Développement d'une méthode d'inventaire de la qualité de la fibre au Québec

Thèse

Guillaume Giroud

Doctorat en sciences forestières
Philosophiae Doctor (Ph.D.)

Québec, Canada

© Guillaume Giroud, 2017

Développement d'une méthode d'inventaire de la qualité de la fibre au Québec

Thèse

Guillaume Giroud

Sous la direction de :

Jean Bégin, directeur de recherche
Chhun-Huor Ung, codirecteur de recherche

Résumé

La valeur du panier de produits des peuplements résineux dépend des dimensions et du défilement des tiges, de la présence de défauts internes, mais aussi des propriétés physiques et mécaniques du bois, principalement de la rigidité du bois, puisque le bois d'œuvre résineux est utilisé essentiellement à des fins structurales. La rigidité du bois d'œuvre résineux est estimée en usine lors du classement visuel ou mécanique des sciages. En forêt, cette connaissance n'existe pas et il n'est pas possible aujourd'hui de localiser les régions ou les peuplements avec un fort potentiel de bois rigide, ni d'évaluer la valeur des bois ou encore de comparer la rentabilité des scénarios sylvicoles, en considérant ce critère de qualité déterminant. Cette absence de connaissances s'explique principalement par les efforts et les coûts considérables associés à la réalisation d'un inventaire de la qualité de la fibre, lequel suppose en effet l'échantillonnage de milliers d'arbres et des analyses en laboratoire très exigeantes. C'est dans ce contexte que la spectroscopie proche infrarouge a été évaluée, comme technologie rapide et non destructive, pour mesurer les propriétés physiques et mécaniques du bois.

Dans un premier temps, nous avons évalué la variabilité écogéographique des propriétés du bois de l'épinette noire pour les deux principales végétations potentielles de la forêt boréale aménagée du Québec (chapitre 1). Nous avons observé que le bois poussant dans les peuplements purs d'épinettes noires avait des fibres matures plus longues, un bois significativement plus dense et de meilleures caractéristiques mécaniques que le bois poussant dans des peuplements mélangés avec le sapin baumier. Une approche de modélisation par saut d'échelle, basée sur des mesures de cernes provenant de 3350 placettes d'inventaire, a permis d'améliorer la performance de tous les modèles, en expliquant, à l'échelle du peuplement, 47%, 57%, 63% et 63% de la variabilité de la densité du bois, du module d'élasticité, de l'angle des microfibrilles, et de la longueur des fibres matures, avec des erreurs quadratiques moyennes, de 8.9 kg/m^3, 0.52 GPa, 0.60° et 0.06 mm respectivement.

Nous avons ensuite évalué le potentiel de la spectroscopie proche infrarouge pour mesurer les propriétés du bois de l'épinette noire (chapitre 2). De bonnes et d'excellentes statistiques de calibration (R^2, rapport de la performance à l'écart) ont été obtenues pour la densité basale (0.85, 1.8), l'angle des microfibrilles (0.79, 2.2), et le module d'élasticité (0.88, 2.9). Une régression segmentée a également été appliquée au profil radial de l'angle des microfibrilles afin de déterminer l'âge de transition du bois juvénile au bois mature. Les valeurs obtenues avec SilviScan ont été comparées à celles obtenues par spectroscopie. L'âge moyen de transition (23 ans ± 7 ans) a été légèrement sous-estimé, par spectroscopie proche infrarouge, avec une erreur de prédiction moyenne de −2.2 ± 6.3 ans et des intervalles de confiance à 95% de −14.6 et 10.1. Ces résultats suggèrent que l'âge de transition du bois juvénile au bois mature peut également être prédit par spectroscopie proche infrarouge.

Finalement, la spectroscopie proche infrarouge a été utilisée pour évaluer la variabilité régionale de la densité basale et de la rigidité du bois des principales essences boréales du Québec (épinette noire, sapin baumier, pin gris, bouleau à papier et peuplier faux-tremble) (chapitre 3). Un système automatisé a été développé à cette fin et calibré à partir de données SilviScan. La densité basale et la rigidité du bois ont été estimées sur 30159 carottes de bois provenant de 10573 placettes d'inventaire. Les observations de densité et de rigidité étaient spatialement autocorrélées sur de plus longues distances chez les feuillus que chez les résineux. Un gradient latitudinal uniforme relié au climat était apparent pour le bouleau à papier et le peuplier faux-tremble. La distribution spatiale de ces mêmes propriétés n'était pas uniforme chez les résineux, suggérant une adaptabilité environnementale plus restreinte en comparaison aux essences feuillues étudiées.

Cette thèse présente de grandes avancées dans le développement d'une méthode d'inventaire de la qualité de la fibre au Québec. La variabilité régionale de la densité et de la rigidité du bois est maintenant connue pour les principales essences boréales du Québec. Les prochains travaux porteront sur l'estimation de ces propriétés à l'échelle du peuplement forestier.

Abstract

The value of forest products from softwood stands depends on stems volume and taper, internal defects, but also on physical and mechanical wood properties, especially stiffness, since softwood lumber is primarily used for structural purposes. The lumber stiffness is evaluated in sawmills through visual or mechanical gradings. In forest, this knowledge does not exist and it is not possible to locate the regions or the forest stands with a high lumber stiffness, neither to evaluate the value of forest products and the economic profitability of forest management scenarios considering this key attribute. This lack of knowledge is mainly due to substantial investments associated with an inventory of wood fibre quality, which involves the sampling of thousands of trees and very demanding laboratory tests. It is in this context that the near-infrared spectroscopy was evaluated as a rapid, non-destructive method for estimating physical and mechanical wood properties.

Ecogeographic variation in black spruce clear wood properties was first investigated for the two main vegetation types of the managed boreal forest of the province of Quebec (chapter 1). Wood growing in pure black spruce stands had longer mature fibers, a significantly denser wood with better mechanical characteristics than the wood growing in stands mixed with balsam fir. A scaling-up modeling approach, based on ring data from 3,350 inventory plots, has improved the performance of all models, explaining, at the stand level, 47%, 57%, 63% and 63% of variance in wood density, modulus of elasticity, microfibril angle and mature fiber length with estimated root mean square errors of 8.9 kg/m^3, 0.52 GPa, 0.60° and 0.06 mm respectively.

The potential of near-infrared spectroscopy to determine the transition from juvenile to mature wood in black spruce was then assessed (chapter 2). Good to excellent calibration statistics (R^2, ratio of performance to deviation) were obtained for basic density (0.85, 1.8), microfibril angle (0.79, 2.2), and modulus of elasticity (0.88, 2.9). Two-segment linear regressions were applied to microfibril angle profiles to determine the transition age. The values obtained using SilviScan data were compared with those obtained using near-infrared spectroscopy predicted data. The average transition age (23 years ± 7 years) was slightly underestimated by near-infrared spectroscopy with a mean prediction error (and 95% limits of agreement) of -2.2 ± 6.3 years (-14.6/10.1). These results suggest that the transition age from juvenile to mature wood could be predicted by near-infrared spectroscopy.

Finally, the near-infrared spectroscopy was used for estimating the regional variation in wood density and stiffness for the main boreal species of Quebec (black spruce, balsam fir, jack pine, paper birch, trembling aspen) (chapter 3). An automated near-infrared system was developed for this purpose and calibrated using SilviScan data. Basic density and wood stiffness were estimated on 30,159 increment cores from 10,573 inventory plots. The observations in wood density and stiffness were spatially autocorrelated on longer distances in hardwoods

than softwoods. A uniform latitudinal gradient related to climate was observed in paper birch and trembling aspen. Conversely, spatial distribution in wood density and modulus of elasticity was not uniform in softwoods, suggesting a more limited environmental adaptability in comparison to the hardwood species studied.

This thesis has made major advances in the development of a method for inventorying wood fibre quality in Quebec. Regional variation in wood density and stiffness is now known for the main boreal species of Quebec. Future work will focus on estimating these properties at the forest stand level.

Table des matières

Liste des tableaux

Liste des figures

À mes deux champions, Arthur et Victor

Remerciements

Avant tout, je remercie sincèrement mon directeur de thèse, Jean Bégin, de m'avoir accompagné et guidé dans la conception et la réalisation de ce projet de recherche, de m'avoir accordé sa totale confiance, et toute la latitude dont j'avais besoin, compte tenu de mes contraintes professionnelles et personnelles. Merci Jean!

Tout projet naît d'une problématique, mais aussi d'une vision. En ce sens, je remercie mon codirecteur de thèse, Chhun-Huor Ung, pour sa confiance, son enthousiasme et sa passion. Cette thèse et le projet d'inventaire de la qualité de la fibre au Québec repose sur une décision judicieuse et éclairée, celle d'avoir conservé les fameuses rondelles de bois du programme d'analyse de tiges de la Direction des inventaires forestiers du du Ministère des Forêts, de la Faune et des Parcs (MFFP).

Un tel projet n'aurait pu voir le jour sans la rigueur, et l'expertise incomparable sur le bois, de Maurice Defo. Je te remercie, Maurice, d'avoir cru en ce projet et d'y avoir collaboré si étroitement.

J'aimerais particulièrement remercier les différents gestionnaires de la Direction des inventaires forestiers qui ont appuyé l'évaluation et la réalisation d'un d'inventaire de la qualité de la fibre de bois au Québec et, par le fait même, soutenu le développement de mon expertise. Ce projet de recherche aura des retombées certaines pour les gestionnaires forestiers à court et moyen termes. Je remercie particulièrement Luc Tellier, Frédéric Dufour, Jean-Pierre Saucier, Jean-Marie Bilodeau, André Larouche ainsi que tous mes collègues du MFFP qui ont participé à ce projet.

Cette thèse, je la dédis totalement à mes deux garçons Arthur et Victor, « beaux comme des anges, forts comme des dieux », les deux plus belles rencontres de ma vie. J'espère leur transmettre cette curiosité, cette passion, cette persévérance qui feront d'eux des grands hommes au cœur tendre. J'embrasse mes parents, mon frère et ma sœur qui me manquent.

Je remercie finalement des personnes qui ont été très importantes pour moi au cours des dernières années et qui m'ont permis de terminer cette thèse avec le sourire: Sonia, Mike, Pascal et Antoine. Merci ☺.

Avant-Propos

La présente thèse a été réalisée sous la direction de M. Jean Bégin, professeur titulaire au Département des sciences du bois et de la forêt de l'Université Laval et sous la codirection de M. Chhun-Huor Ung, professeur associé au même Département et chercheur à la retraite du Centre canadien sur la fibre de bois (CCFB) du Service canadien des forêts de Ressources naturelles Canada. Cette thèse a été réalisée en étroite collaboration avec M. Maurice Defo, initialement professionnel de recherche à l'Université Laval, aujourd'hui agent de recherche au Conseil national de recherches du Canada.

Les résultats de cette thèse sont présentés aux chapitres 1, 2 et 3, sous la forme de trois publications scientifiques, écrites en anglais, et publiées dans des revues internationales. Le reste du document, en français, comprend une introduction et une conclusion générale. L'introduction présente le contexte, la problématique et les objectifs de l'étude. La conclusion générale présente l'originalité et la cohérence des travaux ainsi que les retombées éventuelles et les perspectives d'améliorations. Je suis l'auteur principal de ces trois publications scientifiques. Les coauteurs sont MM. Jean Bégin, Maurice Defo et Chhun-Huor Ung.

Chapitre 1: Giroud, G., Bégin, J., Defo, M. et Ung, C.H. 2016. Ecogeographic variation in black spruce wood properties across Quebec's boreal forest. Forest Ecology and Management, 378, 131-143.

Chapitre 2: Giroud, G., Defo, M., Bégin, J. et Ung, C.H. 2015. Application of near-infrared spectroscopy to determine the juvenile–mature wood transition in black spruce. Forest Products Journal, 65(3), 129-138.

Chapitre 3. Giroud, G., Bégin, J., Defo, M. et Ung, C. H. 2017. Regional variation in wood density and modulus of elasticity of Quebec's main boreal tree species. Forest Ecology and Management, 400, 289-299.

J'ai effectué, de façon autonome, l'ensemble du traitement des données et des analyses statistiques. Les analyses de référence sur le bois (SilviScan, FQA) ont été réalisées par FPInnovations à Vancouver. Les mesures spectrales, en lien avec le premier chapitre, ont été réalisées sous la responsabilité de M. Maurice Defo dans les laboratoires du Centre de recherche sur les matériaux renouvelables de l'Université Laval. Les mesures spectrales, en lien avec le troisième chapitre, ont été réalisées sous ma responsabilité au Ministère des Forêts, de la Faune et des Parcs (MFFP), à Québec.

Ce projet de recherche a été financé par le Fonds de recherche du Québec - Nature et technologies et par le MFFP. Les échantillons de bois de référence ont été mis à disposition par le CCFB qui a également offert la révision linguistique des deux premiers chapitres de cette thèse.

Introduction

La valeur du panier de produits des peuplements résineux dépend des dimensions et du défilement des tiges, de la présence de défauts internes, mais aussi des propriétés physiques et mécaniques du bois, principalement de la rigidité du bois, puisque le bois d'œuvre résineux est utilisé principalement à des fins structurales (Shmulsky and Jones 2011). Au Canada, la plupart des sciages résineux sont classés visuellement selon les règles de classification pour le bois d'œuvre canadien définies par la Commission nationale de classification des sciages (NLGA 2014). Les propriétés mécaniques sont estimées indirectement par le classement visuel des sciages résineux, puisqu'elles sont fortement influencées par la présence des nœuds, du bois de compression, et par l'inclinaison du fil, naturelle ou conséquente au débitage, en accord avec la norme ASTM D245-06 (ASTM International 2011). Dans le calcul des contraintes admissibles, les ingénieurs utilisent donc un facteur de réduction de la résistance du bois exempt de défaut, lequel varie selon la classe visuelle du sciage, en accord avec la norme ASTM D2555 (ASTM International 2016). Toutefois, plusieurs usines classent aussi mécaniquement leurs bois afin d'en connaître précisément la rigidité par le biais d'équipements spécialisés. Sur le marché, on retrouve actuellement deux produits similaires : le bois classé par contrainte mécanique (MSR, machine stress-rating) et le bois classé par résistance mécanique (MEL, machine evaluated lumber) (Forintek Canada Corp. 2000). Ces bois à valeur ajoutée sont appréciés des ingénieurs parce qu'ils réduisent l'incertitude sur la résistance réelle des sciages permettant ainsi de les utiliser à leur plein potentiel dans des applications d'ingénierie, comme les poutrelles, les fermes de toit ou encore le lamellé-collé. Il existe, en principe, plusieurs grades MSR allant d'une rigidité moyenne de 8,3 à 16,5 GPa, démontrant ainsi la variabilité naturelle de la rigidité des sciages résineux, même si en pratique seulement trois classes MSR sont principalement utilisées (NLGA 2017). La rigidité des bois résineux est donc estimée en usine par le biais du classement visuel ou mécanique.

En forêt, cette connaissance n'existe pas et il n'est pas possible aujourd'hui de localiser les régions ou les peuplements à fort potentiel de bois rigide, ni d'évaluer la valeur des bois ou de comparer la rentabilité des scénarios sylvicoles en considérant ce critère de qualité pourtant déterminant. Dans le meilleur des mondes, les usines, produisant du bois classé mécaniquement, devraient pouvoir s'approvisionner à partir de régions ou de peuplements à fort potentiel. Par extension, ces usines devraient se situer dans ces régions ou à proximité de ces peuplements afin de réduire leurs coûts d'opération. De façon générale, l'épinette noire (*Picea mariana* (Mill.) B. S. P.) est privilégiée des industriels puisque son bois se classe MSR en plus grande proportion (Forintek Canada Corp. 2000). Nous savons également que les autres essences résineuses, incluant le sapin (*Abies balsamea* (L.) Mill.), peuvent également produire du bois MSR, mais en plus faible proportion. Il serait ainsi pertinent de pouvoir localiser les régions ou les peuplements à fort potentiel pour ces essences, particulièrement s'ils se situent à proximité des usines produisant du bois classé mécaniquement. Cette réflexion sur la

localisation des peuplements ou des régions à fort potentiel peut se transposer au contexte des pâtes et papiers, mais en considérant les propriétés de la fibre importantes pour le papier, comme la densité du bois, la longueur des fibres et la masse linéique. La localisation des peuplements ou des régions à fort potentiel de bois rigide est de moindre importance dans le cas des essences boréales feuillues, comme le bouleau à papier (*Betula papyrifera* Marsh.) et le peuplier faux-tremble (*Populus tremuloides* Michx.), puisque l'utilisation de ces essences à des fins structurales est marginale. Par contre, la localisation des peuplements ou des régions à faible densité est déterminante pour la fabrication de panneaux, notamment pour le bouleau à papier. La fabrication de panneaux de lamelles orientées (OSB, *Oriented Strand Board*) est en effet adaptée à des essences de faible densité, comme le peuplier faux-tremble au Québec. L'utilisation d'essences comme le bouleau à papier s'avère prometteuse, mais requiert des adaptations au niveau du procédé en raison de sa densité du bois plus élevée (Beck et al. 2010).

La rigidité et la densité du bois sont des éléments qui créent de la valeur et qui devraient faire partie des stratégies de production de bois dans la mesure où il est possible de les évaluer adéquatement. En ce sens, il apparait judicieux de mieux connaître l'influence des conditions de croissance et des traitements sylvicoles sur ces propriétés. Cette connaissance pourrait devenir un intrant déterminant pour le modèle d'évaluation de rentabilité des investissements sylvicoles (MÉRIS) du MFFP, particulièrement en ce qui a trait aux prescriptions de reboisement. L'orientation sur la densité de reboisement est en effet celle qui a le plus d'impact économique pour les forêts résineuses au Québec (Thiffault et al. 2003). En théorie, une densité de reboisement trop faible peut retarder l'âge de transition du bois juvénile au bois mature et avoir pour conséquence de diminuer les propriétés mécaniques du bois en raison de la proportion plus élevée de bois juvénile dans l'arbre au moment de la récolte (Jozsa et Middleton 1994). Cet effet s'accentue dans le cas des plantations d'espèces à croissance rapide en raison des courtes révolutions qui limitent la production de bois mature. Cette situation problématique est particulièrement étudiée dans les plantations de pins du sud-est des États-Unis. Plusieurs études ont en effet été publiées dans le but de déterminer l'âge optimal de récolte afin de produire un bois de qualité sciage, en considérant notamment la variabilité régionale de la rigidité et de la densité du bois en plantations (Antony et al. 2010, Antony et al. 2011, Butler et al. 2016, Jordan et al. 2008). Cette région des États-Unis est un compétiteur important puisqu'il répond actuellement à 60% de la demande intérieure en bois et à 16% de la demande mondiale (Antony et al. 2015). On estime en outre que la surface des plantations de cette région devrait croître de 67% d'ici 2040, en passant de 13 à 22 millions d'hectares, soit très près des 27 millions d'hectares de forêt publique destinée actuellement à la production forestière au Québec, superficie qui ne devrait pas varier fortement d'ici 2040 (BFEC 2017). De plus, la croissance de ces plantations ne cesse de s'améliorer en raison des améliorations génétiques, de la préparation intensive des sites et de l'usage d'herbicides et de fertilisants (Butler et al. 2016). Le bois d'œuvre est désormais récoltable entre 20 et 25 ans dans certaines plantations de pins, avec des dimensions commerciales pouvant être atteintes après 16 années de croissance.

De façon globale, la densité et la rigidité du bois d'œuvre canadien issu de forêts naturelles, poussant en zones tempérée nordique et boréale, devraient être considérées comment un avantage concurrentiel en comparaison de celui issu des plantations de pins du sud-est des États-Unis et récolté à des révolutions très courtes.

L'absence de connaissances au Québec sur la variabilité de la densité et de la rigidité du bois en forêt s'explique principalement par les efforts et les coûts considérables associés à la réalisation d'un inventaire de la qualité de la fibre, lequel suppose en effet l'échantillonnage de milliers d'arbres et des analyses en laboratoire très exigeantes. Sans cette connaissance, il devient difficile de connaître le potentiel réel des forêts en termes de densité et de rigidité du bois, ni de connaître l'influence réelle des traitements sylvicoles sur ces propriétés. Le document « Résistance et propriétés connexes des bois indigènes au Canada » de Jessome (1977) est le document le plus utilisé depuis 40 ans, lorsqu'il s'agit de faire référence aux propriétés physiques et mécaniques des bois canadiens. Ces propriétés ont été mesurées en laboratoire en respectant les normes de référence très exigeantes en la matière. Toutefois, ce document repose sur un nombre très restreint d'arbres et de sites échantillonnés. En exemple, les propriétés de densité et de résistance de l'épinette noire ont été mesurées sur 32 arbres provenant de 6 sites échantillonnés dans quatre provinces différentes. De plus, aucune considération ne semble avoir été portée à l'âge des arbres, à la station écologique ou aux conditions de croissance. Considérant la variabilité naturelle importante des propriétés physiques et mécaniques du bois, les valeurs de Jessome (1977) doivent être utilisées avec prudence. En effet, ces valeurs ne peuvent être représentatives de toute la variabilité observable dans les forêts du Québec et du Canada. Récemment, un partenariat entre l'industrie et la recherche, financé par le CCFB et le Service canadien des forêts de Ressources naturelles Canada, a permis de réaliser un inventaire de la qualité de la fibre de l'épinette noire et du sapin baumier à l'échelle de Terre-Neuve, démontrant ainsi toute une variabilité naturelle et régionale, et la faisabilité de modéliser ces propriétés à l'échelle des peuplements (Lessard et al. 2014, Luther et al. 2014). La papetière, partenaire de ce projet, a également mentionné des retombées substantielles sur ses coûts d'opération, en s'approvisionnant davantage en sapin, ayant les qualités désirées, laquelle ressource se situait plus proche de l'usine que l'épinette noire habituellement recherchée.

C'est dans ce contexte que la Direction des inventaires forestiers du MFFP a décidé d'évaluer la faisabilité technique et scientifique d'un inventaire de la qualité de la fibre de bois au Québec (Defo et al. 2013a, 2013b). Les résultats de cette étude ont permis de démontrer l'influence de la station et des conditions de croissance sur les propriétés du bois de l'épinette noire. De plus, après avoir comparé l'ensemble des technologies disponibles, il s'est avéré que l'usage de la spectroscopie proche infrarouge était la technologie la plus appropriée afin de mettre à profit l'échantillonnage unique que représentent les milliers de carottes de bois récoltées annuellement dans les placettes temporaires de la Direction des inventaires forestiers. Ces carottes sont prélevées systématiquement à 1 mètre de hauteur, encollées, sablées de la même manière, offrant une

finition parfaite pour la mesure spectrale. D'autre part, le bois de ces carottes est généralement exempt de défauts, considérant que ces carottes sont prélevées avec soin pour permettre la mesure précise des cernes. Toutefois, lorsque des défauts sont apparents sur la carotte, tels que du bois de compression, des résidus de colle, ou autres, ils sont alors systématiquement annotés; l'objectif étant d'analyser des mesures relatives et comparables de propriétés physiques et mécaniques de bois exempt de défauts. Le terme d'indice de qualité du bois (IQB) est ainsi utilisé au MFFP pour décrire ces mesures.

Les applications de la spectroscopie proche infrarouge au bois sont nombreuses (Tsuchikawa and Kobori, 2015; Tsuchikawa 2007). Il s'agit d'une technique, rapide et non destructive, requérant peu ou pas de préparation. La spectroscopie proche infrarouge utilise la gamme infrarouge du spectre électromagnétique comprise entre 780 et 2500 nm. Il s'agit d'une spectroscopie d'absorption dont le principe repose sur l'absorption du rayonnement proche infrarouge par la matière organique, laquelle est intimement reliée à la nature chimique du bois. La calibration consiste à relier les spectres d'absorbance à des mesures de propriétés physiques et mécaniques du bois, au moyen d'analyses multivariées. Ce modèle de calibration nécessite des mesures précises provenant de méthodes de référence. SilviScan est l'instrument de référence lorsqu'il s'agit de calibrer des modèles proche infrarouge destinés à prédire les propriétés physiques et mécaniques du bois à partir de carottes d'inventaire (Schimleck 2008). De nombreuses calibrations proche infrarouge ont ainsi été développées pour des essences variées, incluant notamment le sapin baumier et l'épinette noire (Xu et al. 2011). Avec SilviScan, les propriétés physiques et mécaniques du bois sont mesurées par densitométrie à rayons X, diffractométrie à rayons X et analyse d'images (Evans and Ilic 2001; Evans 1994). Il est à noter que la rigidité du bois mesurée avec SilviScan est environ 10% plus élevée que la rigidité, dite statique, c'est-à-dire mesurée avec des tests mécaniques en flexion, et que les résultats des deux méthodes sont hautement corrélés (Raymond et al. 2007). Les mêmes auteurs rapportent des différences plus importantes pour les essences feuillues, de l'ordre de 30%, entre des mesures dynamiques et des mesures statiques de rigidité.

Les travaux de la présente thèse s'inscrivent donc dans une démarche visant dans un premier temps à établir des preuves de concept avec l'épinette noire (chapitres 1 et 2) et, dans un second temps, à proposer une méthode d'inventaire de la qualité de la fibre pour les principales essences boréales du Québec (épinette noire, épinette blanche (*Picea glauca* (Moench) Voss), sapin baumier, pin gris (*Pinus banksiana* Lamb.), bouleau à papier, peuplier faux-tremble (chapitre 3). Les principaux objectifs de cette thèse sont :

1. D'évaluer l'influence de la station écologique et des conditions de croissance sur la densité basale, la rigidité, l'angle des microfibrilles et la longueur des fibres matures de l'épinette noire (chapitre 1).

2. D'évaluer la faisabilité de modéliser au peuplement la densité basale, la rigidité, l'angle des microfibrilles et la longueur des fibres matures de l'épinette noire (chapitre 1).

3. D'évaluer le potentiel de la spectroscopie proche infrarouge pour estimer la densité basale, la rigidité et l'angle des microfibrilles de l'épinette noire, incluant l'âge de transition du bois juvénile au bois mature (chapitre 2).

4. De développer des modèles spectroscopiques pour les principales essences boréales du Québec afin de mesurer la densité basale et la rigidité du bois de carottes d'inventaire (chapitre 3).

5. D'évaluer la variabilité naturelle et régionale de la densité basale et de la rigidité du bois des principales essences boréales du Québec (chapitre 3).

Références

Antony, F., Schimleck, L.R., Daniels, R.F., Clark, A. et Hall D.B. 2010. Modeling the longitudinal variation in wood specific gravity of planted loblolly pine (*Pinus taeda* L.) in the United States. Can. J. For. Res. 40(12), 2439 –2451.

Antony, F., Jordan, L., Schimleck, L.R., Clark, A., Souter, R.A. et Daniels, R.F. 2011. Regional variation in wood modulus of elasticity (stiffness) and modulus of rupture (strength) of planted loblolly pine in the United States. Can. J. For. Res. 41, 1522–1533.

Antony, F., Schimleck, L.R., Daniels, R.F., Clark, A., Borders, B.E., Kane, M.B. et Burkhart, H.E. 2015. Whole-tree bark and wood properties of loblolly pine from intensively managed plantations. Forest Science, 61(1), 55-66.

ASTM International 2011. ASTM D245-06: standard practice for establishing structural grades and related allowable properties for visually graded lumber. American society for testing and materials. West Conshohocken, PA. 17 pages.

ASTM International 2016. ASTM D2555-16: standard practice for establishing clear wood strength values. American Society for Testing and Materials. American society for testing and materials. West Conshohocken, PA. 18 pages.

Beck, K., Cloutier, A., Salenikovich, A. et Beauregard, R. 2010. Comparison of mechanical properties of oriented strand board made from trembling aspen and paper birch. European Journal of Wood and Wood Products, 68(1), 27-33.

BFEC 2017. Possibilités forestières en vigueur du 1er avril 2018 au 31 mars 2023. Synthèse provinciale. http://forestierenchef.gouv.qc.ca/wp-content/uploads/2016/05/synthese_provinciale.pdf (consulté le 8 mai 2017). Bureau du forestier en Chef. Roberval, QC.

Butler, M. A., Dahlen, J., Daniels, R.F., Eberhardt, T.L. et Antony, F. 2016. Bending strength and stiffness of loblolly pine lumber from intensively managed stands located on the Georgia Lower Coastal Plain. European journal of wood and wood products, 74(1), 91-100.

Defo, M., Giroud, G. et Bégin, J. 2013a. Étude de faisabilité portant sur la caractérisation de la qualité de la fibre de bois à partir des données de l'inventaire écoforestier du Québec méridional (IÉQM). Rapport

no. 1, étude de faisabilité technologique. Ministère des Ressources naturelles, Direction des inventaires forestiers, Québec, QC. 49 pages.

Defo, M., Giroud, G. et Bégin, J. 2013b. Étude de faisabilité portant sur la caractérisation de la qualité de la fibre de bois à partir des données de l'inventaire écoforestier du Québec méridional (IÉQM). Rapport no. 2, étude de faisabilité scientifique. Ministère des Ressources naturelles, Direction des inventaires forestiers, Québec, QC. 50 pages.

Evans R. 1994. Rapid measurement of the transverse dimensions of tracheids in radial wood sections from Pinus radiate. Holzforschung 48(2), 168-172.

Evans, R. et Ilic, J. 2001. Rapid prediction of wood stiffness from microfibril angle and density. Forest Prod. J. 51(3), 53.

Forintek Canada Corp. 2000. Lumber and value-added wood products: special report. Sainte-Foy, QC. 129 pages.

Jessome, A.P. 1977. Résistance et propriétés connexes des bois indigènes au Canada. Forintek Canada Corp. Sainte-Foy, QC. 37 pages.

Jordan, L., Clark, A., Schimleck, L.R., Hall, D.B., et Daniels, R.F. 2008. Regional variation in wood specific gravity of planted loblolly pine in the United States. Can. J. For. Res. 38(4): 698 –710.

Jozsa, L.A. et Middleton, G.R. 1994. A discussion of wood quality attributes and their practical implications. Forintek Canada Corp. Vancouver, BC. 42 pages.

Lessard, E., Fournier, R.A., Luther, J. E., Mazerolle, M.J. et Van Lier, O.R. 2014. Modeling wood fiber attributes using forest inventory and environmental data for Newfoundland's boreal forest. Forest Ecology and Management, 313, 307-318.

Luther, J.E., Skinner, R., Fournier, R.A., van Lier, O.R., Bowers, W.W., Coté, J.-F., Hopkinson, C. et Moulton, T. 2014. Predicting wood quantity and quality attributes of balsam fir and black spruce using airborne laser scanner data. Forestry 87, 313–326.

NLGA 2014. Standard grading rules for Canadian lumber (Règles de classification pour le bois d'œuvre canadien). National Lumber Grades Authority (Commission nationale de classification des sciages). Vancouver, BC. 274 pages.

NLGA 2017. SPS 2 - Special products standard for machine graded lumber (SPS 2 - Norme de produits spéciaux pour le bois classé par machine). National Lumber Grades Authority (Commission nationale de classification des sciages). Vancouver, BC. 35 pages.

Raymond, C.A., Joe, B., Evans, R. et Dickson, R.L. 2007. Relationship between timber grade, static and dynamic modulus of elasticity, and SilviSvan properties for Pinus radiata in New South Wales. New Zeal. J. For. Sci. 37(2), 186.

Schimleck, L.R. 2008. Near-infrared spectroscopy: a rapid, non-destructive method for measuring wood properties and its application to tree breeding. New Zeal. J. For. Sci. 38(1), 14-35.

Shmulsky, R. et Jones, P.D. 2011. Forest products and wood science. John Wiley & Sons. 477 pages.

Thiffault, N., Roy, V., Prégent, G., Cyr, G., Jobidon, R., et Ménétrier, J. 2003. La sylviculture des plantations résineuses au Québec. Nat. can, 127(1), 63-80.

Tsuchikawa, S. 2007. A review of recent near infrared research for wood and paper. Appl. Spectrosc. Rev. 42(1), 43-71.

Tsuchikawa, S. et Kobori, H. 2015. A review of recent application of near infrared spectroscopy to wood science and technology. J. Wood Sci. 61(3), 213-220.

Xu, Q., Qin, M., Ni, Y., Defo, M., Dalpke, B. et Sherson, G. 2011. Predictions of wood density and module of elasticity of balsam fir (*Abies balsamea*) and black spruce (*Picea mariana*) from near infrared spectral analyses. Can. J. For. Res. 41(2), 352–358.

Chapitre 1. Ecogeographic variation in black spruce wood properties across Quebec's boreal forest.

Résumé

La variabilité écogéographique des propriétés du bois de l'épinette noire exempt de défaut a été étudiée pour les deux principales végétations potentielles de la forêt boréale aménagée de la province de Québec, Canada. Le bois poussant dans les peuplements purs d'épinettes noires (RE2) avait des fibres matures légèrement plus longues, un bois significativement plus dense et de meilleures caractéristiques mécaniques que le bois poussant dans des peuplements mélangés avec le sapin baumier (RS2). Une approche de modélisation par saut d'échelle, basée sur des mesures de cernes provenant de 3350 placettes d'inventaire, a permis d'améliorer la performance de tous les modèles, en expliquant, à l'échelle du peuplement, 47%, 57%, 63% et 63% de la variance de la densité du bois, du module d'élasticité, de l'angle des microfibrilles, et de la longueur des fibres matures, avec des erreurs quadratiques moyennes de 8.9 kg/m^3, 0.52 GPa, 0.60° et 0.06 mm respectivement.

Abstract

Ecogeographic variation in black spruce clear wood properties was investigated for the two main vegetation types of the managed boreal forest of the province of Quebec, Canada. In total, 409 co-dominant and dominant trees from 82 mature stands were sampled. Basic wood density, modulus of elasticity and microfibril angle were measured using SilviScan. Mature fiber length was determined using a high-resolution Fiber Quality Analyzer. Wood growing in pure black spruce stands had longer mature fibers, a significantly denser wood with better mechanical characteristics than the wood growing in mixed stands with balsam fir. All wood properties were clearly influenced by radial growth and species composition.

Given the limited number of sample plots for mapping purposes, a two-stage modeling approach was assessed to predict stand-level estimates of black spruce clear wood properties. This scaling-up method, based on field measurements and ring data from 3350 inventory plots, has improved the performance of all models. Stand-level models explained 47%, 57%, 63% and 63% of variance in wood density, modulus of elasticity, microfibril angle and mature fiber length respectively with estimated root mean square errors of 8.9 kg/m^3, 0.52 GPa, 0.60° and 0.06 mm.

An east-west gradient in black spruce clear wood properties was revealed as possibly the by-product of the change in relative proportions of both studied vegetation types across the study area. The results indicate that the black spruce wood from western regions of the managed boreal forest has a better potential for producing pulp and paper, lumber or engineered products due to its longer mature fibers and higher mechanical properties.

Introduction

Spatial variation in wood properties is still not well known in natural forests (Briggs 2010). Wood density, however, has been studied as a functional trait of plants at the landscape scale (Chave et al. 2009, Malhi et al. 2006, Swenson and Enquist 2007). The data of these studies were mainly compiled from the literature in order to compare the evolution of wood density between angiosperms and gymnosperms across geographic and topographic gradients. Wood density has always created a lot of interest given its close relationship with mechanical support, water transport and storage capacity (Chave et al. 2009). Performing large-scale research on wood properties for a given species requires significant investments to collect samples and perform laboratory measurements. That reality has always been an impediment to research in this field. Most studies focus on a few sites and, consequently, the scope of results is often narrow.

Black spruce (*Picea mariana* (Mill.) B. S. P.) grows in a variety of conditions, suggesting differences in wood fiber quality between sites. Its reproduction is particularly adapted to fire because of its serotinous cones (Gauthier et al. 2001). In regions with high fire frequency, black spruce forms extensive and even-aged stands. Otherwise, it mainly reproduces by vegetative layering forming irregular stands particularly in open sites with abundant humus. Black spruce largely dominates Quebec's boreal forest. It represents approximately 75% of the total gross merchantable volume of this region, followed by balsam fir (*Abies balsamea* (L.) Mill.) (15%) and jack pine (*Pinus banksiana* Lamb.) (8%), according to data provided by the Ministère des Forêts, de la Faune et des Parcs du Québec (MFFPQ). Black spruce wood is highly desirable for lumber, pulp manufacturing and engineered wood products (Viereck and Johnston 1990, Zhang and Koubaa 2008). Compared with balsam fir, black spruce has a denser wood, a higher modulus of elasticity (MOE) and modulus of rupture (MOR), and a higher coarseness for a similar fiber length (Jessome 2000, Lessard et al. 2014). Compared with jack pine, black spruce has relatively similar values for wood density and mechanical properties (MOE, MOR), but smaller knots and much less resin (Jessome 2000, Panshin and Zeeuw 1980).

Numerous studies have focused on the influence of growth conditions on black spruce wood properties across Canada, given its merchantable importance. However wood fiber quality in relation to ecological site conditions has not been studied much until now. The importance of ecological land classification to predict black spruce wood properties was investigated in the boreal forest of northeastern Ontario (Pokharel et al. 2014, Townshend et al. 2015). Ecosite group was the most important explanatory variable for these studies. Higher values in wood density and latewood proportion were observed for intermediate and poor swamp ecosites. Pokharel et al. (2014) explained these results as the constraining effects of wet, nutrient-poor conditions in swamp ecosites. Townshend et al. (2015) found that longer fiber length was associated with more productive ecosites that supported faster growth. The influence of growing conditions on wood formation was also recently investigated in black spruce and balsam fir by Groot and Luther (2015). Negative correlations of wood density to radial growth

rate at the ring, tree, and plot levels of aggregation were found from 330 black spruce and 680 balsam fir increment cores collected across Newfoundland. However, the authors mentioned that growth rate alone was insufficient to explain variation in wood density at all levels. Model performance was also particularly improved with the aggregation level of wood density models: ring to tree to plot. This improvement was mainly explained by the decrease in wood density variance with the aggregation level. Torquato et al. (2013) have assessed the influence of stand origin and structure on the mechanical properties of black spruce in 28 sites across Quebec. MOE and MOR were found significantly higher for samples from regular stands compared with those from older, irregular stands. The authors suggested that a higher incidence of mild compression wood associated with vegetative layering in irregular stands could explain these differences.

Spatial variation in black spruce wood properties was also little investigated, and the available results are often divergent. Latitudinal variations in tree-ring and wood cell characteristics were observed in 15 black spruce mature stands sampled along a 500 km transect from 47°N to 52°N across the Quebec's boreal forest (St-Germain and Krause 2008). Tree ring, earlywood, and latewood widths, cell numbers, latewood radial cell diameter, and cell wall thickness declined with latitude, but no significant variations were observed on tracheid length and latewood proportion. Rossi et al. (2015) found higher wood density and mechanical properties for sites located at lower latitudes and altitudes. In both studies, the influence of ecosite was however not considered. Spatial variation in wood properties has also been investigated in other North American species. To our knowledge, Lenz et al. (2014) were the first to use the ecological land classification of Quebec to study spatial variation in wood fiber properties. Significant differences in white spruce (*Picea glauca* (Moench) Voss) wood properties among ecological regions were observed in 56 sites across Quebec. Maximum temperature, degree days, geographic location, tree height, and diameter were the best predictors of white spruce wood properties. Significant regional variations in wood properties were also observed in planted loblolly pine (*Pinus taeda* L.) in the United States. Latewood proportion, wood density and mechanical properties were higher in southern and coastal regions characterized by more abundant summer precipitation and longer growing seasons (Finto et al. 2011, Jordan et al. 2008).

Several studies concluded that stand-level models could theoretically be developed to map wood properties over broad areas (Briggs 2010, Lenz et al. 2014, Pokharel et al. 2014, Van Leeuwen et al. 2011). For practical reasons as previously mentioned, very few studies have gone so far to date. The proof of concept was recently done for black spruce and balsam fir in Newfoundland (Lessard et al. 2014). Stand-level estimates were predicted using climate, geographic and photo-interpreted data. Maps were produced for Newfoundland. These models were developed using the average plot values of wood properties measured in 77 black spruce and 117 balsam fir sites. Sample size is the main limitation to the production of accurate regional maps of wood properties in order to take into account, as widely as possible, the ecological variability of the study area. To our knowledge, a two-

stage modeling approach has never been investigated to predict stand-level estimates of wood properties. In the present study, the two-stage modeling approach consisted in developing tree-level models to predict individual tree values from provincial inventory plots, in order to increase the sampling intensity to develop stand-level models. The two-stage modeling approach refers to the concept of double sampling, or two-phase sampling, which is used in forest inventories for several decades (Tuominen et al. 2006).

The present study was based on Quebec's ecological land classification and on a large provincial forest resources inventory dataset. This study aimed to investigate the spatial variation of black spruce clear wood properties in different site types across the managed boreal forest of Quebec. More specifically, the objectives were (i) to assess the influence of ecological conditions on black spruce clear wood properties, and (ii) to develop a modeling approach to produce regional maps.

Materials and methods

Study area and sampled ecosites

The study area was the “black Spruce – moss” bioclimatic domain, located approximately from 48°N to 52°N, in the boreal forest of Quebec, Canada (Figure 1.1) (Blouin and Berger 2004, Blouin and Berger 2005, Morneau and Landry 2007, Morneau and Landry 2010a, Morneau and Landry 2010b). Bioclimatic domain is the highest level of the ecological land classification of the province of Quebec. It is characterized by a particular type of vegetation in the final stage of succession, reflecting the balance between climate and potential vegetation on mesic sites (well-drained soils). The climate of the “black Spruce – moss” domain is continental, with a short growing season. It is divided into two precipitation-based subdomains. Unlike the western subdomain, the eastern subdomain is characterized by more precipitation, a longer fire cycle and more balsam fir than the western subdomain.

Potential vegetation is the typical vegetation of end succession for a given site. The two main potential vegetations are the “balsam Fir – black Spruce” vegetation (“RS2”) and the “black Spruce – moss or ericaceous” vegetation (“RE2”), representing 74% and 14% of the total forest area of the eastern subdomain, and 21% and 48% of the total forest area of the western subdomain, according to data provided by MFFPQ, respectively. The forest dynamics are very different in both types of potential vegetation (Blouin and Berger 2004, Blouin and Berger 2005, Morneau and Landry 2007, Morneau and Landry 2010a, Morneau and Landry 2010b). The stands associated with RE2 vegetation are almost always black spruce even-aged stands continuously renewed by recurring fires, and characterized by seed reproduction. On the other hand, the main natural disturbances related to RS2 vegetation are fires, windthrows and insect outbreaks (mainly spruce budworm). The fire frequency is longer compared with RE2 vegetation and the gap dynamics related to windthrow and insect outbreaks form irregular stands with a predominance of vegetative reproduction for black spruce.

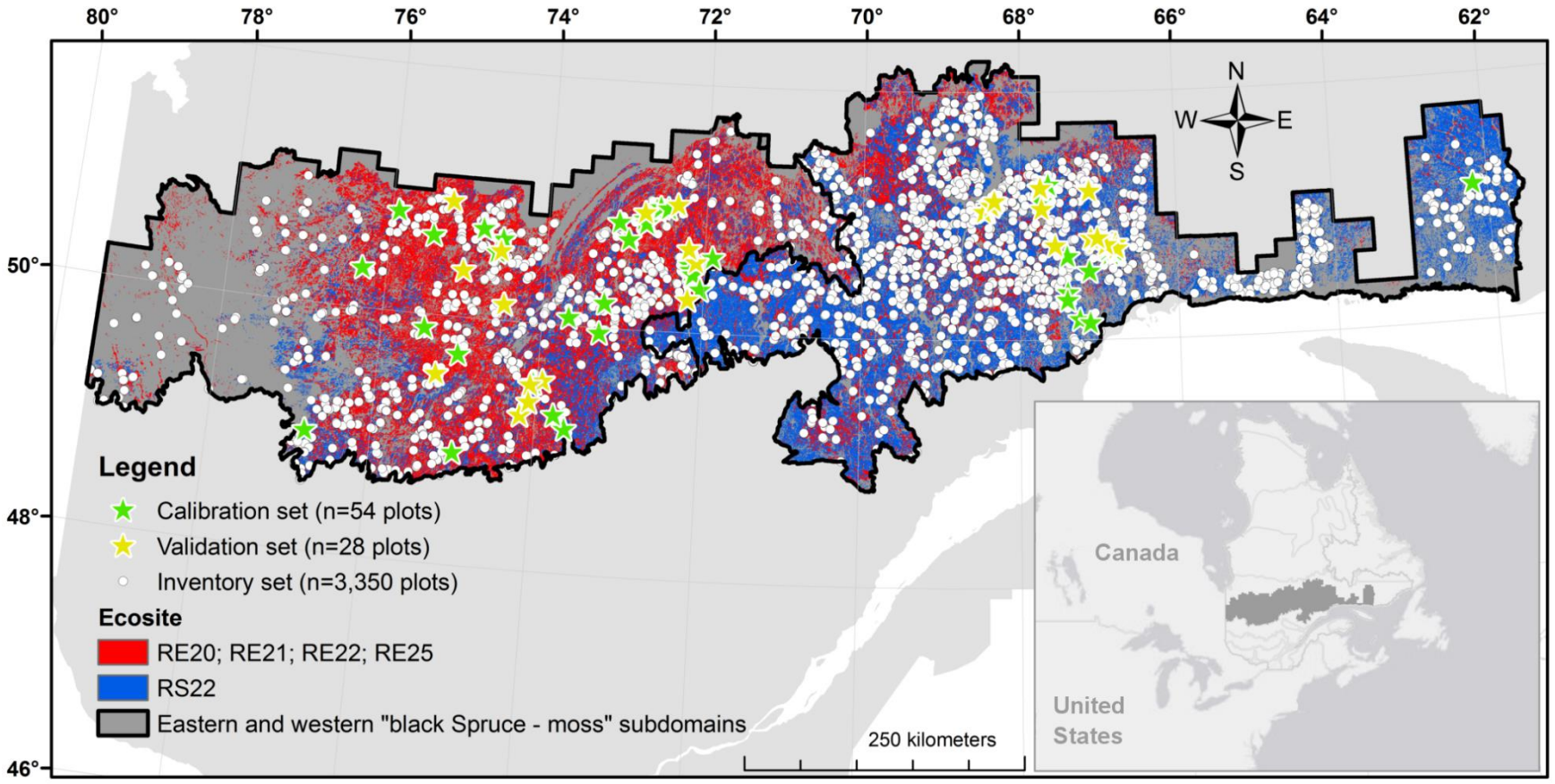

Figure 1.1 Location of calibration, validation, and inventory plots. The natural distribution of studied ecosites is shown across the "black Spruce – moss" bioclimatic domain as well as the boundary between both subdomains.

Different physical features can also be found for a same potential vegetation in terms of soil drainage and texture conditions. A second number is thus added to the potential vegetation code to specify the physical features. This combination of potential vegetation and physical features is here called “ecosite”. Ecosite is determined for every plot and photo-interpreted stand in the provincial forest resources inventory. For the purpose of this study, a gradient of physical features was sampled (Table 1.1). The soil drainage is defined as “rapidly to well-drained” in RE20 ecosite, “well-drained” in RE21, RE22 and RS22 ecosites, and “imperfectly drained” in RE25 ecosite. The surface deposit thickness is “very thin” in RE20 ecosite, and “thin to thick” in RE21, RE22, RE25 and RS22 ecosites. Finally, the soil texture is defined as “varied” in RE20 ecosite, “coarse” in RE21 ecosite, and “medium” in RE22, RE25 and RS22 ecosites. Every ecosite was sampled in both subdomains, except RE20 which was only available in the western subdomain. These five ecosites represent 59% of the total forest area of the “black Spruce – moss” bioclimatic domain, according to data provided by MFFPQ. Figure 1.1 shows the natural distribution of studied ecosites across the “black Spruce – moss” bioclimatic domain as well as the boundary between both subdomains.

Table 1.1 Characteristics of ecosites and number of plots and trees used in this study.

Ecosite				Calibration set		Validation set		Inventory set	
Potential vegetation	Soil drainage	Surface deposit thickness	Soil texture	n (plots)	n (trees)	n (plots)	n (trees)	n (plots)	n (trees)
Black Spruce – moss or ericaceous (RE20)	Rapidly to well-drained	Very thin	Varied	2	10	2	11	179	583
Black Spruce – moss or ericaceous (RE21)	Well-drained	Thin to thick	Coarse	9	44	4	18	213	550
Black Spruce – moss or ericaceous (RE22)	Well-drained	Thin to thick	Medium	11	52	6	28	1322	4339
Black Spruce – moss or ericaceous (RE25)	Imperfectly drained	Thin to thick	Medium	13	66	6	31	473	1365
Balsam Fir – black Spruce (RS22)	Well-drained	Thin to thick	Medium	19	96	10	53	1163	3261
Total				54	268	28	141	3350	10,098

Estimation of the influence of ecological conditions on clear wood properties

Several thousands of trees were measured, felled and cut in disks across the province to develop stem taper equations and site index estimates in the 2000s (Laflèche et al. 2013). A part of this program wood disks was kept frozen by the federal government for future research on wood fiber. From this collection, 409 black spruce clear wood samples from 82 sites met our selection criteria in terms of study area (“black Spruce – moss” bioclimatic domain) and selected ecosites: RE20 (4 plots, 21 trees), RE21 (13 plots, 62 trees), RE22 (17 plots, 80 trees), RE25 (19 plots, 97 trees), and RS22 (29 plots, 149 trees). Four to six samples, collected at breast height, were available for each site. Only co-dominant and dominant trees from mature stands were sampled.

Basic density (BD), MOE and microfibril angle (MFA) were measured on these wood samples using SilviScan-3 at FPInnovations in Vancouver, British Columbia (Giroud et al. 2015). These properties were averaged by calculating the area-weighted mean, assuming a circular shape of the rings. Average values of mature fiber length (FL) were determined for 313 of 409 black spruce wood samples using a high-resolution Fiber Quality Analyzer (HiRes FQA, OpTest Equipment Inc, Hawkesbury, Ontario, Canada) at the FPInnovations lab. Only

mature wood (51 years and older) was analyzed. FL is a relevant variable considering that the sawmill residues, used for pulp manufacturing, are mainly mature wood (Watson and Bradley 2009). Fiber length determination requires boiling small blocks of wood for 4 h and simmering them at 70 °C overnight in deionized water (FPInnovations communications). These blocks are then soaked in maceration solution for 48 h at 70 °C to separate fibers. The pulp solution can then be analyzed using the HiRes FQA. This system collects and analyzes images of fibers of the pulp solution. It measures length and other fiber morphological properties. The length-weighted fiber length was used in this study, as recommended in the literature, since it corrects the natural bias associated with fiber-wall fragments, also called fines (Robertson et al. 1999).

Linear mixed regressions were performed to assess the effects of bioclimatic subdomain, potential vegetation and physical features on BD, MOE, MFA, and FL (PROC MIXED, SAS 9.3, SAS Institute Inc., Cary, North Carolina, USA). The average values of the first 50 rings from the pith for BD, MOE and MFA were used to control the effect of age. The interaction between bioclimatic subdomain and potential vegetation was also investigated. The plot effect was considered as a random effect and its contribution to the variance was estimated. The goodness of fit was assessed by calculating the marginal and conditional pseudo-R^2 as described by Nakagawa and Schielzeth (2013). The marginal pseudo-R^2 is concerned with variance explained by fixed effects, and the conditional pseudo-R^2 is concerned with variance explained by both fixed and random effects. Furthermore, a LSMEANS statement was added to the MIXED SAS procedure to compute least-squares means and estimate treatment differences.

The influence of ecological conditions was also investigated on the radial variation of RW, BD, MOE and MFA at breast height using penalized smoothing splines, as described by Jordan et al. (2008) and Ngo and Wand (2004) (PROC MIXED, SAS 9.3, SAS Institute Inc., Cary, North Carolina, USA). The smoothing splines were represented as mixed models with fixed effects (ring number) and random effects (tree, plot). Fixed and random coefficients were thus estimated for each knot of the smoothing variable. Smoothing splines with confidence intervals were plotted by potential vegetation for each property. The number of sampled trees over 100 years was too limited to perform the penalized smoothing splines beyond this point.

Development of a modeling approach to produce regional maps

Given the limited number of plots for mapping purposes, a first approach with two-stage modeling was assessed to predict stand-level estimates of black spruce wood properties (Figure 1.2). For statistical purposes, 54 sites were randomly chosen for a calibration set (268 samples) and 28 others for an independent validation set (141 samples). Fiber length data were only available for a subset of 53 calibration plots (209 samples) and 26 validation plots (104 samples). The forest resources inventory data, collected by the provincial government since 1995, were investigated to form the "inventory set" (Figure 1.2). In total, 10,098 black spruce trees from 3350 plots met our selection criteria in terms of study area and selected ecosites. Only inventory plots with a height class of 7 m and higher and an age class of 50 years and older were retained. Furthermore, only co-dominant and dominant black spruce trees were chosen. Table 1.1 presents the distribution of calibration, validation and inventory plots and trees by ecosite. It should be noted that RE20 was poorly represented in calibration and validation sets. Figure 1.1 shows the location of calibration, validation and inventory plots across the "black Spruce – moss" bioclimatic domain.

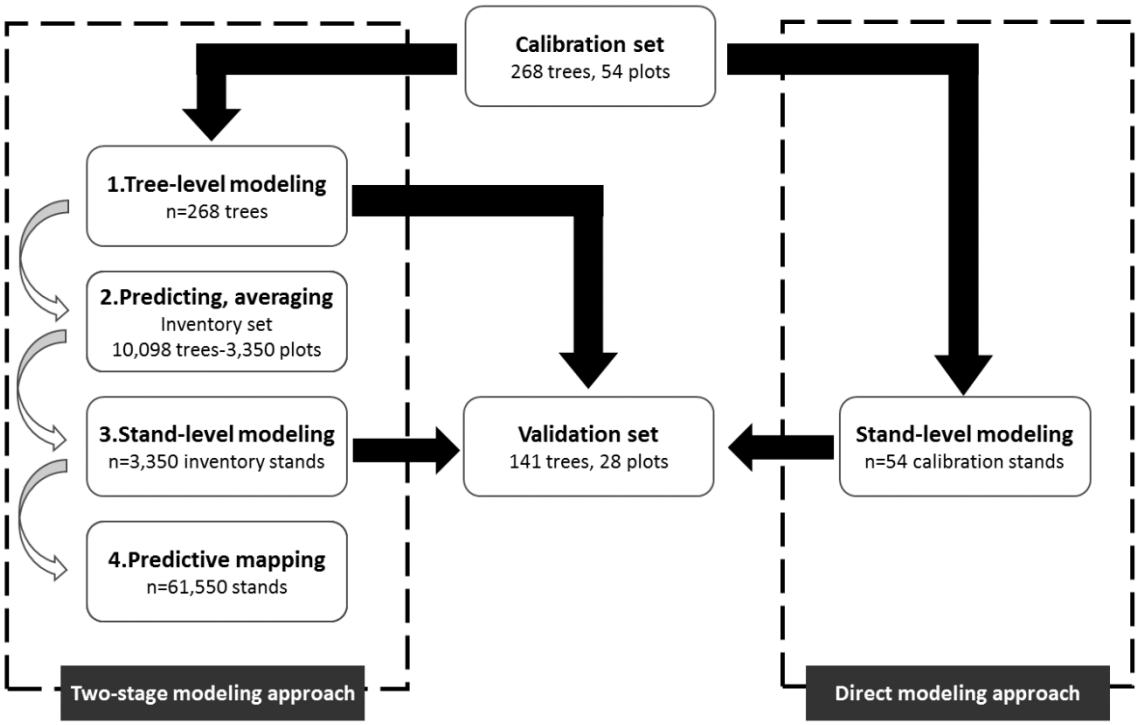

Figure 1.2 Diagram summarizing both scaling-up methods assessed to predict stand-level estimates of wood properties.

The two-stage modeling approach consisted in (i) developing tree-level models using calibration set, (ii) using these models to predict values of the 10,098 trees of the inventory set, and (iii) developing stand-level models using the average plot values of the inventory set (3350 plots). This two-stage modeling approach was compared with a more direct approach that involved predicting stand-level estimates of wood properties using only the average plot values of the calibration set (Figure 1.2). The best modeling approach, based on validation statistics, was finally applied to the photo-interpreted stands in the 70-year-old age class corresponding to the study area and selected ecosites (61,550 stands) for mapping in ArcGIS (ESRI®, Redlands, California, USA). The proportion in area of each ecosite in the selected photo-interpreted stands was 5%, 12%, 30%, 9%, and 44% for RE20, RE21, RE22, RE25, and RS22, respectively. An analysis of variance was finally used to test for differences in wood properties between groups of ecological regions.

Table 1.2 presents the core-, tree-, plot-, and stand-scale attributes available for calibration, validation and inventory sets. The core-, tree-, and plot-scale attributes were only used to develop tree-level models in the two-stage approach. Ring width (RW) and age (AGE) were measured using WinDENDRO (Regent Instruments Inc., Quebec City, Quebec, Canada). Cross-sectional wood samples were collected at breast height while the increment cores of inventory trees were collected at 1 m above ground. It is assumed that the differences in age and wood properties are minor between these two heights and can be ignored. Latewood proportion (LW%) and RGB (red, green, and blue) colors were determined using customized macros developed in ImageJ software (National Institutes of Health, Bethesda, Maryland, USA). Several color combinations were assessed as explanatory variables. LW% and RGB colors were not available for the increment cores of inventory trees. Indeed scanner calibration was never done, consequently, color variation between increment cores cannot be analyzed. In addition, LW% has never been measured on these cores. Its automatic determination by image analysis seems to be too hazardous because of possible errors related to wood defects and due to the quantity of images to validate. Tree- and plot-scale attributes were measured on field according to provincial standards and procedures.

Tree-level models were developed for BD, MOE, MFA, and FL using linear mixed regressions, and stepwise variable selection, on the calibration set (PROC MIXED, SAS 9.3, SAS Institute Inc., Cary, North Carolina, USA). The plot effect was considered as a random effect and its contribution to the variance was estimated. Three types of models were assessed. “DBH (diameter at breast height) models” were performed using only DBH class (DBHcl) and the ratio of DBH class to quadratic mean site diameter (DBHrel). “Core models” were then assessed using DBH, tree height (TH), the ratio of tree height to DBH (HD), AGE, and RW. Finally, “Core+ models” were developed by adding RGB colors and LW% to previous variables. The same plot-level explanatory variables were used in all models: species composition, basal area (BA), slope, exposition, and a Shannon index calculated on the DBH distribution. A full leave-one-out cross-validation procedure was applied in all models.

The calibration performance was assessed using the marginal (R^2c) and the conditional pseudo- R^2 (R^2cc), and the root mean square error (RMSEc). The calibration models were then tested on the validation set. The models were compared using the pseudo-R^2 (R^2v), and the root mean square error (RMSEv) validation statistics.

Stand-level models were developed for mapping purposes, so only spatially comprehensive variables were used as explanatory variables. Same geographic, climate and photo-interpreted vegetation attributes were used in both approaches (Table 1.2). Data of annual climate variables, elevation (Z) and slope were estimated, for the centroid of the polygon, using "BioSIM 10" (Régnière et al. 2014). This software, developed by Natural Resources Canada, generates climate data by simulation models using regional air temperature and precipitation interpolated from nearby weather stations, adjusted for elevation and location differentials with regional gradients. Stand-level models were developed for BD, MOE, MFA, and FL using multi-linear regressions, and stepwise variable selection (PROC GLMSELECT, SAS 9.3, SAS Institute Inc., Cary, North Carolina, USA). These models were developed with the average plot values of the calibration set for the direct approach (54 plots), and with the average plot values of the inventory set, predicted from the tree-level models, for the two-stage approach (3350 plots) (Figure 1.2). A full leave-one-out cross-validation procedure was applied in all models. The calibration performance was assessed using the pseudo-R^2 (R^2c), and the root mean square error (RMSEc). The stand-level models of both approaches were then tested on the validation set (28 plots). The models were compared using validation statistics: the pseudo-R^2 (R^2v), and the root mean square error (RMSEv).

Table 1.2 Descriptive statistics of core-, tree-, plot-, and stand-scale attributes for calibration, validation and inventory sets.

Attributes	Abbreviation	Calibration set				Validation set				Inventory set			
		Mean	S.D.	Min.	Max.	Mean	S.D.	Min.	Max.	Mean	S.D.	Min.	Max.
Stand-level geography													
Latitude (m, NAD 1983 Quebec Lambert)	X	−178,249	260,437	−603,185	528,518	−131,052	232,724	−486,027	121,322	−147,654	264,926	−793,903	482,021
Longitude (m, NAD 1983 Quebec Lambert)	Y	734,877	59,385	566,656	810,728	737,488	58,487	599,898	801,969	724,820	70,751	542,079	884,384
Elevation (m)	Z	441	105	134	669	459	72	321	612	463	135	0	870
Slope (%)	SLOPE	9%	8%	0%	34%	12%	9%	0%	34%	9%	10%	0%	37%
Stand-level climate													
Number of degree-days for T > 5 °C (°C_day)	°CDAY	1023	115	823	1329	1003	110	871	1234	1024	123	720	1408
Annual mean temperature (°C)	TEMP	−1.1	0.8	−2.5	0.8	−1.2	0.5	−1.9	−0.1	−1.0	0.9	−3.7	1.2
Annual precipitation (mm)	TPRECI	379	43	302	475	395	43	329	477	379	51	248	538
Precipitation from June to August (mm)	UPRECI	321	19	280	362	324	15	284	346	327	26	259	393
Annual snow (mm)	SNOW	986	47	902	1094	1004	45	930	1083	1000	59	819	1201
Stand-level vegetation													
Black spruce composition (% of cover)	BS%	76%	26%	10%	100%	81%	26%	33%	100%	86%	23%	10%	100%
Height class (m)	HTcl	12	3	7	17	11	3	7	17	11	3	7	22
Age class (year)	AGEcl	88	22	50	120	87	22	50	120	101	27	50	120
Canopy cover class (%)	CANcl	46%	9%	41%	61%	45%	8%	41%	61%	40%	13%	25%	81%
Plot-level vegetation													
Basal area (m^2/ha)	BA	32.1	9.6	13.1	56.3	31.8	10.3	13.2	50.6	20.7	8.3	1.3	59.1
Black spruce composition (% of basal area)	BS%	69%	26%	11%	100%	77%	22%	32%	100%	84%	18%	3%	100%
Balsam fir composition (% of basal area)	FIR%	13%	21%	0%	88%	9%	17%	0%	66%	11%	16%	0%	86%
Tree-level attributes													
Diameter at breast height in 2-cm class	DBHcl	17.3	3.9	10.0	30.0	17.5	3.9	10.0	30.0	17.6	4.6	10.0	38.0
Ratio of DBHcl to plot's quadratic mean diameter	DBHrel	1.2	0.2	0.8	1.7	1.2	0.2	0.8	1.7	1.1	0.2	0.5	2.2
Diameter at breast height (mm)	DBH	174	39	99	291	177	38	99	289	175	45	91	378
Tree height (m)	TH	14.5	2.7	9.2	22.3	15.0	2.9	8.5	22.1	14.1	3.2	6.1	28.1
Slenderness, ratio of tree height to DBH (m/cm)	HD	0.85	0.10	0.57	1.12	0.85	0.10	0.65	1.11	0.82	0.14	0.40	1.50
Core-level attributes													
Age at 1 m above ground (year)	AGE	82.9	23.2	41.0	140.0	82.8	21.5	48.0	175.0	118.9	49.0	12.0	243.0
Ring width (mm)[a]	RW	1.2	0.4	0.3	2.4	1.2	0.3	0.4	1.9	0.9	0.4	0.1	6.7
Latewood proportion (%)[a]	LW%	23%	5%	14%	42%	23%	5%	13%	37%	–	–	–	–
Basic wood density (kg/m^3)[a]	BD	421.7	34.3	321.3	507.1	424.2	32.4	336.9	491.7	–	–	–	–
Modulus of elasticity (GPa)[a]	MOE	12.8	2.3	5.6	18.3	12.9	2.3	5.9	18.6	–	–	–	–
Microfibril angle (°)[a]	MFA	15.8	3.9	8.9	36.1	15.5	3.6	9.9	27.9	–	–	–	–
Mature fiber length (mm)[b]	FL	3.01	0.23	2.19	3.63	3.00	0.24	2.13	3.59	–	–	–	–

[a] Average value calculated on the 50 first rings.
[b] Average value calculated on the rings 51 years and older.

Results

Influence of ecological conditions

Table 1.3 summarizes the statistics of linear mixed regressions applied on BD, MOE, MFA and FL. Bioclimatic subdomain and its interaction with potential vegetation had no significant effect on black spruce wood properties when potential vegetation was included in the models. Black spruce growing in RE2 vegetation produced a significantly denser wood (433.7 kg/m^3) with better mechanical properties (13.4 GPa for MOE, and 14.9° for MFA) and longer mature fibers (3.05 mm) compared with trees growing in RS2 vegetation (417.3 kg/m^3, 11.4 GPa, 17.8°, 2.89 mm). Soil physical feature was only significant for BD. Black spruce growing in imperfectly drained soils thus produced a significantly denser wood (RE25: 437.3 kg/m^3) compared with trees growing in well-drained soils (RE22 and RS22: 414.3 kg/m^3, and RE21: 420.2 kg/m^3). Wood growing in rapidly to well-drained soils (RE20) was not significantly different from other ecosites in BD. Model performance was improved by including a random plot effect as illustrated by the observed differences between conditional and marginal pseudo-R^2 for BD (59% vs. 23%), MOE (44% vs. 21%), MFA (34% vs. 12%) and FL (54% vs. 6%). Consequently, wood properties were also influenced substantially by local growth conditions, different from those explained by the ecological land classification.

Figure 1.3 presents the pith-to-bark patterns of distribution for RW, BD, MOE, and MFA by potential vegetation (RE2 and RS2). The obtained patterns were consistent with those observed and discussed for black spruce in the literature (Alteyrac et al. 2006, Pokharel et al. 2014, St-Germain and Krause 2008, Xiang et al. 2014). RW increases first very rapidly for approximately the first ten rings in both potential vegetation, and then decreases gradually with age. RW is significantly higher for trees growing in RS2 vegetation for approximately rings 30–80. Both curves become closer thereafter. BD decreases very rapidly in the first 15–20 rings, and gradually increases thereafter with age. BD is significantly higher in RE2 vegetation for rings 20–80. Both curves become closer after ring 80. MOE continuously increases from pith to bark with a rate that decreases with age. This rate is faster in RE2 vegetation for rings 1–25. MOE is significantly higher in RE2 vegetation for rings 10–100. However, both curves also become closer thereafter. MFA continuously decreases from pith to bark with a rate that decreases with age, presenting a typical inverted J shape as described by Giroud et al. (2015). MFA is significantly higher in RS2 vegetation for rings 1–35 and then both curves became closer thereafter.

Table 1.3 Summary of statistics for linear mixed regression models applied to wood properties. Values within the column within the same letter are not significantly different.

	Basic density (kg/m^3)[a]		Modulus of elasticity (GPa)[a]		Microfibril angle (°)[a]		Mature fiber length (mm)[b]	
Fixed effects	F value	Pr > F	F value	Pr > F	F value	Pr > F	F value	Pr > F
Bioclimatic subdomain	0.4	0.5192	2.4	0.1230	1.4	0.2375	0.1	0.7308
Potential vegetation	5.2	0.0252	23.7	<0.0001	18.3	<0.0001	7.5	0.0077
Interaction between bioclimatic domain and potential vegetation	1.0	0.3303	0.1	0.7638	0.4	0.5453	0.0	0.9553
Soil physical feature	3.7	0.0154	0.2	0.8849	1.2	0.3186	0.9	0.4439
Adjusted marginal pseudo-R^2	23%		21%		12%		6%	
Adjusted conditional pseudo-R^2	59%		44%		34%		54%	
Least squares means of potential vegetation	Mean (S.D.)		Mean (S.D.)		Mean (S.D.)		Mean (S.D.)	
Black Spruce – moss or ericaceous (RE2)	433.7a(3.8)		13.4a(0.2)		14.9a(0.3)		3.05a(0.03)	
Balsam Fir – black Spruce (RS2)	417.3b(6.9)		11.4b(0.4)		17.8b(0.7)		2.89b(0.06)	
Least squares means of soil physical feature	Mean (S.D.)		Mean (S.D.)		Mean (S.D.)		Mean (S.D.)	
0 (RE20)	430.2ab(12.3)		12.1a(0.7)		16.3a(1.2)		2.99a(0.10)	
1 (RE21)	420.2b(7.1)		12.4a(0.4)		16.1a(0.7)		2.94a(0.06)	
2 (RS22,RE22)	414.3b(3.7)		12.5a(0.2)		15.9a(0.3)		3.02a(0.03)	
5 (RE25)	437.3a(6.3)		12.7a(0.3)		17.1a(0.6)		2.93a(0.05)	

[a] Average value calculated on the 50 first rings (n = 409 trees).
[b] Average value calculated on the rings 51 years and older (n = 313 trees).

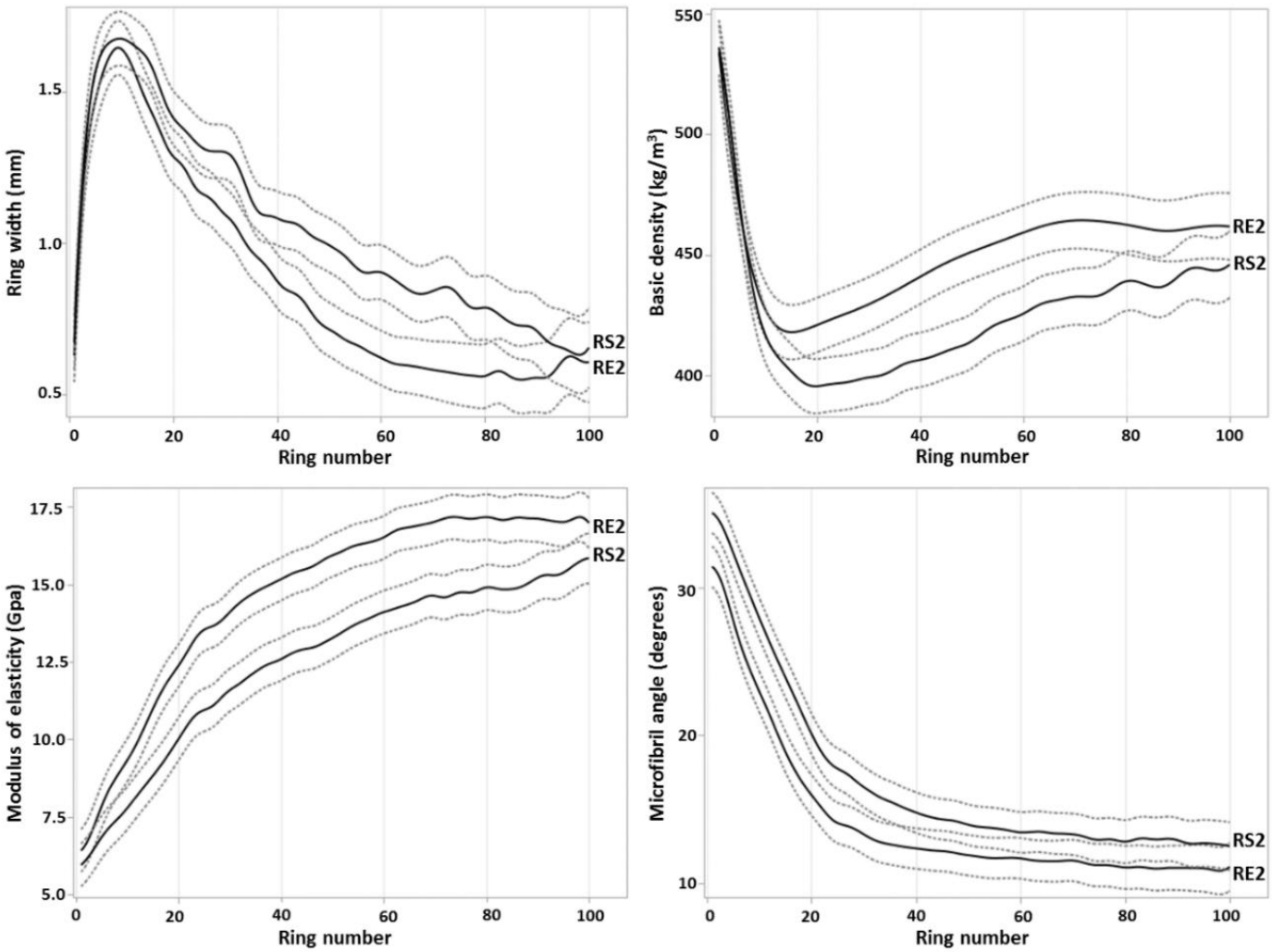

Figure 1.3 Pith-to-bark patterns of distribution for ring width (top-left panel), basic density (top-right panel), modulus of elasticity (bottom-left panel), and microfibril angle (bottom-right panel) by potential vegetation (RE2: "black Spruce – moss or ericaceous"; RE2: "balsam Fir – black Spruce"). The confidence intervals are shown in dashed lines.

Tree-level modeling

Table 1.4 summarizes the calibration and validation statistics for tree-level linear mixed models applied on wood properties. Better performances were obtained with “core” or “core+” models and the lowest with “DBH” models. The conditional pseudo-R^2 (R^2cc) were generally slightly higher than the marginal pseudo-R^2 (R^2c), but the improvement in performance by adding a random plot effect was minor in all calibrations, suggesting that the total variance was mostly explained by the fixed effects. The results are described in detail according to the group of explanatory variables.

The calibration statistics (R^2c (RMSEc)) of “DBH” models were 35% (27.0 kg/m^3), 21% (2.13 GPa), 14% (2.76°) and 18% (0.21 mm) for BD, MOE, MFA and FL, respectively. Tree-level attributes (DBHcl or DBHrel) accounted for 63%, 31%, and 42% of the variation that was explained by the model for BD, MOE, and FL, respectively. Tree-level attributes were not significant for the MFA model. The signs of parameter coefficients for DBH variables were negative for BD and MOE, and positive for FL. The plot-level variance component was essentially explained by species composition. Black spruce composition (BS%) accounted for 37% of the explained variation in BD with a positive coefficient. Balsam fir composition (FIR%) accounted for 70%, 100%, and 58% of the explained variation in MOE, MFA, and FL, respectively. The parameter coefficient was negative for MOE and FL, and positive for MFA. The validation statistics (R^2v (RMSEv)) were similar to calibration statistics for BD (33% (26.4 kg/m^3)) and MOE (19% (2.15 GPa)). The validation statistics dropped off from 14% (2.76°) to 1% (2.80°) for MFA, and from 18% (0.21 mm) to 10% (0.23 mm) for FL. The “DBH” model failed to predict MFA values using an independent set.

The performance of tree-level models was improved by adding RW, TH and HD as explanatory variables. The calibration statistics (R^2c (RMSEc)) of “core” models were 46% (24.7 kg/m^3), 26% (2.06 GPa), 21% (2.65°) and 23% (0.20 mm) for BD, MOE, MFA and FL, respectively. HD accounted for 38% and 20% of the explained variation in BD and MOE, with a positive coefficient in both cases. TH accounted for 8% and 19% of the explained variation in MFA and FL. Its coefficient was negative for MFA and positive for FL. RW accounted for 32%, 39%, 32% and 27% of the variation that was explained by the model for BD, MOE, MFA, and FL, respectively. Its coefficient was negative for BD and MOE and positive for MFA and FL. Finally, the plot-level variance component was essentially explained by a species composition similar to what was observed for “DBH” models. The validation statistics (R^2v (RMSEv)) were similar to calibration statistics for BD (46% (23.7 kg/m^3)), MOE (31% (1.98 GPa)) and MFA (17% (2.56°)), and higher for FL (43% (0.19 mm)).

Table 1.4 Summary of calibration and validation statistics for tree-level linear mixed models applied to wood properties. Signs of parameter coefficients and percentages of total variance explained by the models are illustrated for significant core-, tree- and plot-scale explanatory variables. For statistical purposes, 54 sites were randomly chosen for a calibration set (268 samples) and 28 others for an independent validation set (141 samples). Fiber length data were only available in 53 calibration plots (209 trees) and 26 validation plots (104 samples).

Wood property	Model	Calibration set			Validation set		Core-level attributes					Tree-level attributes				Plot-level attributes		
		R^2_{cc}	R^2_c	$RMSE_c$	R^2_v	$RMSE_v$	RW	LW%	GREEN	BLUE	Bl/Rd	DBHcl	DBHrel	TH	HD	BA	BS%	FIR%
Basic density (kg/m^3)	DBH	0.42	0.35	27.0	0.33	26.4						– 63%					+ 37%	
	Core	0.48	0.46	24.7	0.46	23.7	– 32%								+ 38%	– 17%	+ 13%	
	Core+	0.75	0.69	18.8	0.59	20.6		+ 74%		– 19%						– 7%		
Modulus of elasticity (GPa)	DBH	0.28	0.21	2.13	0.19	2.15							– 31%					– 70%
	Core	0.31	0.26	2.06	0.31	1.98	– 39%								+ 20%			– 40%
	Core+	0.37	0.35	1.93	0.36	1.91		+ 28%	+ 8%		– 41%				+ 10%			– 13%
Microfibril angle (°)	DBH	0.16	0.14	2.76	0.01	2.80												+ 100%
	Core	n.s.	0.21	2.65	0.17	2.56	+ 32%							– 8%			+ 11%	+ 48%
	Core+	n.s.	0.23	2.62	0.14	2.61	+ 28%				+ 21%						+ 11%	+ 40%
Mature fiber length (mm)	DBH	0.32	0.18	0.21	0.10	0.23						+ 42%						– 58%
	Core	0.32	0.23	0.20	0.43	0.19	+ 27%							+ 19%				– 54%
	Core+	0.34	0.24	0.20	0.10	0.23	+ 46%				– 11%							– 42%

R^2cc: adjusted conditional pseudo-R^2 for calibration set; R^2c: adjusted marginal pseudo-R^2 for calibration set; RMSEc: root mean square error for calibration set; R^2v: adjusted pseudo-R^2 for validation set; RMSEv: root mean square error for validation set; n.s.: not significant; GREEN: average value of green intensity in wood sample; BLUE: average value of blue intensity in wood sample; Bl/Rd: ratio of blue to red modes in wood sample.

The performance of tree-level models was even more improved by adding LW% and RGB colors to previous explanatory variables. The calibration statistics (R^2c (RMSEc)) of "core+" models were 69% (18.8 kg/m^3), 35% (1.93 GPa), 23% (2.62°) and 24% (0.20 mm) for BD, MOE, MFA and FL, respectively. Compared with "core" models, the explained variance by core- and tree-level attributes was higher, with 89%, 87%, 49% and 57% for BD, MOE, MFA, and FL, respectively. LW% accounted for 68% and 28% of the variation that was explained by the model for BD and MOE, respectively, with positive coefficients in both cases. BD was thus highly and positively correlated to LW%. Color information accounted for 19%, 49%, 21% and 11% of the explained variation in BD, MOE, MFA and FL, respectively. MOE was highly and negatively correlated to a color combination (ratio of blue mode to red mode). Plot-level variance component was low, except for MFA and FL, for which the species composition represented 51% and 42% of the explained variation, respectively. The validation statistics (R^2v (RMSEv)) were similar to calibration statistics for MOE (36% (1.91 GPa)), and lower for BD (59% (20.6 kg/m^3)), MFA (14% (2.61°)) and FL (10% (0.23 mm)).

Finally, the "core" models were chosen to predict the black spruce wood properties of the 10,098 trees in the inventory set. The "core+" models were not retained since LW% and RGB colors were not available for the inventory samples. Given its performance, the "core+" model would have been particularly interesting to investigate for the spatial variation of black spruce wood density.

Stand-level modeling

Table 1.5 summarizes the calibration and validation statistics for stand-level linear models applied to wood properties. According to the validation statistics (R^2v (RMSEv)), the best performances were obtained with the two-stage approach compared with the direct approach for BD (42 vs. 27%), MOE (51 vs. 17%), and MFA (34 vs. 9%). Similar performance was obtained for FL (16 vs. 16%). The proportion of the explained variance by vegetation attributes were higher in the two-stage modeling approach compared with the direct approach for BD (76 vs. 63%), MFA (99 vs. 71%) and FL (99 vs. 31%), except for MOE (75 vs. 100%). Inversely, the proportion of the explained variance by geographic and climate attributes were lower in the two-stage modeling approach compared with the direct approach for BD (24 vs. 37%), MFA (1 vs. 29%) and FL (1 vs. 69%), except for MOE (25 vs. 0%). The most important predictor variables were AGEcl, HTcl, and BS% in the two-stage modeling approach, and BS%, potential vegetation (PVEG), slope and number of degree-days (°CDAY), in the direct modeling approach.

Based on validation performance, the two-stage modeling approach was chosen for its better ability to predict the black spruce wood properties across the managed boreal forest of Quebec. This approach was applied to 61,550 photo-interpreted stands in the 70-year-old age class corresponding to the study area and selected ecosites (Figure 1.4). Using these stand-level estimates, significant differences in wood properties between the groups of regions of the ecological land classification were calculated (Table 1.6). Ecological region is defined as an area characterized by the composition and dynamics of the vegetation growing on mesic sites, and by the distribution of ecological types within the landscape. The regions are commonly grouped according to their resemblance (Blouin and Berger 2004, Blouin and Berger 2005, Morneau and Landry 2007, Morneau and Landry 2010a, Morneau and Landry 2010b). It is obvious there is a longitudinal gradient, with a significant and continuous increase in BD, MOE and FL from eastern to western regions, and inversely for MFA. The highest mean values in BD (450 kg/m^3), MOE (14.5 GPa), and FL (3.0 mm) were found in the most western regions of the "black Spruce – moss" bioclimatic domain (6a, Plaine du lac Matagami; 6b, Plaine de la baie de Rupert) (Table 1.6). Inversely, the lowest mean values in BD (414 kg/m^3), MOE (11.8 GPa), and FL (2.8 mm), and the highest mean value in MFA (16.1°), were found in the most eastern regions (6m, Collines de Havre-Saint-Pierre et de Blanc-Sablon; 6n, Collines du lac Musquaro).

Table 1.5 Summary of calibration and validation statistics for stand-level linear models applied to wood properties. Signs of parameter coefficients and percentages of total variance explained by the models are illustrated for significant explanatory variables. Signs of coefficients are not shown for class variables. HTcl, AGEcl, CANcl were converted into continuous variables.

Wood property	Model	Calibration set			Validation set			Photo-interpreted vegetation								Geography			Climate					
		n	R^2_c	RMSEc	n	R^2_v	$RMSE_v$	Species	BS%	HTcl	STRU	AGEcl	CANcl	PVEG	ECO	X	Z	SLOPE	°CDAY	TEMP	TPRECI	UPRECI	SNOW
Basic density	Direct	54	0.46	14.7	28	0.27	21.1		+ 40%	– 23%								– 24%				– 13%	
(kg/m^3)	Two-stage	3350	0.47	8.9	28	0.42	18.7		+ 22%	– 5%	3%	+ 44%	– 1%		1%		– 6%		+ 6%	– 10%			– 2%
Modulus of	Direct	54	0.35	0.91	28	0.17	1.58		+ 41%					59%									
elasticity (GPa)	Two-stage	3350	0.57	0.52	28	0.51	1.21	10%		– 1%	4%	+ 56%	– 3%		1%		– 6%		+ 5%	– 10%			– 4%
Microfibril	Direct	54	0.28	1.05	28	0.09	1.80				26%			45%							+ 29%		
angle (°)	Two-stage	3350	0.63	0.60	28	0.34	1.53	8%		– 6%	3%	– 81%			1%	+ 1%							
Mature fiber	Direct	53	0.14	0.09	26	0.16	0.16							31%				+ 27%	+ 42%				
length (mm)	Two-stage	3350	0.63	0.06	26	0.16	0.16		+ 9%	+ 47%	1%	– 40%			2%		– 1%						

R^2c: adjusted pseudo-R^2 for calibration set; RMSEc: root mean square error for calibration set; R^2v: adjusted pseudo-R^2 for validation set; RMSEv: root mean square error for validation set; Species: photo-interpreted species group; STRU: structure stand (irregular or regular); DRAIcl: soil drainage class; PVEG: potential vegetation (RE2 or RS2); ECO: ecosite (RE20, RE21, RE22, RE25, RS22).

Table 1.6 Least squares means of stand-level coefficients of wood properties by group of ecological regions with their corresponding standard errors (in parentheses). Values within the column within the same letter are not significantly different. Only 70-year-old stands were used (n = 61,550 stands).

Group of ecological regions	Basic density (kg/m^3)	Modulus of elasticity (GPa)	Microfibril angle (°)	Mature fiber length (mm)
6a – Plaine du lac Matagami 6b – Plaine de la baie de Rupert	449.76a(0.11)	14.519a(0.007)	14.028f(0.009)	3.024a(0.001)
6c – Plaine du lac Opémisca 6d – Coteaux du lac Assinica 6e – Coteaux de la rivière Nestaocano 6f – Coteaux du lac Mistassini 6g – Coteaux du lac Manouane	442.16b(0.04)	14.210b(0.003)	13.838g(0.003)	3.009b(0.000)
6h – Collines du lac Péribonka 6i – Hautes collines du réservoir aux Outardes	435.17d(0.06)	13.612e(0.004)	14.448c(0.005)	2.949c(0.001)
6j – Hautes collines du lac Cacaoui	427.27e(0.14)	13.068f(0.009)	14.912b(0.011)	2.906e(0.001)
6k – Coteaux de la rivière à la Croix et du lac au Griffon 6l – Collines du lac Grandmesnil	437.49c(0.13)	13.846c(0.009)	14.273e(0.011)	2.935d(0.001)
6m – Collines de Havre-Saint-Pierre et de Blanc-Sablon 6n – Collines du lac Musquaro	413.51f(0.46)	11.814g(0.030)	16.087a(0.037)	2.848f(0.003)
6o – Coteaux du lac Fonteneau 6p – Coteaux du lac Caopacho 6q – Coteaux des lacs Matonipi et Jonquet 6r – Massif des monts Groulx	437.36c(0.31)	13.766d(0.021)	14.370d(0.025)	2.932d(0.002)

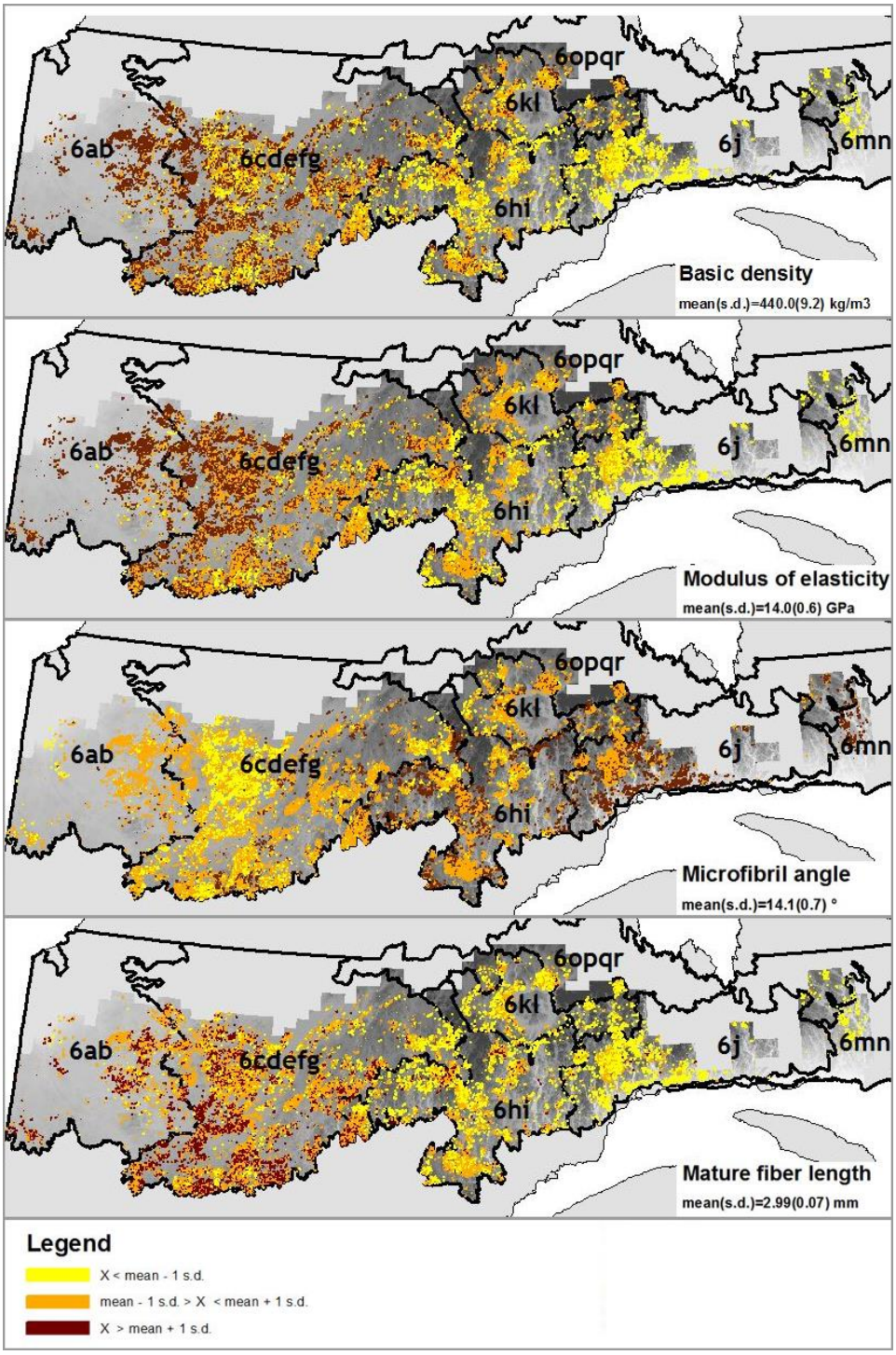

Figure 1.4 Spatial distribution of black spruce wood properties across the black Spruce – moss bioclimatic domain: basic density (first panel from the top), modulus of elasticity (second panel), microfibril angle (third panel) and mature fiber length (fourth panel). Only the estimates of 70-year-old stands corresponding to studied ecosites (RE20, RE21, RE22, RE25, RS22) are shown (n = 61,550 stands). The boundaries of ecological regions are illustrated by black lines.

Discussion

The influence of ecological conditions and local growth conditions on wood properties was clearly demonstrated. First, all clear wood properties were significantly different between sites characterized as having different potential vegetation. Trees growing in RE2 potential vegetation thus had a denser wood with better mechanical characteristics than those growing in RS2 vegetation, where the constraints on growth imposed by site conditions are usually less severe. BD was also influenced by drainage conditions since trees growing in imperfectly drained soils (RE25) produced a denser wood. In ecological field guides, the site relative richness of RS2 vegetation is classified as medium, and that of RE2 vegetation as poor (Blouin and Berger 2004, Blouin and Berger 2005, Morneau and Landry 2007, Morneau and Landry 2010a, Morneau and Landry 2010b). This indicator of soil fertility is based on humus classification, pH, presence or absence of seepage, length of the back slope and plant diversity. Based on field and ring data, RS2 and RE2 vegetations had similar ages (87 vs. 81 years), but different RW (1.3 vs. 1.1 mm) and TH (16.0 vs. 13.9 m). Laflèche et al. (2013) found that the RS22 site productivity in the "black Spruce – moss" bioclimatic domain was similar to or higher than that of other studied ecosites as follows RS22 $\geqslant$ (RE22, RE21) $\geqslant$ (RE20, RE25). Torquato et al. (2013) suggested also that a higher incidence of mild compression wood in black spruce trees of layer origin may explain lower mechanical properties (MOE, MOR). However, this hypothesis remains to be validated. BD and MOE were negatively related to radial growth (Table 1.4). These observations are consistent with the literature. Indeed, inverse relationships with radial growth have frequently been reported in black spruce for wood density (Groot and Luther 2015, St-Germain and Krause 2008), and mechanical properties (Liu et al. 2007, Zhang and Morgenstern 1995).

The differences in BD and mechanical properties between potential vegetations were related to site richness, but also to juvenility period. The first growth rings from the pith form the juvenile wood (Panshin and Zeeuw 1980). Its formation is controlled by the action of phytohormones and the aging process. The mechanical properties of juvenile wood are weaker and vary greatly, unlike those of mature wood. The transition age from juvenile to mature wood can be determined using different wood properties and mathematical methods. Using the same wood samples as those used in the present study, Giroud et al. (2015) estimated the transition age in applying two-segment linear regressions on MFA profiles. Based on the visual examination of the pith-to-bark patterns of distribution for MFA, the transition from juvenile to mature wood takes a few more years in RS2 vegetation (Figure 1.3). In addition, the rapid decrease in BD close to the pith takes a few more years in RS2 vegetation suggesting also a longer juvenility period. More intense self-pruning caused by a higher stand density in the first stages of stand development may explain a shorter juvenility period as observed for RE2 vegetation. Furthermore, higher values in BD and mechanical properties were mainly explained by a lower radial growth in RE2 vegetation for approximately rings 20–80. Finally, genetic control may also influence the transition age from juvenile to mature wood and the values at maturity in wood fiber properties.

Trees growing in RE2 potential vegetation have longer mature fibers than those growing in RS2 vegetation. There is no clear trend in the literature on the relationship between FL, growth rate and site conditions (Townshend et al. 2015, Yang and Hazenberg 1993). However, its pith-to-bark pattern of distribution is well known. FL increases with cambial age and then reaches a plateau at maturity. Townshend et al. (2015) found that longer fiber length, averaged on the first 50 years of growth, was associated with more productive ecosites that supported faster growth in black spruce trees from the boreal forest of northeastern Ontario. In the present study, mature fiber length was also positively related to radial growth as shown in Table 1.4. However, mature fiber length was also strongly and negatively influenced by the proportion of balsam fir in the stand.

The performance of tree-level models was determinant for the success of the two-stage modeling approach. The availability of ring measurements at a large scale explains the success of this approach. The performance of tree-level models could be improved for BD and MOE, by including LW% and wood color as explanatory variables. Indeed, BD was highly and positively correlated to LW% and MOE was also highly and negatively correlated to a color combination (ratio of blue mode to red mode). The close relationship between BD and LW% is well known (Pokharel et al. 2014). However, the positive relationship between MOE and wood color does not seem to have been investigated. The variation in natural wood color may reflect differences in chemical composition and indirectly in mechanical properties. LW% and color information can easily be measured using image and ring analysis software. Another way to improve substantially the precision of tree-level estimates could be to scan the increment cores by near infrared spectroscopy (NIRS), a cost and time effective method of wood characterization. NIR light interacts with material, and the spectral response can be interpreted in real time using multivariate analysis in order to predict wood properties. NIRS was recently successfully assessed on black spruce wood (Giroud et al. 2015, Xu et al. 2011). Using the same wood samples as those used in the present study, Giroud et al. (2015) obtained the following validation statistics (R^2c (RMSEc)): 85% (5.1 kg/m^3), 88% (1.14 GPa) and 79% (1.90°) for BD, MOE and MFA, respectively.

Compared with the direct modeling approach, the two-stage approach helped us to improve the precision of stand-level estimates. Consequently, the tree-level relationships were strong enough to correctly estimate the spatial variation in wood properties using the field and ring data of the inventory plots corresponding to the study area and selected ecosites. Stand-level models performed better than tree-level models. Mäkinen et al. (2007) suggested that it is much easier to predict between-stand variation than between-tree variation in wood properties because the genetic variation averaged over a stand is considerably lower than the genetic variation between trees. In comparison with models developed for black spruce wood properties in Newfoundland (Lessard et al. 2014, Luther et al. 2014), similar R^2 values but substantially lower RMSE were obtained despite a lower number of trees sampled by plot (4–6 vs. 10 trees/plot). For example, RMSE values, estimated by leave-one-out cross-validation, and related to BD stand-level estimates, were 8.9, 30.6, and 33.9 kg/m^3 for the current

study, Lessard et al. (2014) and Luther et al. (2014), respectively. This higher precision may be explained by an ecosite-based sampling that allowed us to better control variance, and partly, by a lower range of BD.

Ecosite, and particularly potential vegetation, are good indicators for a wood quality differentiation as suggested by Pokharel et al. (2014) and Townshend et al. (2015). Spatial variation in wood fiber properties shows close similarities with the natural distribution of both potential vegetations across the study area (Figure 1.4 vs. Figure 1.1). An east-west gradient in the black spruce clear wood properties was thus revealed. Black spruce wood growing in western ecological regions had longer mature fibers, a denser wood with better mechanical properties for the 70-year-old age class. Wood cell formation may be influenced by the maritime influence and the abundant precipitation of eastern regions. However, climate and local growth conditions are closely related and it makes it difficult to clearly bring out the effect of climate in the current study. Bioclimatic subdomain was not significant concerning wood properties when tested with potential vegetation and ecosite, which were sampled in both subdomains. Furthermore, spatial variation in wood properties was mainly explained by vegetation attributes and very little directly by climate attributes, using the two-stage modeling approach. This east-west gradient is possibly a by-product of the change in relative proportions of potential vegetations between both bioclimatic subdomains.

The spatial variation in wood properties was mainly explained by the variation in vegetation attributes, age class, black spruce proportion, and height class. These attributes were also important predictors for the spatial distribution of black spruce fiber properties in Newfoundland (Lessard et al. 2014). However, these attributes are not measured but are photo-interpreted. Furthermore, age class is partially derived from the height of codominant and dominant trees and from the stand structure. Recently, Luther et al. (2014) obtained a similar performance to predict stand-level estimates of black spruce and balsam fir wood properties using only LiDAR (light detection and ranging) metrics in comparison with models derived using geographic, climate and vegetation variables. A large-scale acquisition of airborne laser scanner data in Quebec may thus provide interesting metrics for wood fiber modeling and mapping.

Conclusion

An ecogeographic gradient in black spruce clear wood properties was revealed across the “black Spruce – moss” bioclimatic domain of the province of Quebec. The influence of ecological conditions was clearly demonstrated. All properties were significantly different between sites characterized as having different potential vegetation. Spatial variation in wood fiber properties showed close similarities with the natural distribution of both potential vegetations across the study area. The current study fills the knowledge gap in spatial variation of wood fiber properties for the study area. These results could rapidly find practical implications for decision making in forest management and wood allocation. Based on the results of the current study, conducting a provincial inventory on wood fiber properties is thus technically possible.

A two-stage modeling process is recommended to produce regional maps. Higher precision was indeed obtained using the extensive field and ring data collected by the provincial forest resources inventory. The two-stage modeling approach is an innovative way to address the high cost of measuring wood properties. However, the proposed method presents some limits. First, the two-stage approach requires strong relationships at the tree level. Although the performance of developed models was similar to other models in the literature, the part of unexplained variance was still too high. Secondly, the stand-level models were mainly built on photo-interpreted vegetation attributes, which leave too much room for subjective judgement despite improved tools. The combined use of NIRS wood estimates and LiDAR stand metrics would greatly enhance the proposed method. Finally, a two-stage modeling approach requires access to substantial datasets and modeling expertise. A direct modeling approach could be considered as a useful alternative if the data are not available to support a two-stage modeling.

Acknowledgements

This research was funded by the Fonds de Recherche du Québec - Nature et Technologies of the province of Quebec and the Ministère des Forêts, de la Faune, et des Parcs du Québec, Canada. The wood samples were provided by the Canadian Wood Fibre Centre, Canadian Forest Service, Natural Resources Canada. Special thanks to my MFFPQ colleague Vincent Laflèche for his valuable advice about ecology and to Martin Riopel, researcher at Université Laval, for statistical support and advice. We thank the two anonymous reviewers for their constructive comments, which helped us to improve the manuscript.

References

Alteyrac, J., Cloutier, A., and Zhang, S.Y. (2006). Characterization of juvenile wood to mature wood transition age in black spruce (Picea mariana (Mill.) B.S.P.) at different stand densities and sampling heights. Wood Sci. Technol. 40, 124–138.

Blouin, J., and Berger, J.-P. (2004). Guide de reconnaissance des types écologiques des régions écologiques 6c – Plaine du lac Opémisca, 6d – Coteaux du lac Assinica, 6e – Coteaux de la rivière Nestaocano, 6f – Coteaux du lac Mistassini et 6g – Coteaux du lac Manouane. Ministère des Ressources naturelles, de la Faune et des Parcs (provincial Department of Natural Resources, Wildlife and Parks). Quebec, Canada. 210 pp.

Blouin, J., and Berger, J.-P. (2005). Guide de reconnaissance des types écologiques de la région écologique 6a - Plaine du lac Matagami et 6b - Plaine de la baie de Rupert. Ministère des Ressources naturelles et de la Faune (provincial Department of Natural Resources and Wildlife). Quebec, Canada. 188 pp.

Briggs, D. (2010). Enhancing forest value productivity through fiber quality. J. For. 108, 174–182.

Chave, J., Coomes, D., Jansen, S., Lewis, S.L., Swenson, N.G., and Zanne, A.E. (2009). Towards a worldwide wood economics spectrum. Ecol. Lett. 12, 351–366.

Finto, A., Jordan, L., Schimleck, L.R., Clark, A., Souter, R.A., and Daniels, R.F. (2011). Regional variation in wood modulus of elasticity (stiffness) and modulus of rupture (strength) of planted loblolly pine in the United States. Can. J. For. Res. 41, 1522–1533.

Gauthier, S., Leduc, A., Harvey, B., Bergeron, Y., and Drapeau, P. (2001). Les perturbations naturelles et la diversité écosystémique. Nat. Can. 125, 1–35.

Giroud, G., Defo, M., Bégin, J., and Ung, C.-H. (2015). Application of near-infrared spectroscopy to determine the juvenile-mature wood transition in black spruce. For. Prod. J. 65, 129–138.

Groot, A., and Luther, J.E. (2015). Hierarchical analysis of black spruce and balsam fir wood density in Newfoundland. Can. J. For. Res. 45, 805–816.

Jessome, A.P. (2000). Strength and related properties of woods grown in Canada. Special Publication SP-514E. Forintek Canada Corp., Quebec, Canada. 37 pp.

Jordan, L., Clark, A., Schimleck, L.R., Hall, D.B., and Daniels, R.F. (2008). Regional variation in wood specific gravity of planted loblolly pine in the United States. Can. J. For. Res. 38, 698–710.

Laflèche, V., Bernier, S., Saucier, J.-P. and Gagné, C. (2013). Indices de qualité de station des principales essences commerciales en fonction des types écologiques du Quebec méridional. Ministère des Ressources naturelles (provincial Department of Natural Resources). Quebec, Canada. 115 pp.

Lenz, P., Deslauriers, M., Ung, C.-H., MacKay, J., and Beaulieu, J. (2014). What do ecological regions tell us about wood quality? A case study in eastern Canadian white spruce. Can. J. For. Res. 44, 1383–1393.

Lessard, E., Fournier, R.A., Luther, J.E., Mazerolle, M.J., and van Lier, O.R. (2014). Modeling wood fiber attributes using forest inventory and environmental data for Newfoundland's boreal forest. For. Ecol. Manag. 313, 307–318.

Liu, C., Zhang, S.Y., and Jiang, Z.H. (2007). Models for predicting lumber grade yield using tree characteristics in black spruce. For. Prod. J. 57, 60–67.

Luther, J.E., Skinner, R., Fournier, R.A., Lier, O.R. van, Bowers, W.W., Coté, J.-F., Hopkinson, C., and Moulton, T. (2014). Predicting wood quantity and quality attributes of balsam fir and black spruce using airborne laser scanner data. Forestry 87, 313–326.

Mäkinen, H., Jaakkola, T., Piispanen, R., and Saranpää, P. (2007). Predicting wood and tracheid properties of Norway spruce. For. Ecol. Manag. 241, 175–188.

Malhi, Y., Wood, D., Baker, T.R., Wright, J., Phillips, O.L., Cochrane, T., Meir, P., Chave, J., Almeida, S., Arroyo, L., et al. (2006). The regional variation of aboveground live biomass in old-growth Amazonian forests. Glob. Change Biol. 12, 1107–1138.

Morneau, C., and Landry, Y. (2007). Guide de reconnaissance des types écologiques des régions écologiques 6h - Collines du lac Péribonka et 6i - Hautes collines du réservoir aux Outardes. Ministère des Ressources naturelles et de la Faune (provincial Department of Natural Resources and Wildlife). Quebec, Canada. 101 pp.

Morneau, C., and Landry, Y. (2010a). Guide de reconnaissance des types écologiques de la région écologique 6j – Hautes collines du lac Cacaoui. Ministère des Ressources naturelles et de la Faune (provincial Department of Natural Resources and Wildlife). Quebec, Canada. 96 pp.

Morneau, C., and Landry, Y. (2010b). Guide de reconnaissance des types écologiques des régions écologiques 6k - Coteaux de la rivière à la Croix et du lac au Griffon et 6l - Collines du lac Grandmesnil. Ministère des Ressources naturelles et de la Faune (provincial Department of Natural Resources and Wildlife). Quebec, Canada. 196 pp.

Nakagawa, S., and Schielzeth, H. (2013). A general and simple method for obtaining R2 from generalized linear mixed-effects models. Methods Ecol. Evol. 4, 133–142.

Ngo, L., and Wand, M. (2004). Smoothing with mixed model software. J. Stat. Softw. 9, 1–54.

Panshin, A.J., and Zeeuw, C.D. (1980). Textbook of Wood Technology: Structure, Identification, Properties, and Uses of the Commercial Woods of the United States and Canada. 4th ed. McGraw-Hill, New York. 722 pp.

Pokharel, B., Dech, J.P., Groot, A., and Pitt, D. (2014). Ecosite-based predictive modeling of black spruce (Picea mariana) wood quality attributes in boreal Ontario. Can. J. For. Res. 44, 465–475.

Régnière, J., St-Amant, R., and Béchard, A. (2014). BioSIM 10 – User's manual. Natural Resources Canada, Canadian Forest Service, Laurentian Forestry Centre, Quebec, Canada. LAU-X-137E. 66 pp.

Robertson, G., Olson, J., Allen, P., Chan, B., and Seth, R. (1999). Measurement of fiber length, coarseness, and shape with the fiber quality analyzer. Tappi J. 82, 93–98.

Rossi, S., Cairo, E., Krause, C., and Deslauriers, A. (2015). Growth and basic wood properties of black spruce along an alti-latitudinal gradient in Quebec, Canada. Ann. For. Sci. 72, 77–87.

St-Germain, J.-L., and Krause, C. (2008). Latitudinal variation in tree-ring and wood cell characteristics of Picea mariana across the continuous boreal forest in Quebec. Can. J. For. Res. 38, 1397–1405.

Swenson, N.G., and Enquist, B.J. (2007). Ecological and evolutionary determinants of a key plant functional trait: Wood density and its community-wide variation across latitude and elevation. Am. J. Bot. 94, 451–459.

Torquato, L.P., Auty, D., Hernández, R.E., Duchesne, I., Pothier, D., and Achim, A. (2013). Black spruce trees from fire-origin stands have higher wood mechanical properties than those from older, irregular stands. Can. J. For. Res. 44, 118–127.

Townshend, E., Pokharel, B., Groot, A., Pitt, D., and Dech, J.P. (2015). Modeling wood fibre length in black spruce (Picea mariana (Mill.) BSP) based on ecological land classification. Forests 6, 3369–3394.

Tuominen, S., Holopainen, M., and Poso, S. (2006). Multiphase sampling. In Forest Inventory. Springer Netherlands. 235–252.

Van Leeuwen, M., Hilker, T., Coops, N.C., Frazer, G., Wulder, M.A., Newnham, G.J., and Culvenor, D.S. (2011). Assessment of standing wood and fiber quality using ground and airborne laser scanning: A review. For. Ecol. Manag. 261, 1467–1478.

Viereck, L.A., and Johnston, W.F. (1990). Picea mariana (Mill.) B.S.P.-Black spruce. In Silvics of North America: Volume 1. Conifers. USDA Forest Service, Washington, D.C. 227–237.

Watson, P., and Bradley, M. (2009). Canadian pulp fibre morphology: superiority and considerations for end use potential. For. Chron. 85, 401–408.

Xiang, W., Leitch, M., Auty, D., Duchateau, E., and Achim, A. (2014). Radial trends in black spruce wood density can show an age- and growth-related decline. Ann. For. Sci. 71, 603–615.

Xu, Q., Qin, M., Ni, Y., Defo, M., Dalpke, B., and Sherson, G. (2011). Predictions of wood density and module of elasticity of balsam fir (Abies balsamea) and black spruce (Picea mariana) from near infrared spectral analyses. Can. J. For. Res. 41, 352–358.

Yang, K.C., and Hazenberg, G. (1993). Impact of spacing on tracheid length, relative density, and growth rate of juvenile wood and mature wood in Picea mariana. Can. J. For. Res. 24, 996–1007.

Zhang, S.Y., and Koubaa, A. (2008). Softwoods of Eastern Canada. Their silvics, characteristics, manufacturing and end-uses. Special Publication SP-526E. FPInnovations. Quebec, Canada. 363 pages.

Zhang, S.Y., and Morgenstern, E. (1995). Genetic variation and inheritance of wood density in black spruce (Picea mariana) and its relationship with growth: implications for tree breeding. Wood Sci. Technol. 30, 63–75.

Chapitre 2. Application of near-Infrared spectroscopy to determine the juvenile–mature wood transition in black Spruce.

Résumé

Le potentiel de la spectroscopie proche infrarouge pour mesurer les propriétés du bois de l'épinette noire a été évalué. De bonnes et d'excellentes statistiques de calibration (R^2, rapport de la performance à l'écart) ont été obtenues pour la densité basale (0.85, 1.8), l'angle des microfibrilles (0.79, 2.2), et le module d'élasticité (0.88, 2.9). Une régression segmentée a également été appliquée au profil radial de l'angle des microfibrilles afin de déterminer l'âge de transition du bois juvénile au bois mature. Les valeurs obtenues avec SilviScan ont été comparées à celles obtenues par spectroscopie. L'âge moyen de transition (23 ans ± 7 ans) a été légèrement sous-estimé par spectroscopie proche infrarouge avec une erreur de prédiction moyenne de −2.2 ± 6.3 ans et des intervalles de confiance à 95% de −14.6 et 10.1. Ces résultats suggèrent que l'âge de transition peut également être prédit par spectroscopie proche infrarouge.

Abstract

The potential of near-infrared spectroscopy (NIRS) to determine the transition from juvenile to mature wood in black spruce (*Picea mariana* (Mill.) B. S. P.) was assessed. In total, 127 wood samples were harvested from 50 sites located across the black spruce-moss domain in the province of Québec, Canada. Mechanical wood properties were determined by SilviScan. NIR spectra were collected on the transverse face of the samples. Good to excellent calibration statistics (R^2, ratio of performance to deviation) were obtained for basic density (0.85, 1.8), microfibril angle (0.79, 2.2), and modulus of elasticity (0.88, 2.9). Two-segment linear regressions were applied to microfibril angle profiles to determine the transition age and then calculate the juvenile and mature wood properties. The values obtained using SilviScan data were compared with those obtained using NIRS predicted data. Using SilviScan data, the average transition age was 23 years, with a standard deviation of 7 years. The correlation was moderate for the transition age ($r = 0.592$, $P < 0.0001$), which was slightly underestimated by NIRS with a mean prediction error (and 95% limits of agreement) of -2.2 ± 6.3 years (-14.6/10.1). These results suggest that the transition age from juvenile to mature wood could be predicted by NIRS. This article makes some recommendations to improve method accuracy for operational use.

Introduction

Natural variation in black spruce (*Picea mariana* (Mill.) B. S. P.) wood properties is known, which is not the case for its spatial variation. There is presently no spatial information produced by the provincial forest inventory programs of Canada on fiber quality. This lack of knowledge is problematic for wood supplies. This knowledge could be integrated into decision support systems in order to improve and optimize forest management and the entire value chain (Briggs 2010). Black spruce is one of the main commercial species in the Canadian boreal forest (Viereck and Johnston 1990). Its principal commercial use is for high-quality pulp manufacturing. It is also largely used for lumber and high-value building products. Black spruce grows on a wide variety of sites, suggesting a potential spatial variation in wood properties. Lessard et al. (2014) recently demonstrated that it was possible to model and map wood properties at the landscape level for black spruce and balsam fir (*Abies balsamea*) in Newfoundland. In Québec, the provincial government is also planning to model and map wood properties of the main commercial species of the boreal forest by 2020. To this end, the present study aims to evaluate the potential of near-infrared spectroscopy (NIRS) to quickly and accurately characterize the fiber properties of wood samples.

NIRS is used in many industrial applications because of its numerous advantages. It is cost and time effective, relatively accurate, and nondestructive. The use of NIRS by the forest and forest products industries has been increasing over the past 20 years (Tsuchikawa 2007, Meder et al. 2010). During the last decade, a lot of efficient NIRS calibration models were built using SilviScan data (for example, see Schimleck et al. 2001, Jones et al. 2005). Today, NIRS seems to be the most economic method when dealing with thousands of wood samples. NIR light interacts with material, and the spectral response can be interpreted using multivariate analysis (Siesler et al. 2002). NIRS does not directly measure anatomical or physical properties of wood. It measures the absorption of NIR light by the sample. This absorption occurs when the NIR frequency is the same as the vibrational frequency of a molecular bond. The NIR signal is thus sensitive to changes in wood chemistry. Furthermore, the wood chemistry varies with age. For instance, the microfibril orientation in the S2 layer appears related to lignin content in normal wood with a decrease of microfibril angle (MFA) and lignin content from pith to bark (Via et al. 2009, Hein et al. 2010). These findings help give us a better understanding of how MFA can be predicted by NIRS. Xu et al. (2011) have successfully used NIRS data to predict wood density and modulus of elasticity based on SilviScan measurements for black spruce and balsam fir. However, they found that MFA was not well estimated by NIRS, unlike the results obtained with other species (Schimleck and Evans 2002, Jones et al. 2005, So et al. 2013). The potential of NIRS to predict the wood properties of increment cores has largely been demonstrated. Nevertheless, to our knowledge, the potential of NIRS to model MFA in order to automatically determine the transition from juvenile to mature wood has never been studied.

The first growth rings from the pith form the juvenile wood (Panshin and De Zeeuw 1980, Jozsa and Middleton 1994). Its formation is controlled by the action of phytohormones and the aging process. The transition from juvenile to mature wood occurs at a given time called transition age. The mechanical properties of mature wood are stronger and present very few variations, unlike those of juvenile wood. Juvenile wood is undesirable for many applications. Forest managers try to reduce its content by tree breeding and silvicultural treatments. There is no universally accepted definition of the transition age from juvenile to mature wood. It can be determined using different wood properties and different mathematical methods such as the threshold method, polynomial regression, segmented regression, or derivative function. These methods were assessed on different ring properties such as density, surface area, percentage of latewood, MFA, and tracheid length (Yang and Hazenberg 1994, Alteyrac et al. 2006, Clark et al. 2006). As shown by Alteyrac et al. (2006), the transition age varies according to wood property considered and the method used. In our study, MFA and linear segmented regression were used. The two-segment linear regression (TSLR) is one of the most widely used methods to determine the transition point. TSLR has often been applied on MFA profiles (Bhat et al. 2001, Alteyrac et al. 2006, Clark et al. 2006, Wang and Stewart 2012). Wang and Stewart (2012) assessed different forms of two-segmented regression (linear, quadratic, exponential, and constant) to estimate MFA transition point, but concluded that all combinations give essentially the same estimates from a practical viewpoint.

The MFA profile generally follows the same pattern from the pith to the bark which is linked to the cambium maturation process (or aging process) (Donaldson 2008). It decreases rapidly in the juvenile wood portion and remains more or less stable in the mature wood portion, unless compression wood is present. The MFA profile thus presents an inverted J-shaped pattern. However, the rate of decrease in MFA with age varied among species. In hardwoods, similar patterns occur, but with much less variation and much smaller MFAs in juvenile wood. MFA is influenced by environmental factors as shown by its increased values in compression wood, decreased values in tension wood, and often increased values following nutrient or water supplementation (Donaldson 2008). This typical inverted J shape was observed for MFA in black spruce (Alteyrac et al. 2006). Similar profiles were also observed for pine species (Schimleck and Evans 2002, Wang and Stewart 2012), eucalyptus (Evans et al. 2000), and teak (Bhat et al. 2001). MFA profiles show two interesting features in softwoods: a typical behavior in the presence of compression wood and a high variability from the pith to the bark. In a sample with no defect, any sudden increase in MFA can be attributed to compression wood (Barnett and Bonham 2004). Compression wood is formed under stress conditions. The presence of compression wood disturbs the MFA profile and makes it difficult to determine the transition point. However, it is easy to detect and remove the disruptions caused by the presence of compression wood in order to recover the normal pattern. Finally, MFA decreases greatly from the pith to the bark. The values are around three times lower in black spruce mature wood than in juvenile wood (Alteyrac et al. 2006). This characteristic should thus facilitate determination of the transition point by TSLR.

The aim of this study was to develop a quantitative, economic, and accurate method to determine the transition age from juvenile to mature wood in black spruce. The working hypothesis is that the transition age from juvenile to mature wood can be estimated by applying the TSLR method to MFA profiles predicted by NIRS. Once the transition age is known, it becomes possible to calculate the average properties for each wood type. This method could be easily integrated into a NIRS system to produce real-time estimates of transition age and juvenile-mature wood properties for an increment core. In this study, basic density (BD), MFA, and modulus of elasticity (MOE) were investigated in relation to juvenile and mature wood.

Materials and methods

Sample origin and preparation

In the 2000s, the Québec provincial government implemented a large-scale forest inventory program to develop site index and taper equations for the main commercial species. In total, 1,648 plots were sampled in the main ecological regions. About 14,000 trees were harvested and cut into disks for ring analysis. At the end of the program, thousands of disks were selected and kept frozen by the federal government for future research. For this study, 127 wood disks cut at breast height were selected. They were from 50 sites located in the black spruce-moss domain. The sites were chosen to take into account the ecological variability of the study area. The trees were between 45 and 148 years old. The 127 samples were cut in radial sticks of 17 by 10 mm (tangentially by longitudinally). NIRS measurement is sensitive to wood moisture content (Xu et al. 2011), surface preparation (Schimleck et al. 2005a), and cell orientation (Schimleck et al. 2005b). Therefore, more attention was paid to these parameters. Wood surface was sanded using three sandpaper grits (120, 220, and 320) and then cleaned up to remove dust. The radial sticks were conditioned for several days at 60 percent relative humidity and 20°C to reach a wood moisture content of 12 percent.

Near-infrared spectroscopy

Fourier Transform (FT) NIR spectra were acquired with a Perkin Elmer Spectrum 400 FT-MIR/FT-NIR spectrometer, using near-infrared reflectance accessory (NIRA). The diameter of the NIRA opening was 15 mm. Black electrical masking tape, which fully absorbs NIR light, was used to reduce the opening to 5 by 5 mm in order to be closer to the size of increment cores as usually collected in eastern Canada. Only the transverse face of cores is usually prepared and sanded for ring analysis. Hence the NIRS calibrations were developed with the transverse face even though SilviScan works with the radial face. Furthermore Schimleck et al. (2005b) tested NIRS calibrations on both faces of SilviScan samples for air-dry density, MFA, MOE, and several tracheid morphological characteristics. They concluded that the differences between the two sets were small, indicating that either face could be used for NIR analysis. The spectra were collected from the bark side to the pith in 7.5-mm increments. For the purposes of this study, a 5-mm increment size would have been more justified, but the samples were already cut in sticks according to SilviScan's specifications. The spectra were collected over the wavelength range of 680 to 2520 nm, at 1-nm intervals. Thirty-two scans were accumulated and averaged to give a single spectrum by spot. A ceramic standard was used as instrument reference. In total, 1,332 spectra were collected from the 127 samples.

SilviScan analysis

The same 127 radial sticks were then analyzed by SilviScan-3 at FPInnovations in Vancouver, British Columbia. SilviScan processing was precisely described by Cieszewski et al. (2013). The samples were cut into radial

strips of 2 by 7 mm (tangentially by longitudinally) and conditioned at 40 percent relative humidity and 20°C to reach a wood moisture content of 8 percent (dry basis). No acetone extraction was performed because the NIR models are intended to be used on increment cores with no extraction. Wood density was determined at a 25-µm radial resolution using the X-ray densitometer unit of SilviScan. MFA was determined at a 5-mm radial resolution using the X-ray diffractometer unit. MOE was estimated using the density and the coefficient of variation of the X-ray diffraction profile intensity (Evans 1999). The density at 8 percent moisture content was converted into basic density as follows (Siau 1995):

$$BD = \frac{1{,}000 \text{ x } D_8}{1{,}080 + 0.22 \text{ x } D_8}$$

where BD is basic density and D_8 is density at 8 percent moisture content. It is assumed that the fiber saturation point is 30 percent and that the water density is 1,000 kg/m³.

Development of NIR calibrations

SilviScan values were matched with the corresponding NIR spots according to measurement position. Data processing was used to prepare and match the databases (PROC SQL, SAS 9.3). For statistical purposes, 34 sites were randomly chosen for the calibration set (88 samples, 918 spectra) and 16 others for the validation set (39 samples, 414 spectra). Multivariate data analysis was performed using The Unscrambler X software (version 10.2, Camo, Oslo, Norway). The presence of outliers was evaluated using the Hotelling T^2 ellipse on principal components analysis (PCA) scores plots with a 99 percent confidence interval. Model calibration and validation were performed using partial least-squares (PLS) regression. Calibration models were developed with four random cross-validation segments. Several combinations of wavelength ranges and mathematical pretreatments (smoothing, baseline offset, Savitzky-Golay derivatives, and multiplicative scatter correction) were tested. The optimal number of principal components was suggested by the software, based on the significance of the change in explained variance. In addition, to test the model on a validation set, a full cross-validation procedure was also applied on the calibration set. The calibration performance was assessed using the coefficient of determination (R^2c), the standard error of calibration (SEC), the standard error of cross-validation (SECV), and the ratio of performance to deviation (RPDc) calculated as the ratio of standard deviation of the reference data to SECV (Williams and Sobering 1993, Jones et al. 2005). The calibration model was then tested on the validation set. The standard error of prediction (SEP) gave a measure of how well the calibration predicted the wood property of the remaining 414 spots (validation set). The predictive ability of the calibration was also assessed using the ratio of performance to deviation (RPDv).

Segmented regression analysis

TSLRs were applied to MFA profiles to determine the transition age from juvenile to mature wood for the 127 samples. Models were built with MFA values measured by SilviScan and MFA values predicted by NIRS. The transition age is frequently expressed in terms of number of rings from the pith (Wang and Stewart 2012). Each ring MFA value was determined from the 5-mm increment MFA profile using data processing (PROC SQL, SAS 9.3). A mathematical pretreatment was applied on MFA profiles to remove the effect of compression wood. Any sudden MFA increase above 0.025° per mm was removed. This threshold was chosen by trial and error.

A TSLR model can be written as follows (Ryan and Porth 2007):

$$y_i = a_1 + b_1 x_i + \varepsilon \text{ for } x \leq c$$

and

$$y_i = a_2 + b_2 x_i + \varepsilon \text{ for } x > c$$

where yi is the MFA value of the ith ring from the pith, xi is the ith ring, a1 is the intercept of linear fit to data below the estimated breakpoint, b1 is the slope of linear fit to data below the estimated breakpoint, a2 is the intercept of linear fit to data above the estimated breakpoint, b2 is the slope of linear fit to data above the estimated breakpoint, c is the estimated breakpoint, and e is the error term. The transition point (c) is the intersection point of two lines, which is obtained as follows:

$$c = \frac{a_2 - a_1}{b_1 - b_2}$$

The first step in applying a segmented regression is to graph the data to estimate visually where the break occurs (Ryan and Porth 2007). The transition age seemed to vary between 10 and 40 years for the 127 MFA profiles obtained from SilviScan. An automatic procedure was developed (1) to estimate all the possible starting parameters (a1, a2, b1, b2, c) for transitions between 10 and 40 years using regression analysis (PROC REG, PROC NLIN, SAS 9.3) and (2) to choose the model with the smallest mean squared error using data processing (PROC SQL, SAS 9.3). Once the transition point was determined, the proportions of juvenile and mature wood were calculated, as well as the average values of BD, MOE, and MFA. These juvenile and mature wood properties were obtained by calculating the area-weighted mean, assuming a circular shape of the rings.

Methods comparison for the determination of wood properties

The ability of a model to precisely predict the value from a single sample can be assessed using statistics such as RPD for NIRS models. However, the analysis of population statistics is also a good way to assess the calibration performance. Average wood properties and transition ages determined using SilviScan data were thus compared with values obtained using NIRS predicted data. The comparison was assessed using the Pearson correlation coefficient (r), the mean prediction error (bias), and the 95 percent limits of agreement. High correlation means that data from the two methods are linearly related, even if they cannot agree. The mean prediction error is the mean difference between the measurements of the two methods (Bland and Altman 1995). The closer the mean prediction error is to zero, the less bias there is. The lower and upper limits represent the 95 percent limits of agreement of the mean difference (±1.96 x SD). The smaller the range between these two limits, the better the agreement.

Results and discussion

SilviScan wood properties

The statistics of wood properties were calculated using SilviScan data of the 127 samples. Average values were 431.8 ± 31.2 kg/m³ in BD, 14.1 ± 2.3 GPa in MOE, and 14.0° ± 3.1° in MFA. The average BD value was similar to that measured by Jessome (1995). Lessard (2013) obtained similar MOE and MFA values for black spruce samples from 77 sites across Newfoundland, with average values of 13.9 ± 2.3 GPa in MOE and 15.6° ± 3.3° in MFA. The statistics of wood properties were also calculated for the calibration set (88 samples, 918 spectra) and for the independent validation set (39 samples, 414 spectra) for the purpose of comparison (Table 2.1). Average values for the calibration set were slightly lower for MFA (16.9° vs. 18.1°) but very similar to those of the validation set for BD (428.3 vs. 425.8 kg/m³) and MOE (12.4 vs. 12.0 GPa).

Table 2.1 Statistics of wood properties for the near-infrared calibration and validation sets.[a]

	Calibration set				Validation set			
Wood property	*n*	Mean (SD)	Min.	Max.	*n*	Mean (SD)	Min.	Max.
BD (kg/m^3)	918	428.3 (42.8)	324.2	609.4	414	425.8 (47.4)	293.6	632.8
MFA (degrees)	918	16.9 (7.0)	8.0	47.4	414	18.1 (8.0)	8.1	52.1
MOE (GPa)	918	12.4 (3.7)	4.1	21.9	414	12.0 (3.9)	4.7	21.8

[a] BD = basic density; MFA = microfibril angle; MOE = modulus of elasticity.

Development of NIR calibrations

Table 2.2 presents the calibration statistics obtained for BD, MOE, and MFA by PLS regression. No outlier was observed or removed. None of mathematical pretreatments significantly improved the precision of the models. Calibration statistics (R²c, SECV) were higher for MOE (0.89, 1.3) than for BD (0.82, 25.0) or MFA (0.82, 3.1). The wavelength range and the number of principal components (PC) were also smaller for MOE (900 to 1,150 nm, 6 PC) than for BD (900 to 2,500 nm, 8 PC) or MFA (680 to 2,500 nm, 9 PC). The models were then tested on the validation set (39 samples, 16 sites, 414 spectra; Table 2.2). The statistics (R²v, SEP, RPDv) did not drop off when predicting BD (0.85, 26.0, 1.8), MFA (0.79, 3.6, 2.2), or MOE (0.88, 1.3, 2.9). SEC and SEP values were very similar for all wood properties.

Table 2.2 Summary of near-infrared calibration and validation statistics.[a]

	Calibration set							Validation set			
Wood property	*n*	Range	PC	R^2c	SEC	SECV	RPDc	*n*	R^2v	SEP	RPDv
BD (kg/m^3)	918	900–2,500	8	0.82	24.2	25.0	1.71	414	0.85	26.0	1.82
MFA (degrees)	918	680–2,500	9	0.82	3.0	3.1	2.29	414	0.79	3.6	2.22
MOE (GPa)	918	900–1,150	6	0.89	1.2	1.3	2.91	414	0.88	1.3	2.93

[a] PC = number of principal components; R^2c = coefficient of determination for calibration set; SEC = standard error of calibration; SECV = standard error of cross-validation for calibration set; RPDc = ratio of performance to standard deviation for calibration set; R^2v = coefficient of determination for validation set; SEP = standard error of prediction; RPDv = ratio of performance to standard deviation for validation set; BD = basic density; MFA = microfibril ange; MOE = modulus of elasticity.

Good to excellent calibrations were thus obtained for BD, MOE, and MFA. In other words, in this study, strong linear relationships were obtained between the studied wood properties and the absorption values. The validation statistics (R^2v, SEP, RPDv) obtained by Xu et al. (2011) for black spruce and balsam fir were slightly higher for air-dried density (0.87, 25, 2.7), but lower for MOE (0.72, 1.0, 1.9) and MFA (0.56, 3.2, 0.9). A value of RPDv above 2.5 is usually defined as satisfactory for screening in a breeding program, whereas values of 5 to 10 are defined as adequate for quality control (Williams and Sobering 1993). However, based on the references cited in this article, the RPDv value is rarely above 3 for calibrations applied to solid wood. The calibrations obtained for BD, MOE, and MFA can thus be considered robust enough for operational use.

Figure 2.1 shows the correlations between SilviScan data (BD, MFA, MOE) and NIRS values obtained from the calibration and validation sets. Small deviations from linearity were observed for the highest values of BD (500 kg/m³ and more). In this range, BD was underestimated by NIRS. For MFA, small deviations also occurred in extreme values (7° and less, 30° and more). In these ranges, MFA was also underestimated by NIRS. The same trends were observed with the prediction set. For MOE, no deviation was obvious. Several authors have also observed slight deviations from linearity at extreme values in density (Schimleck et al. 2001, Via 2010) and in MFA (Jones et al. 2005, So et al. 2013). The source of nonlinearity for these extreme values seems to be intrinsic to wood material given that the mathematical pretreatments were ineffective (Pérez-Marín et al. 2007). However, these deviations from linearity concern only a few samples in this study.

A large part of the variance in BD (85%), MFA (79%), and MOE (88%) was thus explained by FT-NIR spectra. The unexplained variance may be attributed to many sources. NIR light penetration is limited to a few millimeters from the surface as opposed to X-ray beam, which passes through the sample. NIRS may thus have not exactly captured the same properties as SilviScan. Furthermore, the transverse face was scanned by NIRS, whereas SilviScan scans samples on the radial face as previously discussed. Finally, in this study, MFA and MOE were estimated in 5-mm increments using Silviscan and in 7.5-mm increments using NIRS, which may have caused some discrepancies.

The autocorrelation between the trees from the same sites (site random effect) and between the spots from the same samples (sample random effect) was investigated. The classic PLS regression method proposed by The Unscrambler X software does not take into account the dependence between observations. The random effects were thus assessed on the residuals using mixed regressions (Proc MIXED, SAS 9.3). The random effect was highly significant for the sample and not significant for the site. However, the dependence between the measurements from a same sample is not surprising. This random effect was not considered in the development of calibrations that may have influenced the NIRS predictions at the spot scale and was certainly not considered for the MFA profile, which is the most important to determine the transition point.

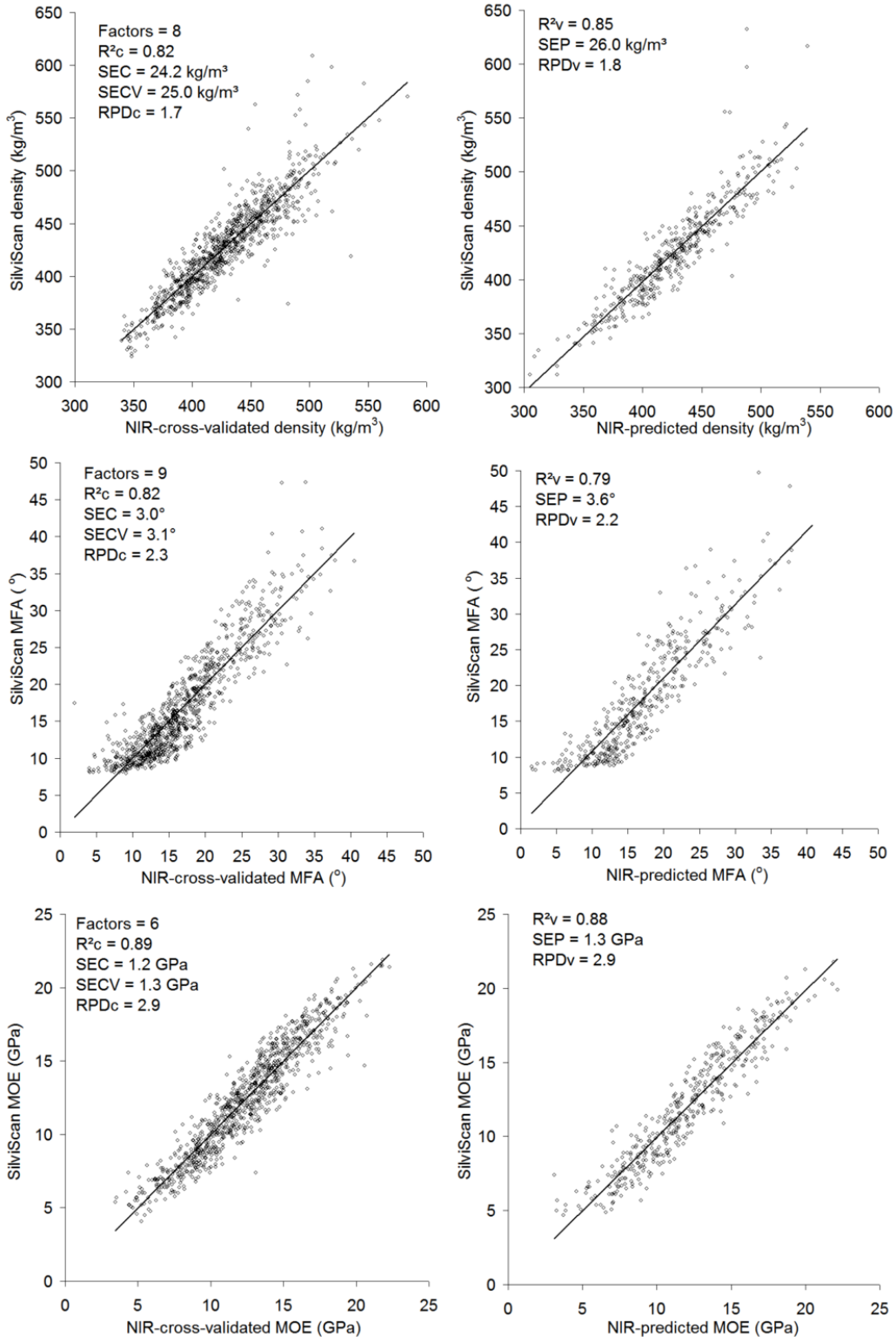

Figure 2.1 (Left) calibrations and (right) predictions for basic density (top panels), microfibril angle (MFA; middle panels), and modulus of elasticity (MOE; bottom panels).

A fixed effect related to the position of the measurement (spot) in the increment cores was also highly significant. The higher biases in BD and MOE were observed for spots collected close to the pith and bark. Via et al. (2003) observed that MOE and MOR were poorly related to NIR spectra for pith wood in Pinus palustris, while density was strongly correlated. The authors explained that this lack of significance was perhaps attributable to the high concentration of resinous extractives near the pith. Furthermore, compression wood is also very frequent close to the pith. It could thus be interesting to consider the spot position as covariable in a PLS regression.

Two segment linear regressions

Table 2.3 shows the results of TSLR applied to the 127 MFA profiles obtained with SilviScan. The average transition age was 23 ± 7 years, varying between 8 and 43 years. The average MFA value at the transition point was 13.9° ± 3.2°. All the MFA profiles presented the same inverted J shape (Figure 2.2). On average, the MFA value close to the pith was 32.3° ± 5.7°, whereas the MFA value close to the bark was 10.5° ± 2.1°. The average MFA value at the transition point was 2.3 times smaller than the MFA value close to the pith. Alteyrac et al. (2006) applied TSLR to ring area, maximum ring density, and ring MFA to determine the transition point of 36 black spruce trees harvested near Chibougamau, Québec. The transition age at 2.4 m was estimated at 14.0, 17.6, and 15.9 years, respectively. Yang and Hazenberg (1994) applied TSLR to tracheid length to determine the transition point of 10 black spruce trees harvested near Thunder Bay, Ontario. The transition varied between 11 and 21 years among the samples taken at breast height. The transition age estimated at 23 years in the present study is thus relatively similar to results presented in the literature.

Table 2.3 Statistics of juvenile and mature wood properties calculated from SilviScan data (n=127).[a]

	Sample wood			Juvenile wood			Mature wood		
Wood property	Mean (SD)	Min.	Max.	Mean (SD)	Min.	Max.	Mean (SD)	Min.	Max.
Transition age (y)	22.8 (7.1)	8.0	43.0	—	—	—	—	—	—
Transition MFA (degrees)	13.9 (3.2)	9.3	25.3	—	—	—	—	—	—
Area proportion (%)	—	—	—	17.5 (13.3)	1.2	76.6	82.5 (13.3)	23.4	98.8
BD (kg/m^3)	431.8 (31.2)	361.7	509.1	417.9 (36.0)	333.6	538.2	436.6 (31.4)	367.5	516.8
MFA (degrees)	14.0 (3.1)	8.7	26.4	20.2 (3.7)	13.9	34.2	12.6 (3.2)	8.4	25.4
MOE (GPa)	14.1 (2.3)	8.7	19.0	10.4 (1.5)	6.2	13.7	15.0 (2.5)	8.9	20.3

[a] BD = basic density; MFA = microfibril angle; MOE = modulus of elasticity.

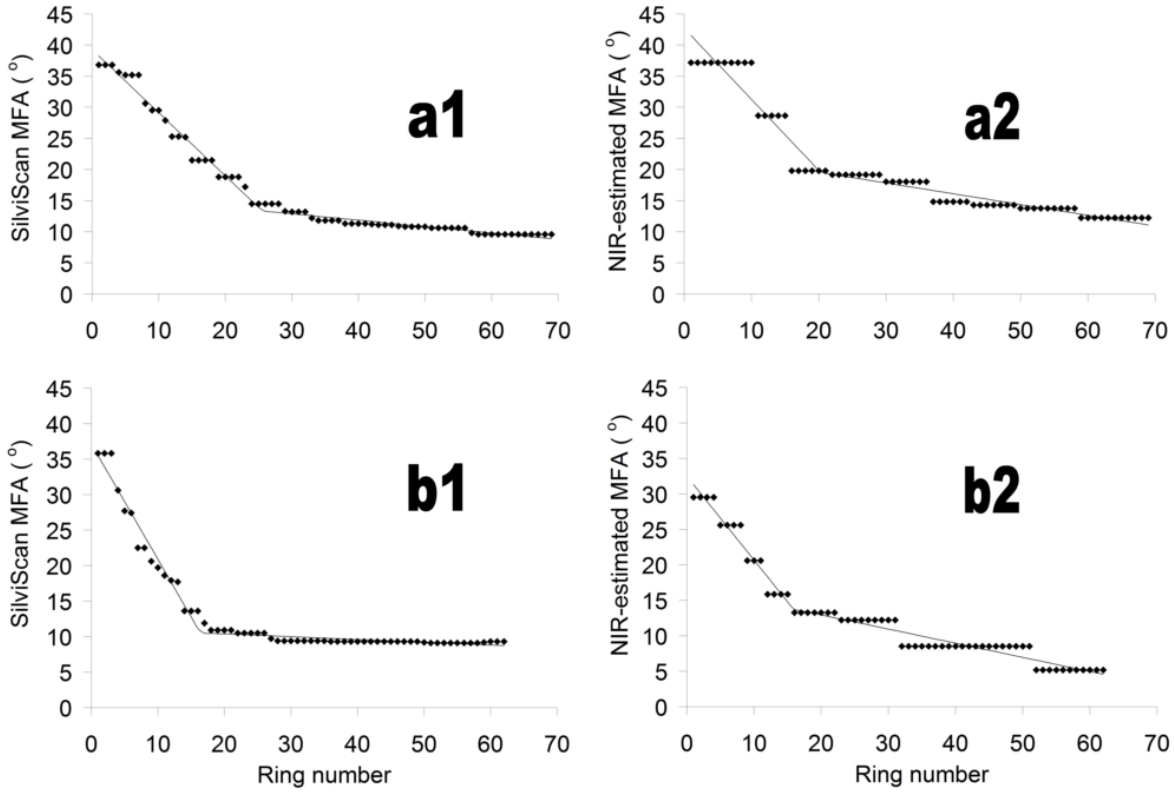

Figure 2.2 Illustrations of segmented regressions fitted on microfibril angle (MFA) profiles obtained by (left) SilviScan and (right) near-infrared (NIR) spectroscopy for two samples (a and b).

Once the transition age became known, juvenile-mature wood properties were calculated. The proportion of mature wood was 82.5 ± 13.3 percent. There were highly significant differences in BD, MFA, and MOE between juvenile and mature wood using t tests for paired observations (Proc TTEST paired, SAS 9.3). Average values for mature wood were significantly higher than those for juvenile wood for BD (436.6 vs. 417.9 kg/m³) and MOE (15.0 vs. 10.4 GPa), whereas for MFA, average value for mature wood was significantly lower than that for juvenile wood (12.6° vs. 20.2°). These results are consistent with the definition of juvenile and mature wood (Panshin and De Zeeuw 1980).

Table 2.4 shows the results of TSLR applied to the 127 MFA profiles obtained by NIRS. Average transition age was 21 ± 7 years, varying between 5 and 40 years. Average MFA value at the transition point was 15.4° ± 3.5°. All the MFA profiles presented the same inverted J shape (Figure 2.2). The proportion of mature wood was 85.5 ± 11.3 percent. There were highly significant differences in BD, MFA, and MOE between juvenile and mature wood using t tests for paired observations (Proc TTEST paired, SAS 9.3). Average values for mature wood were significantly higher than those for juvenile wood for BD (435.4 vs. 426.4 kg/m³) and MOE (14.6 vs. 10.5 GPa), whereas for MFA, average value for mature wood was significantly lower than that for juvenile wood (13.0° vs. 20.5°).

Table 2.4 Statistics of juvenile and mature wood properties calculated from NIRS data (n=127).[a]

Wood property	Sample wood			Juvenile wood			Mature wood		
	Mean (SD)	Min.	Max.	Mean (SD)	Min.	Max.	Mean (SD)	Min.	Max.
Transition age (y)	20.6 (6.9)	5.0	40.0	—	—	—	—	—	—
Transition MFA (degrees)	15.4 (3.5)	6.2	23.2	—	—	—	—	—	—
Area proportion (%)	—	—	—	14.5 (11.3)	0.2	56.7	85.5 (11.3)	43.3	99.8
BD (kg/m^3)	432.6 (30.7)	355.8	511.2	426.4 (32.6)	352.2	549.3	435.4 (31.8)	355.4	515.3
MFA (degrees)	14.1 (3.2)	6.2	23.8	20.5 (3.3)	12.9	31.7	13.0 (3.5)	4.9	23.9
MOE (GPa)	14.0 (2.2)	8.9	19.1	10.5 (1.8)	6.3	14.1	14.6 (2.4)	8.9	20.0

[a] NIRS = near-infrared spectroscopy; BD = basic density; MFA = microfibril angle; MOE = modulus of elasticity.

Of the 127 TSLR models, four and five models failed to converge using SilviScan data and NIRS data, respectively. Each of these cases was investigated. The presence of compression wood seems to be the main reason for nonconvergence when SilviScan data were used. Therefore, the data pretreatment applied to MFA profiles to remove the effect of compression wood was not sufficient for these samples. However the threshold filtering method has corrected 28 percent of the MFA values and helped the convergence of other models while increasing the measurement accuracy of the transition point (Figure 2.3). Such pretreatment is thus strongly recommended for operational use. Moreover, it would be relevant to optimize this threshold filtering in function of transition age results rather than by trial and error. This pretreatment has also made it possible to remove some unlikely NIRS predictions in the MFA profile. Nevertheless, a succession of prediction errors was the main reason for nonconvergence when NIRS data were used. A NIRS calibration is a predictive model. Even with an excellent calibration, errors due to variance (called prediction errors) and slight biases occur. However, after inspection, the transition ages of these nonconvergent models did not seem unlikely and the values were kept.

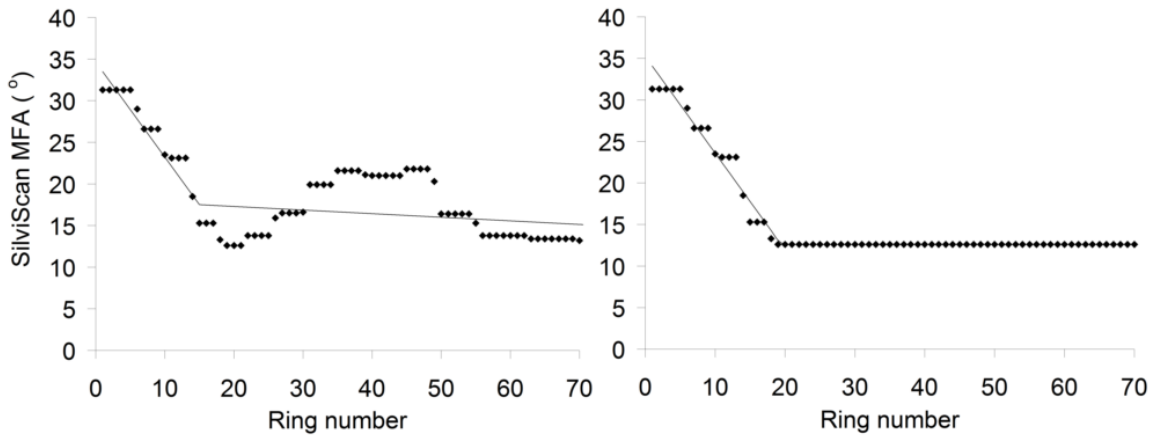

Figure 2.3 Illustrations of segmented regressions fitted on (left) raw microfibril angle (MFA) profile obtained by SilviScan and (right) MFA profile corrected by the threshold filtering

It should also be noted that TSLR was only applied in the present study to mature trees aged 45 years and older. Younger trees, which have less or no mature wood, could be sampled in an inventory. In this case, a standard linear regression should give a better fit than a TSLR, which could signal the absence of mature wood.

Furthermore, MFA was estimated in 5-mm increments with SilviScan and in 7.5-mm increments with NIRS. The average ring width of the 127 samples was 0.95 mm. Consequently, such resolutions could not give a precision to the nearest ring. The determination of the transition age could also be more accurate with MFA determined or predicted at a resolution of 2 mm or less, particularly in the presence of very narrow growth rings.

Methods comparison for the determination of wood properties

The transition age and juvenile-mature wood properties obtained from SilviScan data (Table 2.3) were compared with values obtained from NIRS predicted data (Table 2.4). The two methods were compared using the correlation coefficient and the agreement. Table 2.5 shows that the correlations between the two data sets were moderate to high. The lowest correlations were observed for transition age (r = 0.59, P < 0.001) and juvenile-mature wood proportion (r = 0.65, P < 0.001). The lowest agreements were also observed for these properties. The transition age was slightly underestimated by NIRS with a mean prediction error (and 95% limits of agreement) of -2.2 ± 6.3 years (-14.6/10.1). The juvenile wood proportion was also slightly underestimated by NIRS with a mean prediction error (and 95% limits of agreement) of -3.0 ± 10.4 percent (-23.4/17.5). Excellent correlation (r = 0.95, P < 0.001) and agreement were obtained for transition MFA with -1.5° ± 1.1° (-3.7/0.7). Good to excellent correlations and agreements were also observed for juvenile-mature wood properties (Table 2.5).

Table 2.5 Comparison between the SilviScan and NIRS estimates (n=127).[a]

	Sample wood				Juvenile wood				Mature wood			
Wood property	*r*	Bias (SD)	Lower	Upper	*r*	Bias (SD)	Lower	Upper	*R*	Bias (SD)	Lower	Upper
Transition age (y)	0.59**	−2.2 (6.3)	−14.6	10.1	—	—	—	—	—	—	—	—
Transition MFA (degrees)	0.95**	−1.5 (1.1)	−3.7	0.7	—	—	—	—	—	—	—	—
Area proportion (%)	—	—	—	—	0.65**	−3.0 (10.4)	−23.4	17.5	0.65**	3.0 (10.4)	−17.5	23.4
BD (kg/m^3)	0.95**	0.9 (9.7)	−18.1	19.8	0.89**	8.4 (16.6)	−24.2	41.0	0.93**	−1.3 (11.5)	−23.8	21.3
MFA (degrees)	0.78**	0.1 (2.1)	−4.0	4.1	0.70**	0.3 (2.7)	−5.0	5.7	0.78**	0.4 (2.2)	−4.0	4.8
MOE (GPa)	0.91**	−0.2 (0.9)	−2.0	1.7	0.79**	0.1 (1.1)	−2.0	2.3	0.90**	−0.4 (1.1)	−2.6	1.8

[a] *r* = Pearson correlation coefficient; bias = mean prediction error, average of differences; lower = bias − 1.96 SD; upper = bias + 1.96 SD; asterisks = correlation is highly statistically significant ($P < 0.001$); BD = basic density; MFA = microfibril angle; MOE = modulus of elasticity.

The correlation and the agreement were thus notably higher for transition MFA than for transition age. Close to the transition point, MFA presents very few variations, as opposed to the transition age, which was strongly influenced by the measurement resolution (Figure 2.2). For 86 of 127 (68%) samples, the transition age was similar (±5 y) to that obtained using SilviScan data. A few cases with greater discrepancies occurred despite the good calibration statistics for MFA. Discrepancies above 10 years for the transition age were observed for 12 of 127 (9%) samples, including extreme discrepancies above 15 years for three samples (2%). These cases were investigated, and the main observed cause also was the succession of prediction errors, which disturbed the MFA profile. For operational use, the performance of the NIRS calibration should not be inferior to that obtained for MFA in this study. In addition, some rules should be defined to detect potential outliers. Using the 0.05 and

0.95 percentiles of SilviScan measurements as thresholds, a transition MFA below 9° or above 21° could be considered as suspicious, as well as a transition age below 10 years or above 32 years. A better knowledge of the natural range of black spruce wood properties could help to define stronger rules. A larger sampling of all the natural ranges of growth conditions could thus be required.

Conclusion

NIRS potential to model MFA in order to automatically determine the transition from juvenile to mature wood was confirmed in this study. First, good to excellent calibrations (R^2v, RPDv) were obtained for BD (0.85, 1.8), MFA (0.79, 2.2), and MOE (0.88, 2.9). The TSLR method was then successfully applied to the MFA profile determined by SilviScan and to the MFA profile predicted by NIRS. However, the NIRS transition age was poorly correlated to the SilviScan transition age ($r = 0.59$, $P < 0.001$). The ability of the method to precisely measure the transition age from a single sample should be improved to be ready for operational use. On the other hand, the suggested method was able to correctly estimate an average transition age for a given population with a mean prediction error (and 95% limits of agreement) of -2.2 ± 6.3 years (-14.6/10.1).

The data pretreatment applied to MFA profiles improved the measurement accuracy of the transition point, and its use is strongly recommended for species with high proportions of compression wood. The difference in resolution between SilviScan data (every 5 mm) and NIRS predictions (every 7.5 mm) could partly explain the discrepancies observed in the estimation of transition age by NIRS. A better precision of the transition age could be obtained with MFA determined or predicted at a resolution of 2 mm or less, given the annual growth ring width in natural black spruce. Finally, a better knowledge of the natural range for MFA in black spruce could help to identify unlikely values.

NIRS appears to be a suitable and economic alternative to SilviScan to assess the transition age, even if the method accuracy must still be improved for operational use. Such a method could be integrated into a NIRS system for rapid determination of the transition age and juvenile-mature wood properties of an increment core. Thousands of samples from trees grown in various conditions could be assessed. Large-scale research could thus help to obtain a better understanding of the factors that influence the transition. In addition, this method could be adapted to any species with a MFA profile in an inverted J shape.

Acknowledgements

This research was funded by the Fonds de recherche du Québec-Nature et technologies and the Ministère des Forêts, de la Faune, et des Parcs du Québec, Canada. The samples were provided by the Canadian Wood Fibre Centre, Canadian Forest Service, Natural Resources Canada. The authors thank the Centre de recherche sur le bois de l'Université Laval for material support and are especially grateful to Professor Tatjana Stevanovic for the use of NIR spectrometer. Thanks also to the FPInnovations team for providing the fiber database. Thanks to Sébastien Cortade for help with sample preparation and spectra collection. Thanks to Martin Riopel for statistical support.

References

Alteyrac, J., A. Cloutier, and S. Y. Zhang. 2006. Characterization of juvenile wood to mature wood transition age in black spruce (Picea mariana (Mill.) B.S.P.) at different stand densities and sampling heights. Wood Sci. Technol. 40(2):124-138.

Barnett, J. R. and V. A. Bonham. 2004. Cellulose microfibril angle in the cell wall of wood fibres. Biol. Rev. 79(2):461-472.

Bhat, K. M., P. B. Priya, and P. Rugmini. 2001. Characterisation of juvenile wood in teak. Wood Sci. Technol. 34(6):517-532.

Bland, J. M. and D. G. Altman. 1995. Comparing methods of measurement: Why plotting difference against standard method is misleading. Lancet 346(8982):1085-1087.

Briggs, D. 2010. . J. Forestry 108(4):174-182.

Cieszewski, C. J., M. Strub, F. Antony, P. Bettinger, J. Dahlen, and R. C. Lowe. 2013. Wood quality assessment of tree trunk from the tree branch sample and auxiliary data based on NIR spectroscopy and SilviScan. Math. Comput. Forestry Nat.-Res. Sci. 5(26):86-111.

Clark, A., III, R. F. Daniels, and L. Jordan. 2006. Juvenile/mature wood transition in loblolly pine as defined by annual ring specific gravity, proportion of latewood, and microfibril angle. Wood Fiber Sci. 38(2):292-299.

Donaldson, L. 2008. Microfibril angle: Measurement, variation and relationships--A review. IAWA J. 29(4):345-386.

Evans, R. 1999. A variance approach to the X-ray diffractometric estimation of microfibril angle in wood. Appita J. 52(4):283-289.

Evans, R., S. Stringer, and R. Kibblewhite. 2000. Variation of microfibril angle, density and fibre orientation in twenty-nine Eucalyptus nitens trees. Appita J. 53(6):450-457.

Hein, P., B. Clair, L. Brancheriau, and G. Chaix. 2010. Predicting microfibril angle in Eucalyptus wood from different wood faces and surface qualities using near infrared spectra. J. Near Infrared Spectrosc. 18(6):455-464.

Jessome, A. P. 1995. Strength and related properties of woods grown in Canada. SP-514F. Forintek Canada Corp., Ottawa, Ontario. 37 pp.

Jones, P. D., L. R. Schimleck, G. F. Peter, R. F. Daniels, and A. Clark III. 2005. Nondestructive estimation of Pinus taeda L. wood properties for samples from a wide range of sites in Georgia. Can. J. Forest Res. 35(1):85-92.

Jozsa, L. A. and G. R. Middleton. 1994. A discussion of wood quality attributes and their practical implications. SP-34. Forintek Canada Corp., Vancouver, British Columbia. 42 pp.

Lessard, E. 2013. Modeling and mapping wood fiber attributes using environmental and forest inventory data: Case of Newfoundland's boreal forest. Master's thesis in geographic sciences. Université de Sherbrooke, Québec, Canada. 103 pp. (In French.)

Lessard, E., R. A. Fournier, J. E. Luther, M. J. Mazerolle, and O. R. Van Lier. 2014. Modeling wood fiber attributes using forest inventory and environmental data for Newfoundland's boreal forest. Forest Ecol. Manag. 313:307-318.

Meder, R., T. Trung, and L. Schimleck. 2010. Guest editorial: Seeing the wood in the trees: Unleashing the secrets of wood via near infrared spectroscopy. J. Near Infrared Spectrosc. 18(6):v-vii.

Panshin, A. J. and C. De Zeeuw. 1980. Textbook of Wood Technology: Structure, Identification, Properties, and Uses of the Commercial Woods of the United States and Canada. 4th ed. McGraw-Hill, New York. 722 pp.

Pérez-Marín, D., A. Garrido-Varo, and J. E. Guerrero. 2007. Non-linear regression methods in NIRS quantitative analysis. Talanta 72(1):28-42.

Ryan, S. E. and L. S. Porth. 2007. A tutorial on the piecewise regression approach applied to bedload transport data. General Technical Report RMRS-GTR-189. USDA Forest Service, Rocky Mountain Research Station, Fort Collins, Colorado. 41 pp.

Schimleck, L. R. and R. Evans. 2002. Estimation of microfibril angle of increment cores by near infrared spectroscopy. IAWA J. 23(3):225-234.

Schimleck, L. R., R. Evans, and J. Ilic. 2001. Estimation of Eucalyptus delegatensis wood properties by near infrared spectroscopy. Can. J. Forest Res. 31(10):1671-1675.

Schimleck, L. R., P. D. Jones, A. Clark III, R. F. Daniels, and G. F. Peter. 2005a. Near infrared spectroscopy for the nondestructive estimation of clear wood properties of Pinus taeda L. from the southern United States. Forest Prod. J. 55(12):21-28.

Schimleck, L. R., R. Stürzenbecher, C. Mora, P. D. Jones, and R. F. Daniels. 2005b. Comparison of Pinus taeda L. wood property calibrations based on NIR spectra from the radial-longitudinal and radial-transverse faces of wooden strips. Holzforschung 59(2):214-218.

Siau, J. F. 1995. Wood: Influence of moisture on physical properties. Department of Wood Science and Forest Products, Virginia Polytechnic Institute and State University, Blacksburg. 227 pp.

Siesler, H. W., Y. Ozaki, S. Kawata, and H. M. Heise. 2002. Near-Infrared Spectroscopy: Principles, Instruments, Applications. Wiley-VCH, Weinheim, Germany. 348 pp.

So, C.-L., J. H. Myszewski, T. Elder, and L. H. Groom. 2013. Rapid analysis of the microfibril angle of loblolly pine from two test sites using near-infrared analysis. Forestry Chron. 89(5):639-645.

Tsuchikawa, S. 2007. A review of recent near infrared research for wood and paper. Appl. Spectrosc. Rev. 42(1):43-71.

Via, B. 2010. Prediction of oriented strand board wood strand density by near infrared and Fourier transform infrared reflectance spectroscopy. J. Near Infrared Spectrosc. 18(6):491-498.

Via, B. K., T. F. Shupe, L. H. Groom, M. Stine, and C.-L. So. 2003. Multivariate modelling of density, strength and stiffness from near infrared spectra for mature, juvenile and pith wood of longleaf pine (Pinus palustris). J. Near Infrared Spectrosc. 11(5):365-378.

Via, B. K., C. L. So, T. F. Shupe, L. H. Groom, and J. Wikaira. 2009. Mechanical response of longleaf pine to variation in microfibril angle, chemistry associated wavelengths, density, and radial position. Compos. Part A 40(1):60-66.

Viereck, L. A. and W. F. Johnston. 1990. Picea mariana (Mill.) B.S.P.--Black spruce. In: Silvics of North America. Vol. 1. Conifers. Agricultural Handbook 654. R. M. Burns and B. H. Honkala (Eds.). USDA Forest Service, Washington, D.C. pp. 227-237.

Wang, M. and J. D. Stewart. 2012. Determining the transition from juvenile to mature wood microfibril angle in lodgepole pine: A comparison of six different two-segment models. Ann. Forest Sci. 69(8):927-937.

Williams, P. C. and D. C. Sobering. 1993. Comparison of commercial near infrared transmittance and reflectance instruments for analysis of whole grains and seeds. J. Near Infrared Spectrosc. 1(1):25-32.

Xu, Q., M. Qin, Y. Ni, M. Defo, B. Dalpke, and G. Sherson. 2011. Predictions of wood density and module of elasticity of balsam fir (Abies balsamea) and black spruce (Picea mariana) from near infrared spectral analyses. Can. J. Forest Res. 41(2):352-358.

Yang, K. C. and G. Hazenberg. 1994. Impact of spacing on tracheid length, relative density, and growth rate of juvenile wood and mature wood in Picea mariana. Can. J. Forest Res. 24(5):996-1007.

Chapitre 3. Regional variation in wood density and modulus of elasticity of Quebec's main boreal tree species

Résumé

La spectroscopie proche infrarouge a été utilisée pour évaluer la variabilité régionale de la densité et de la rigidité du bois des principales essences boréales du Québec (épinette noire, sapin baumier, pin gris, bouleau à papier et peuplier faux-tremble), à partir de 30159 carottes de bois provenant de 10573 placettes d'inventaire. Un système automatique a été développé à cette fin et calibré à partir de données SilviScan. Les observations de densité et de rigidité étaient spatialement autocorrélées sur de plus longues distances chez les feuillus que chez les résineux. Un gradient latitudinal uniforme relié au climat était apparent pour le bouleau à papier et le peuplier faux-tremble. La distribution spatiale de ces mêmes propriétés n'était pas uniforme chez les résineux, suggérant une adaptabilité environnementale plus restreinte en comparaison aux essences feuillues étudiées.

Abstract

Regional variation in wood density and modulus of elasticity (MOE) for the main boreal softwoods (black spruce, balsam fir, jack pine) and hardwoods (paper birch, trembling aspen) of Quebec, Canada, were estimated using near-infrared spectroscopy on 30,159 increment cores from 10,573 inventory plots. An automated near-infrared system was developed for this purpose and calibrated using SilviScan data. Large-scale spatial dependence in wood density and MOE was observed. On average, observations were spatially autocorrelated on longer distances in hardwoods (136-157 km) than softwoods (65-74 km). Overall wood density and MOE increased with temperature and precipitation regardless of species. In addition, a uniform latitudinal gradient related to climate was observed in paper birch and trembling aspen. Conversely, spatial distribution in wood density and modulus of elasticity was not uniform in softwoods, suggesting a more limited environmental adaptability in comparison to the hardwood species studied. The natural variability of wood density and MOE in these species is now known for the study area. Regional estimates are thus available for various decision-making processes related to forest management, wood allocation, timber market value, protection priorities in firefighting and insect pest control, and forest carbon estimation.

Introduction

Spatial modeling of wood properties aims to produce local estimates and reveal significant regional differences. Given the importance of physical and mechanical properties in wood processing, this knowledge could provide a competitive advantage and have practical applications to aid decision-making in forestry (Briggs 2010). For this purpose, several models were recently developed in Canada to predict local estimates of wood properties based on a combination of photo-interpreted vegetation (including ecology), climate, geography, and imagery data (Giroud et al. 2016, Lenz et al. 2014, Lessard et al. 2014, Pokharel et al. 2014) or by using only stand vegetation structure derived from LiDAR (Luther et al. 2013, Pokharel et al. 2016). Some of the spatial dependence in wood properties was usually attributed to climate and/or geography, although the number of sampled plots tended to be limited.

Regional variation in wood density and modulus of elasticity (MOE) have also been studied in other parts of the world, specifically loblolly pine (*Pinus taeda* L.) plantations in the US (Antony et al. 2011, Jordan et al. 2008) and Monterey pine (*Pinus radiata* D. Don) plantations in New Zealand (Palmer et al. 2013), and across various species and geoclimatic conditions in Neotropical (Chave et al. 2006; Swenson and Enquist 2007), Bornean (Slik et al. 2010), and Chinese (Zhang et al. 2011) forests. These studies found that wood density and MOE frequently appeared to decrease with latitude and/or altitude including positive correlations with temperature and/or precipitation. Rossi et al. (2015) also observed higher values of wood density and MOE for Quebec's black spruce in lower latitudes or altitudes, where the radial growth rate was higher. Globally, wood formation appeared to be influenced by climate, producing more cells with thicker walls and more latewood when temperature and precipitation increased and the growing season was extended (Antony et al. 2011, Jordan et al. 2008, Rossi et al. 2015).

Spatial dependence or spatial autocorrelation can be measured using geostatistical techniques based on the first law of geography, according to which everything is related to everything else, but near things are more related than distant things (Tobler 1970). The spatial variability pattern is usually described and estimated using a semivariogram. Spatial dependence can be incorporated into a regression model based on semivariogram parameters, including or excluding covariants (Littell et al. 2006). Different geostatistical techniques have already been used to predict and map regional variation in wood density and MOE for large-scale pine plantations (Antony et al. 2011, Jordan et al. 2008, Palmer et al. 2013). These geostatistical models require samples from numerous, widely-distributed sites. However measuring the wood properties of thousands of samples using current technologies is a daunting challenge.

Near-infrared (NIR) spectroscopy and its applications for wood is well-documented (Tsuchikawa and Kobori, 2015; Tsuchikawa 2007). NIR spectroscopy is indeed a fast and relatively accurate technique that requires no

sample preparation. NIR absorption spectra are obtained by exposing wood samples to NIR radiation, which covers the 780– 2500 nm range of the electromagnetic spectrum. The spectra are then used to predict the wood properties using multivariate analysis. NIR calibration requires accurate measurements from reference methods. SilviScan was used in most studies to obtain the necessary data to model wood density and MOE (Schimleck 2008). SilviScan is a system that combines X-ray densitometry, X-ray diffractometry, and image analysis (Evans and Ilic 2001; Evans 1994). Few NIR calibrations were developed using the radial profiles of wood properties measured by SilviScan (Giroud et al. 2015, Meder et al. 2010). Such calibrations are particularly interesting considering the high variability of wood properties from the pith to the bark. NIR spectra were usually collected by manually translating the wood samples or the handheld contact probe at a specific step size (Giroud et al. 2015, Xu et al. 2011). A motorized linear carriage coupled with a 1-mm diameter fibre-optic probe was also conceived for this purpose in Australia (Meder et al. 2010). Most of NIR calibrations, developed for the prediction of wood density and MOE, were species-specific. However, global calibrations (i.e., multi-site, multi-species) were also investigated (Schimleck et al. 2001, Schimleck et al. 2010). Schimleck et al (2001) demonstrated that was possible to develop NIR calibrations for wood density and MOE using a wide range of softwood and hardwood species that displayed extreme variations in wood chemistry, anatomy and physical properties. Such global calibrations are of great interest in resource assessment to estimate the wood properties of many species, grown on a large range of sites (Schimleck et al. 2010).

Regional variation in wood density and MOE were studied for the main tree species of Quebec's managed boreal forests: balsam fir (*Abies balsamea* (L.) Mill.), black spruce (*Picea mariana* (Mill.) B. S. P.), jack pine (*Pinus banksiana* Lamb.), paper birch (*Betula papyrifera* Marsh.), trembling aspen (*Populus tremuloides* Michx.), and white spruce (*Picea glauca* (Moench) Voss). Thousands of increment cores taken from Quebec's provincial forest resources inventory were used for this purpose. More specifically, the objectives were to (i) develop a fast and reliable method to estimate wood density (basic density) and MOE using increment cores, (ii) incorporate spatial dependence into predictive models, and (iii) map and discuss the intraspecific and interspecific spatial distribution of wood density and MOE. To our knowledge, NIR spectroscopy and geostatistics have never been combined to predict and map regional variation in wood density and MOE in natural forests.

Materials and methods

Materials and study area

The study area was located in the center of the Canadian province of Quebec, approximately from 71°W to 79°W and from 45°N to 51°N, covering a large latitudinal gradient across the managed forest and, consequently, a large range of growing conditions (Figure 3.1). Data generated for the study area using BioSIM, a climate simulation software developed by the Canadian Forest Service (Régnière 2014), indicates that for the period covering 1981 to 2010, the normal July mean temperature ranges from approximately 11.9°C to 21.7°C, growing season precipitation ranges from 310 mm to 776 mm, snowfall from 229 mm to 577 mm, and aridity from 1 to 85 mm (Figure 3.2). Aridity was calculated using Thornthwaite's monthly potential evapotranspiration minus monthly growing season precipitation. Forest data and increment cores were provided by Quebec's provincial forest resources inventory, a two-phase inventory design based on photo-interpretation and field sampling. Forest stand composition, structure, and ecology are photo-interpreted every 10 to 15 years. Productive and accessible forest stands of 7 m and higher were sampled in temporary plots in accordance with provincial standards and procedures. This inventory data is used to assess the current state of the forest, including available standing volume. Care was taken to precisely measure the metrics and features of three sample trees per temporary plot. Increment cores were collected from these trees at 1 m above ground. Ring width and age were systematically measured from the increment cores using WinDENDRO (Regent Instruments Inc., Quebec City, Quebec, Canada).

Spectral data acquisition

The wood surface was sanded using three sandpaper grits (120, 220, and 320) and cleaned to remove dust. The increment cores were conditioned for 24 hours at 40% relative humidity and 20°C, before being scanned by NIR spectroscopy to measure the wood properties. A NIR system was developed by Centre de Recherche Industrielle du Québec (CRIQ) to automatically acquire NIR spectra and high resolution images from increment cores (Figure 3.3). For this purpose, a FT-NIR spectrometer (Matrix-F model, Bruker, Billerica, Massachusetts, USA) was equipped with a 2-mm diameter reflector probe (Reflector model, Solvias, Kaiseraugst, Switzerland). A 2-mm diameter probe was chosen because of the size of the increment cores, which are about 4-5 mm wide. The spectra were acquired between 4000 and 12000 cm^{-1} (830 to 2500 nm). Four scans were accumulated and averaged to give a single spectrum per spot. A ceramic standard was used as instrument reference and measured every hour. The spectra were collected in 5-mm increments, from bark side to pith, using a motorized linear carriage, with a 3-mm unscanned gap between each spot. The increment size and the number of scans accumulated were chosen as a result of a compromise between spectral quality and productivity in terms of scanning time.

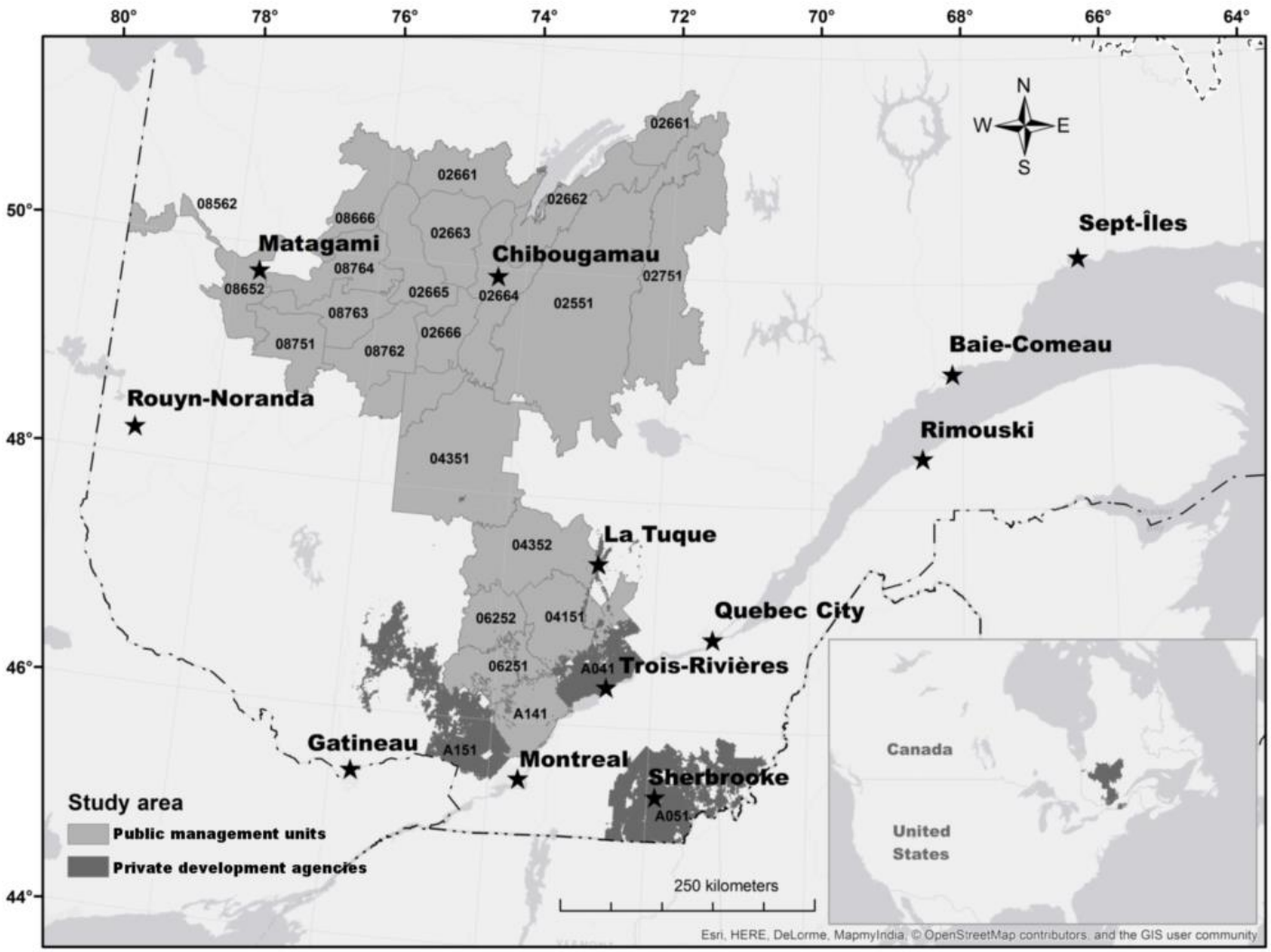

Figure 3.1 Study area including names and boundaries of public forest management units and private forest development agencies.

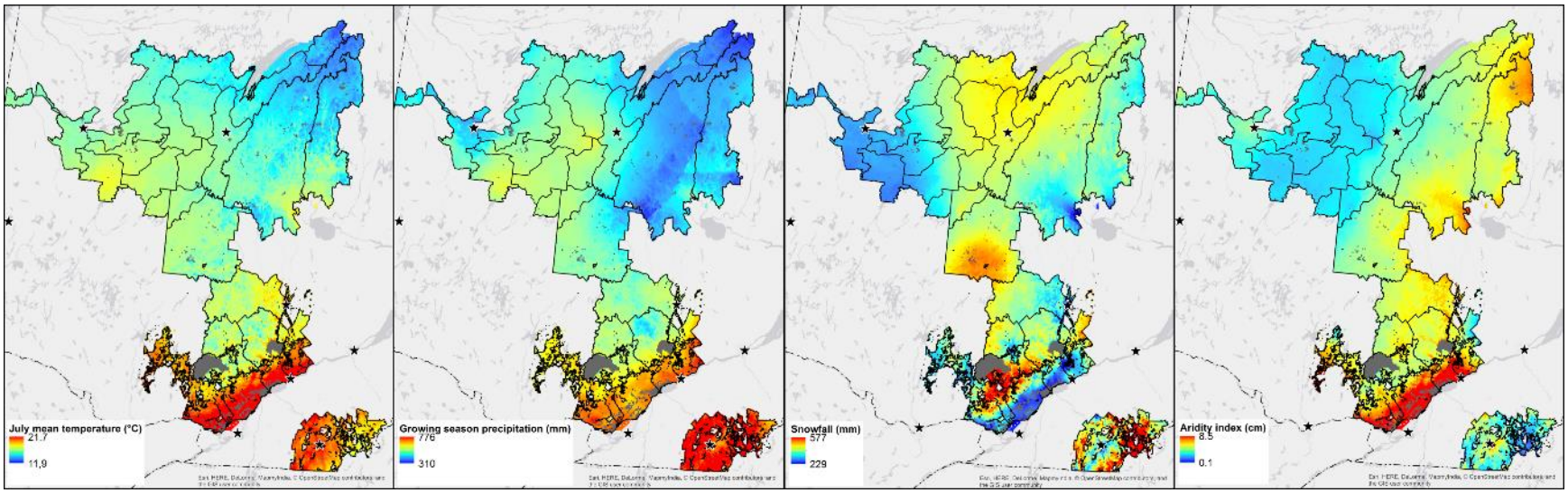

Figure 3.2 Maps for July mean temperature, mean growing season precipitation, total annual snowfall, and aridity index across the study area.

Figure 3.3 Automated system for near-infrared spectra collection from increment cores, developed by Centre de Recherche Industriel du Québec for Ministère des Forêts, de la Faune, et des Parcs du Québec, Canada. This system uses a motorized carriage (top left photo), a high resolution on-line camera (top right photo), and a 2-mm diameter near-infrared probe (bottom left photo) controlled by software (bottom right photo).

Calibration of NIR models

Near-infrared calibrations were based on 1,636 wood samples measured by X-ray diffractometry and X-ray densitometry, using SilviScan-3 at FPInnovations in Vancouver, British Columbia (Table 3.1). These reference samples were chosen from a collection of wooden disks harvested across the province to develop stem taper equations and site index estimates in the 2000s (Laflèche et al. 2013). Only co-dominant and dominant trees from mature stands were sampled. Some of these wooden disks were kept frozen by the federal government for future research on wood fiber. Only wooden disks collected at breast height were retained, since too few samples collected at 1 m above ground were kept. SilviScan processing was described by Giroud et al. (2015). The transverse face of reference samples was scanned by NIR spectroscopy, even though SilviScan works with the radial face. Schimleck et al. (2005) tested NIR calibrations on both faces of SilviScan samples for density, MOE, microfibril angle and several tracheid morphological characteristics. They concluded that either face could be used for NIR analysis. In addition, in our study, only the transverse face of increment cores is prepared and sanded for ring analysis, and can thus be scanned by NIR spectroscopy. Furthermore, no acetone extraction was performed on SilviScan samples because the NIR models are intended to be used on increment cores with no extraction. The wood density was not vessel-free for paper birch and trembling aspen since the vessel proportions were not estimated.

Table 3.1 Descriptive statistics by species of spot-averaged SilviScan wood properties and summary by species of near-infrared calibration statistics.

Wood property	Species	descriptive statistics						global model							species-specific models						
		n_{cores}	n_{spots}	mean	s.d.	L0.025	U0.975	n_{spots}	factors	$n_{wavelengths}$	R^2	RMSE	RMSE%	RPD	n_{spots}	factors	$n_{wavelengths}$	R^2	RMSE	RMSE%	RPD
Basic density (kg/m³)	Balsam fir	272	4350	360	45	280	566	4350	14	881	0.66	26	7%	1.7	4350	14	1049	0.71	24	7%	1.9
	Black spruce	409	5327	424	43	317	573	5325	14	881	0.67	25	6%	1.8	5322	11	1102	0.70	23	5%	1.8
	Jack pine	214	2783	419	47	306	539	2777	14	881	0.53	32	8%	1.5	2781	14	1116	0.68	27	6%	1.8
	Paper birch	250	3426	509	37	412	610	3425	14	881	0.46	27	5%	1.4	3425	14	1101	0.57	25	5%	1.5
	Trembling aspen	250	5651	391	33	305	493	5646	14	881	0.55	22	6%	1.5	5650	13	1063	0.62	20	5%	1.6
	White spruce	241	5426	377	47	281	567	5418	14	881	0.56	31	8%	1.5	5422	15	1116	0.61	29	8%	1.6
Modulus of elasticity (GPa)	Balsam fir	272	4350	10.2	3.5	3.2	18.2	4350	14	881	0.77	1.6	16%	2.1	4350	14	1049	0.81	1.5	15%	2.3
	Black spruce	409	5327	12.1	3.6	4.6	20.9	5325	14	881	0.74	1.8	15%	2.0	5322	11	1102	0.77	1.7	14%	2.1
	Jack pine	214	2783	10.2	3.9	3.2	19.1	2777	14	881	0.76	1.9	19%	2.0	2781	14	1116	0.80	1.7	17%	2.2
	Paper birch	250	3426	16.1	3.1	9.0	22.3	3425	14	881	0.68	1.8	11%	1.8	3425	14	1101	0.76	1.5	10%	2.0
	Trembling aspen	250	5651	14.9	2.5	6.4	21.5	5646	14	881	0.59	1.6	11%	1.6	5650	13	1063	0.69	1.4	9%	1.8
	White spruce	241	5426	10.5	3.4	3.5	18.3	5418	14	881	0.64	2.0	19%	1.7	5422	15	1116	0.74	1.7	16%	2.0

$n_{wavelengths}$: number of wavelength predictors retained

The individual NIR spectra were used to develop species-specific and global calibrations. SilviScan values were matched with the corresponding NIR spot according to measurement position. In total, 26,963 spectra were available for calibration (Table 3.1). Multivariate normality was first evaluated to detect outliers using estimated Mahalanobis distance and QQ-plots (Varmuza and Filzmoser 2016). A multiple-response PLS regression (PLS2) was then used to simultaneously predict basic density and MOE from NIR spectra (PROC PLS, SAS 9.4, SAS Institute Inc., Cary, North Carolina, USA). The multiple-response PLS regression was chosen because of the correlation between basic density and MOE at the spot scale (r=0.47). Several mathematical pre-treatments were tested (i.e., smoothing, baseline offset, Savitzky-Golay derivatives, and multiplicative scatter correction).

The optimal number of PLS factors (principal components) was determined by cross validation using a split-sample validation method with n=7 by default (PROC PLS, SAS 9.4, SAS Institute Inc.). The model was fitted to all groups except one to assess the ability of the model to predict responses for the group omitted. Repeating this for each group, a predicted residual sum of squares (PRESS) statistic was calculated based on the residuals generated by this process. The CVTEST option was also added to test whether the model with the minimum root mean PRESS was significantly different from other models with fewer factors, based on the cross-validated residuals. Furthermore, the addition of another factor should minimally improve the coefficient of determination (R^2) by 0.5%. Finally, predictors (wavelengths) with small absolute regression coefficients (inferior to one standard deviation of the normal distribution of regression coefficients) and small Variance Importance for Projection (VIP inferior to 0.8) were automatically dropped from the models (PROC PLS, SAS 9.4, SAS Institute Inc.). The VIP statistic represents the contribution of each wavelength as a predictor due to the amount of variance explained and was obtained using the option “plots = (parmprofiles vip)” in the SAS PLS procedure. In addition, the predictive ability of the calibration was assessed using the ratio of performance to deviation (RPD), calculated as the ratio of standard deviation of the reference data to the root mean square error (Williams and Sobering 1993). Furthermore, autocorrelation between trees from the same species (species random effect) was studied on the residuals using mixed regressions (Proc MIXED, SAS 9.4, SAS Institute Inc.). Lastly, bootstrap validation was performed using 1,000 replicates to evaluate the performance of the NIR models. For each replicate, 25% of observations were randomly selected for validation.

Tree-level estimates of wood properties

The final NIR calibration was applied to the spectra collected from increment cores. Only increment cores from codominant and dominant trees were retained (n = 30,159 trees). The NIR estimates of wood properties for each increment core were then matched with the corresponding annual growth rings according to measurement position. Extreme prediction values (i.e., those outside the 95% range) were automatically replaced by the mean prediction value of the nearest growth rings. Increment cores with more than two extreme values were excluded. The NIR estimates of wood properties were then averaged by increment cores. Mean values were obtained by calculating the area-weighted mean, assuming a circular shape of the rings. Correlations were tested by species between wood properties and the following tree-level attributes: number of rings, mean ring width, diameter at breast height (DBH), tree height, and ratio of tree height to DBH (slenderness) (PROC CORR, SAS 9.4, SAS Institute Inc.). These correlations were tested on calibration samples and on increment cores to verify the stability of tree-level relationships when NIR spectroscopy was used to estimate the wood properties.

Spatial modeling

NIR estimates of wood properties were averaged by species and stand (n = 10,573 stands). On average, 2.4 increment cores from the same species were sampled by stand. Extreme prediction values (outside the 99%

range) were automatically excluded. The spatial autocorrelation in wood density and MOE was measured by species using Moran's I and Geary's C statistics (PROC VARIOGRAM, SAS 9.4, SAS Institute Inc.). The pattern of spatial variability and the range of plausible spatial covariance parameters (range, nugget, and partial sill) were estimated using the semivariogram. A lag distance of 2 km was used for semivariogram modeling. Different isotropic and anisotropic semivariogram models (spherical, exponential, and Gaussian) were assessed and compared using the Akaike Information Criterion (AIC). The nugget-to-sill ratio was used as a measurement of the proportion of the total variance that could not be explained by the spatial dependence of the variable. The spatial dependence in wood properties was modeled by species with and without stand-level covariates (kriging vs. cokriging). All available spatially comprehensive data was thus tested: geographic, climatic, landsat, and photo-interpreted vegetation attributes. Data for annual climate variables, elevation (Z), and slope were estimated for the centroid of the polygon using BioSIM 10 (Régnière et al. 2014). A stepwise method was initially applied for variable selection, and the multicollinearity between predictors was also measured (PROC GLMSELECT and PROC CORR, SAS 9.4, SAS Institute Inc.). Spatial dependence was incorporated into regression models as described by Littell et al. (2006) (PROC MIXED, SAS 9.4, SAS Institute Inc.). The effect of including spatial dependence into regressions was assessed on the significance of stand-level covariates, and the spatial models were compared using AICC. Bootstrap validation was performed to evaluate the performance of the spatial models. Spatial modeling is very time-consuming. Consequently only 100 replicates were used. For each replicate, 25% of observations were randomly selected within each regional landscape unit for validation. Regional landscape is a level of ecological land classification used by the province of Quebec. It is characterized by a recurrent arrangement of the principal permanent ecological factors and vegetation. The contribution of climate to spatial dependence was also estimated based on the predictions of models without covariates using a PLS procedure. The most significant climatic variables were discussed based on absolute regression coefficients and VIP. The final spatial models were then applied to stands where the studied species were photo-interpreted. Rasters were generated in ArcGis (ESRI®, Redlands, California, USA) for kriging predictions and standard errors with a 2 km cell size resolution.

Results

Near-infrared calibrations

Near-infrared calibrations were developed using wavelengths between 4200 and 8500 cm^{-1} (1176 to 2381 nm). Outside that range the signal was too noisy, and the addition of wavelengths did not significantly improve model performance. Furthermore, none of the mathematical pre-treatments significantly improved the models. Around 2% of spectra were excluded based on the multivariate normality test. The global calibration was developed using 14 factors and 881 wavelengths (Table 3.2). No significant random effect related to species was observed on the model residuals. A simple linear regression model of observed to predicted values was fitted for each species for the purpose of comparison. Overall, the species-specific calibrations provided a slightly better explanation of variations in wood density and MOE than the global calibration when compared by species. The root mean square errors (RMSE) of species-specific calibrations were also slightly lower in all species whereas the ratio of performance to deviation (RPD) were slightly higher. Although the number of retained factors was relatively similar in both approaches, the number of retained wavelengths was higher in the species-specific models than in the global calibration. The global calibration appeared thus reasonably robust to be used at large scale and was chosen to predict wood density and MOE of all increment cores. In addition, very little variation was observed in the bootstrap estimates of R^2 and RMSE for basic density (0.78 to 0.80; 27 to 28 kg/m^3) and MOE (0.77 to 0.78; 1.9 to 2.0 GPa), confirming the reliability of the global calibration (Table 3.2).

Table 3.2 Descriptive statistics of spot-averaged SilviScan wood properties and summary of near-infrared global calibration statistics (range: 1180 to 2380 nm) with bootstrap estimates (1,000 replicates, sample ratio=25%).

Wood property	descriptive statistics					global model						bootstrap estimates of R^2				bootstrap estimates of RMSE				
	n_{spots}	mean	s.d.	L0.025	U0.975	factors	$n_{wavelengths}$	R^2	RMSE	RMSE%	RPD	mean	bias	L0.025	U0.975	mean	CV%	bias	L0.025	U0.975
Basic density (kg/m^3)	26963	408	61	285	589	14	881	0.80	28	7%	2.2	0.79	0.00	0.78	0.80	27.8	7%	0.2	27.3	28.4
Modulus of elasticity (GPa)	26963	12.4	4.0	3.4	21.8	14	881	0.78	1.9	15%	2.2	0.78	0.00	0.77	0.78	1.9	16%	0.0	1.9	2.0

Natural variability in wood density and modulus of elasticity

Natural variability in wood density and MOE was defined by species for the study area using 30,159 increment cores from codominant and dominant trees (Table 3.3). The hierarchy of species for these properties was consistent with the literature, but tree-level estimates were usually higher (Alemdag 1985, Jessome 1977, Singh 1987). However, Raymond et al. (2007) demonstrated that the longitudinal dynamic MOE values from SilviScan were 11% greater than those from the traditional static bending test. The species can be ranked in descending order of basic density as follows: paper birch (575 kg/m^3±12%; 2,708 trees), black spruce (481 kg/m^3±11%; 14,493 trees), jack pine (469 kg/m^3±11%; 2,837 trees), trembling aspen (459 kg/m^3±12%; 2,369 trees), white spruce (431 kg/m^3±10%; 610 trees), and balsam fir (403 kg/m^3±10%; 7,142 trees). The same hierarchy of species in terms of basic density was observed using the calibration samples measured by SilviScan. However, the mean values of wood density and their coefficients of variation were lower in all species when compared

with those calculated from the increment cores, possibly because of the larger sampling. Furthermore, the species can also be ranked in descending order of MOE as follows: paper birch (17.1 GPa±16%), trembling aspen (15.5 GPa±16%), black spruce (12.3 GPa±23%), jack pine (10.9 GPa±24%), white spruce (10.8 GPa±21%), and balsam fir (10.0 GPa±19%). The same hierarchy of species in terms of MOE was also observed using the calibration samples measured by SilviScan. The mean values of MOE were higher for balsam fir, black spruce, and jack pine when compared with those calculated from the increment cores. Similar mean values of MOE were observed for paper birch, trembling aspen, and white spruce. The coefficients of variation were higher in all species when calculated from the increment cores. Finally, little changes in basic density had a major impact on MOE. Basic density was indeed moderately to highly correlated to MOE among species. An increase of 25 kg/m^3 in black spruce basic density was equivalent to an increase of 1 GPa in MOE (results not presented).

Table 3.3 Descriptive statistics by species of ring area-weighted wood properties, number of rings and ring width for calibration samples measured by SilviScan (n = 1,636) and for increment cores measured by near-infrared spectroscopy (n = 30,159). Only codominant and dominant trees were used.

Wood property	Species	calibration samples measured by SilviScan						increment cores measured by NIRS					
		n	mean	s.d.	cv	min	max	n	mean	s.d.	cv	min	max
Basic density (kg/m³)	Balsam fir	272	368	27	7%	294	448	7142	403	42	10%	281	575
	Black spruce	409	439	32	7%	337	514	14493	481	55	11%	285	652
	Jack pine	214	439	28	6%	366	511	2837	469	51	11%	295	629
	Paper birch	250	521	30	6%	440	605	2708	575	72	12%	289	740
	Trembling aspen	250	395	22	6%	335	464	2369	459	53	12%	284	604
	White spruce	241	391	33	8%	304	505	610	431	45	10%	295	567
	All species	1636	425	29	7%	294	605	30159	470	53	11%	281	740
Modulus of elasticity (GPa)	Balsam fir	272	11.0	1.6	15%	5.8	15.4	7142	10.0	1.9	19%	3.2	19.6
	Black spruce	409	13.4	2.3	17%	5.9	19.2	14493	12.3	2.8	23%	2.7	24.0
	Jack pine	214	12.4	1.6	13%	8.1	16.5	2837	10.9	2.6	24%	3.4	20.5
	Paper birch	250	17.2	2.0	12%	12.4	22.6	2708	17.1	2.8	16%	7.7	23.8
	Trembling aspen	250	15.2	1.7	11%	9.9	20.1	2369	15.5	2.5	16%	6.5	23.3
	White spruce	241	11.2	1.9	17%	6.0	15.6	610	10.8	2.2	21%	4.9	18.8
	All species	1636	13.4	1.9	14%	5.8	22.6	30159	12.8	2.5	19%	2.7	24.0
Number of rings	Balsam fir	272	84	23	27%	50	157	7142	54	26	47%	12	177
	Black spruce	409	83	23	27%	41	175	14493	90	45	50%	13	252
	Jack pine	214	77	12	16%	49	117	2837	57	30	52%	11	180
	Paper birch	250	57	12	20%	26	104	2708	64	28	43%	11	170
	Trembling aspen	250	64	11	18%	41	105	2369	52	27	51%	12	152
	White spruce	241	74	21	28%	47	137	610	63	32	50%	13	220
	All species	1636	73	17	23%	26	175	30159	64	31	49%	11	252
Ring width (mm)	Balsam fir	272	1.1	0.4	37%	0.4	2.7	7142	2.2	0.9	39%	0.4	5.9
	Black spruce	409	1.0	0.3	31%	0.3	2.1	14493	1.5	0.7	49%	0.2	4.6
	Jack pine	214	1.0	0.3	30%	0.6	2.2	2837	2.8	1.2	42%	0.7	8.3
	Paper birch	250	1.4	0.4	29%	0.7	4.8	2708	2.2	0.9	38%	0.7	6.9
	Trembling aspen	250	1.9	0.5	24%	0.7	3.1	2369	2.9	1.0	35%	0.9	9.9
	White spruce	241	1.7	0.6	33%	0.7	3.6	610	3.1	1.5	48%	0.9	8.5
	All species	1636	1.4	0.4	30%	0.3	4.8	30159	2.4	1.0	42%	0.2	9.9

Correlative relationships

Highly significant ($p \leq 0.001$) linear correlations were usually observed between wood properties and tree-level attributes (Table 3.4). However, these significant linear relationships were weak. Indeed, a magnitude of between 0.3 and 0.5 usually indicates low correlation, whereas a magnitude of less than 0.3 indicates little or no linear correlation. No strong linear relationship between wood properties and tree-level attributes were therefore observed in any species based on SilviScan or NIR measurements. For a given correlative relationship, the sign of correlation coefficients was usually consistent across species, while the MOE of the relationship could vary slightly. When significant, number of rings and slenderness were usually positively related to basic density and MOE. Mean ring width and DBH were negatively related to basic density and MOE. Tree height was negatively related to basic density, except for paper birch, but positively related to MOE.

Using NIR estimates rather than SilviScan estimates of wood properties did not change the characteristics of the linear relationships observed in the calibration samples. Indeed, the magnitude and the sign of correlation coefficients were similar, except in a few cases. For example, a non-significant correlation between the SilviScan estimate of MOE and tree height became highly significant using NIR estimates in jack pine. Overall, the magnitude of significant linear relationships decreased when measured on the increment cores. The magnitude of correlation coefficients was less than 0.3 in most cases. The relationship was not significant in several cases. When significant, the signs of correlation coefficients were usually consistent with those obtained using calibration samples.

Spatial dependence

White spruce was excluded from the spatial modeling due to insufficient sampling intensity for the study area. For the remaining species, spatial autocorrelation in wood density and MOE was positive and highly significant based on the Moran's I and Geary's C statistics (results not presented). The spherical function performed better for modeling semivariograms in all species. The mean proportion of the total variance that could not be explained by spatial dependence (nugget-to-sill ratio) was high in basic density (71%) and in MOE (77%) (Table 3.5). Spatial variation in wood properties was weakly explained by stand-level attributes only. Furthermore, most of these attributes became non-significant when included in spatial models. Kriging models without covariates were finally chosen based on AIC statistics. On average, similar coefficients of determination (R^2) were obtained for basic density and MOE (33% and 26%, respectively). Lower average values of relative root mean square errors (RMSE%) were obtained for basic density and MOE (6% and 12%, respectively). Very little variation was observed in bootstrap estimates of RMSE in all models. More variation was observed in bootstrap estimates of R^2 in all models. However, spatial models did not drop off when predicting wood density and MOE for new locations.

Table 3.4 Magnitude and significance of linear correlations between wood properties and tree-level attributes in calibration samples measured by SilviScan and near-infrared spectroscopy and in increment cores measured by near-infrared spectroscopy only.

Wood property	Attribute	Sample	Method	Balsam fir	Black spruce	Jack pine	Paper birch	Trembling aspen	White spruce
Basic density (kg/m³)	Number of rings	calibration samples	SilviScan	0.39 **	0.28 **	-0.01 n.s.	0.37 **	-0.09 n.s.	0.46 **
		calibration samples	NIR	0.33 **	0.23 **	-0.13 n.s.	0.39 **	-0.11 n.s.	0.33 **
		increment cores	NIR	0.04 **	0.11 *	0.20 **	0.08 *	-0.06 **	0.07 n.s.
	Ring width (mm)	calibration samples	SilviScan	-0.47 **	-0.61 **	-0.25 **	-0.25 **	-0.16 *	-0.66 **
		calibration samples	NIR	-0.46 **	-0.55 **	-0.29 **	-0.42 **	-0.17 **	-0.63 **
		increment cores	NIR	-0.12 **	-0.23 **	-0.18 **	-0.08 **	0.02 n.s.	-0.23 **
	DBH (mm)	calibration samples	SilviScan	-0.28 **	-0.28 **	-0.34 **	0.11 n.s.	-0.28 **	-0.42 **
		calibration samples	NIR	-0.30 **	-0.25 **	-0.45 **	-0.12 n.s.	-0.34 **	-0.49 **
		increment cores	NIR	-0.13 **	-0.21 **	0.05 **	0.02 n.s.	-0.04 n.s.	-0.23 **
	Tree height (cm)	calibration samples	SilviScan	-0.25 **	-0.39 **	-0.13 n.s.	0.34 **	-0.05 n.s.	-0.37 **
		calibration samples	NIR	-0.28 **	-0.33 **	-0.16 *	0.13 *	-0.15 *	-0.42 **
		increment cores	NIR	-0.08 **	-0.10 **	0.19 **	0.13 **	0.00 n.s.	-0.10 *
	Slenderness (m/cm)	calibration samples	SilviScan	0.11 *	0.37 **	0.42 **	0.18 **	0.22 **	0.14 *
		calibration samples	NIR	0.11 *	0.36 **	0.57 **	0.26 **	0.23 **	0.20 **
		increment cores	NIR	0.12 **	0.23 **	0.22 **	0.08 **	0.04 *	0.30 **
Modulus of elasticity (GPa)	Number of rings	calibration samples	SilviScan	0.16 **	0.23 **	0.18 **	0.38 **	0.08 n.s.	0.18 **
		calibration samples	NIR	0.15 **	0.14 **	0.09 n.s.	0.27 **	-0.02 n.s.	0.27 **
		increment cores	NIR	0.06 **	0.04 **	0.14 **	0.10 **	0.00 n.s.	0.10 **
	Ring width (mm)	calibration samples	SilviScan	-0.07 n.s.	-0.42 **	-0.24 **	-0.35 **	-0.37 **	-0.33 **
		calibration samples	NIR	-0.11 n.s.	-0.28 **	0.13 n.s.	-0.23 **	-0.18 **	-0.39 **
		increment cores	NIR	-0.22 **	-0.21 **	-0.21 **	-0.17 **	-0.08 **	-0.36 **
	DBH (mm)	calibration samples	SilviScan	0.00 n.s.	-0.11 *	-0.14 *	-0.03 n.s.	-0.33 **	-0.16 *
		calibration samples	NIR	-0.06 n.s.	-0.09 n.s.	0.11 n.s.	0.00 n.s.	-0.23 **	-0.19 **
		increment cores	NIR	-0.13 **	-0.12 **	0.04 *	0.00 n.s.	-0.03 n.s.	-0.19 **
	Tree height (cm)	calibration samples	SilviScan	0.17 **	-0.09 n.s.	0.11 n.s.	0.24 **	-0.01 n.s.	0.14 *
		calibration samples	NIR	0.11 *	-0.03 n.s.	0.39 **	0.21 **	0.01 n.s.	0.10 n.s.
		increment cores	NIR	0.04 **	0.06 **	0.23 **	0.20 **	0.07 **	0.03 n.s.
	Slenderness (m/cm)	calibration samples	SilviScan	0.18 **	0.31 **	0.35 **	0.28 **	0.24 **	0.39 **
		calibration samples	NIR	0.20 **	0.28 **	0.27 **	0.19 **	0.20 **	0.36 **
		increment cores	NIR	0.30 **	0.32 **	0.30 **	0.17 **	0.09 **	0.38 **

Table 3.5 Summary of kriging statistics with bootstrap estimates (100 replicates, sample ratio=10%).

Wood property	Species	n_{stands}	kriging model								bootstrap estimates of $R^2_{SPATIAL}$				bootstrap estimates of RMSE				
			nugget	partial sill	nugget/sill	range (km)	$R^2_{SPATIAL}$	RMSE	RMSE%	$R^2_{CLIMATE}$	mean	bias	L0.025	U0.975	mean	CV%	bias	L0.025	U0.975
Basic density (kg/m³)	Balsam fir	2742	662	320	67%	58	39%	23.9	6%	23%	19%	0.02	15%	22%	27	7%	0.5	26	29
	Black spruce	4580	1073	403	73%	57	30%	30.7	6%	32%	14%	0.01	10%	16%	34	7%	0.5	33	35
	Jack pine	1059	1061	409	72%	80	35%	29.8	6%	27%	11%	0.02	6%	16%	35	7%	1.0	32	37
	Paper birch	1200	2128	912	70%	135	31%	43.7	8%	43%	15%	0.02	10%	20%	49	8%	1.2	45	51
	Trembling aspen	992	1267	453	74%	142	29%	33.8	6%	57%	16%	0.03	9%	24%	37	8%	1.1	33	39
Modulus of elasticity (GPa)	Balsam fir	2757	1.5	0.4	81%	72	24%	1.17	12%	29%	10%	0.01	6%	13%	1.3	13%	0.0	1.2	1.3
	Black spruce	4573	2.8	0.9	75%	64	27%	1.60	13%	35%	13%	0.01	10%	16%	1.7	14%	0.0	1.7	1.8
	Jack pine	1060	2.6	0.9	73%	86	35%	1.50	14%	43%	15%	0.02	11%	23%	1.7	16%	0.0	1.6	1.9
	Paper birch	1199	3.6	1.1	77%	137	24%	1.81	11%	40%	10%	0.02	6%	17%	2.0	11%	0.0	1.8	2.1
	Trembling aspen	983	3.0	0.7	81%	176	22%	1.66	10%	65%	13%	0.02	7%	19%	1.8	11%	0.1	1.6	1.9

On average, observations were spatially autocorrelated on longer distances (ranges) in hardwoods than softwoods for basic density (139 vs. 65 km) and MOE (157 vs. 74 km). The climate dependence was also higher in hardwoods than softwoods for basic density (50% vs. 27%) and for MOE (52% vs. 36%). Climatic variables were highly autocorrelated and made it difficult to clearly identify the most important variables. However, precipitation under different forms (total, growing season only, and snow), aridity, and July mean temperature were among the most important variables in terms of VIP values in all models. Spatial similarities were obvious between wood properties and species (Figure 3.4). A clear latitudinal gradient related to climate was observed in paper birch and trembling aspen wood properties, with the highest values usually in the warmest and rainiest regions of the study area (Figure 3.2 and Figure 3.4). The spatial distribution of wood properties was not uniform in softwoods, and climatic dependence was less apparent. No elevation gradient was observed in wood properties, possibly due to its limited range across the study area (395±102 meters).

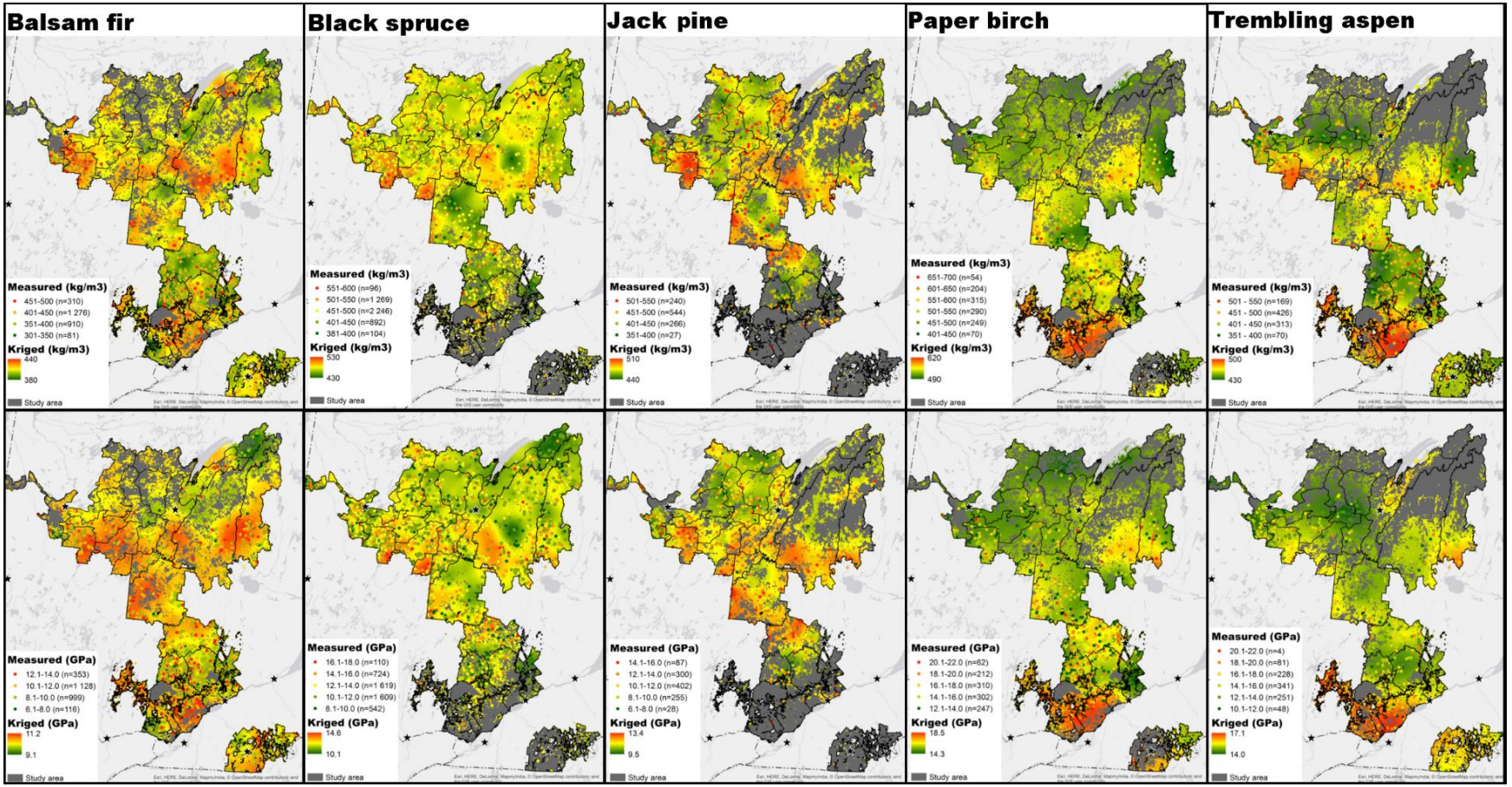

Figure 3.4 Maps for basic density (top images) and modulus of elasticity (bottom images) in balsam fir, black spruce, jack pine, paper birch, and trembling aspen across the study area.

Discussion

The development of a global, multi-response NIR calibration for simultaneously predicting basic density and MOE was explored for the main boreal softwoods (black spruce, balsam fir, jack pine) and hardwoods (paper birch, trembling aspen) of Quebec, Canada. Good and reliable statistics (R^2, RMSE, RPD) were obtained for basic density (0.80, 28 kg/m^3, 2.2) and MOE (0.78, 1.9 GPa, 2.2). This study confirms that it is possible to develop global calibrations for important wood properties using species that display large variations in wood chemistry, anatomy and physical properties, as already demonstrated by Schimleck et al. (2001). The fit statistics (R^2, RPD) were slightly higher for the species-specific calibrations. However, it would be relevant to compare the predictive ability of species-specific and global calibrations using independent wood samples from different regions. Moreover, it would be interesting to test the global calibration on unsampled species in the range of measured wood properties.

The statistics of species-specific calibrations appeared comparable to those reported in the literature. Giroud et al. (2015) have developed a similar NIR calibration using the radial profiles of wood properties measured by SilviScan. For this purpose, 127 clear wood black spruce samples were used. The fit statistics (R^2, RPD) were better than those obtained in our study for basic density (0.82, 1.7 vs. 0.70, 1.8) and MOE (0.89, 2.9 vs. 0.77, 2.1). These differences are probably related to larger spot sizes (15 vs 2-mm diameter) and the analysis of clear wood samples only (i.e., without compression wood). In addition, the fit statistics (R^2, RPD) obtained by Xu et al. (2011) for black spruce and balsam fir were slightly higher for wood density (0.85, 2.4), and relatively similar for MOE (0.78, 2.0).

This study demonstrated a spatial dependence in wood density and MOE in Quebec's main boreal tree species. The spatial distribution of these properties was mainly driven by climate. As observed in other studies around the world, wood density and MOE increased with a rise in temperature and precipitation, regardless of species (Antony et al. 2011; Chave et al. 2006; Jordan et al. 2008; Palmer et al. 2013; Slik et al. 2010; Zhang et al. 2011). The observations were spatially correlated on longer distances in paper birch and trembling aspen, which were more climate dependant. The patterns of spatial distribution in wood density and MOE appear to be patchy in softwoods and uniform in paper birch and trembling aspen. The remaining spatial dependence could result from either unmeasured attributes (e.g. soil, physical environment) or biotic processes that cause spatial clustering (e.g., gene flow) (Miller et al. 2007). Gene flow in softwoods may be limited by shorter distances of seed dispersal in comparison to paper birch and trembling aspen, and by specific factors such as a widespread clonal growth in black spruce and serotinous cones in jack pine. The unexplained spatial dependence was highest in balsam fir, as shown by the limited range of its regional variation in wood density and MOE. Thus, the environmental adaptability of balsam fir wood appears to be very weak even though this species grows in a variety of conditions. An analysis of the phylogenetic variation may help provide a better understanding of the

intraspecific and interspecific spatial distribution of wood density and MOE (Zhang et al. 2011). Hung et al. (2016) have recently demonstrated that it was possible to assess the genetic variation in wood density, MOE and microfibril angle of *Corymbia citriodora* using NIR estimates of these wood properties.

Comparisons with other Canadian regions and provinces were possible using the results of the current study. For example, the plot-level estimates of wood density were lower than those measured by SilviScan in Newfoundland for black spruce (480±40 kg/m^3 vs. 547±39 kg/m^3) and balsam fir (403±34 kg/m^3 vs. 425±30 kg/m^3) (Lessard et al. 2014). The plot-level estimates of MOE were also lower for black spruce (12.2±2.1 GPa vs. 13.9±2.3 GPa) and balsam fir (10.0±1.5 GPa vs. 11.2±1.5 GPa). These differences are probably related to a lower growing rate in Newfoundland. Indeed, the mean ring widths measured in Quebec's increment cores were higher than those measured in Newfoundland for black spruce (1.31±0.64 mm vs. 0.86±0.72 mm) and balsam fir (1.45±0.83 mm vs. 1.21±0.90 mm) (Groot and Luther 2015). A negative relationship between growth rate and wood density is usually observed in softwoods with gradual transition from earlywood to latewood (*Picea* spp. and *Abies* spp.) (Zobel and van Buijtenen 1989).

The kriged estimates of wood density and MOE must be interpreted as regional population estimates since no local variable was included in the spatial models. Intraspecific and interspecific regional differences were observed for the study area. For example, balsam fir appeared to produce a wood as dense and stiff as black spruce in some areas. Within each species, populations also presented a higher potential to produce a denser wood with higher MOE. In eastern Canada, black spruce, balsam fir, and jack pine are combined to produce SPF (spruce, pine or fir) softwood lumber, which is visually graded in sawmills. Nevertheless, several sawmills use mechanical grades as the machine-stress-rated (MSR) grades for producing engineered wood products (Paradis et al. 2013). Among the Canadian Wood Council, the most common MSR grades are 1650f-1.5E, 2100f-1.8E and 2400f-2.0E, which require MOE of 10.3, 12.4, and 13.8 GPa, respectively. The regions with a strong potential in MSR lumber could be easily differentiated using the color chart on the black spruce wood MOE map (Fig. 3.4). However, technically speaking, SilviScan wood stiffness was calibrated using acoustic tests and cannot be compared without correction with standard (static) MOE, which is measured by static bending tests (Mora et al. 2009).

Local random noise, represented by the nugget of semivariograms, was high in all models. Random noise is usually caused by a combination of some inherent short-scale variation and sampling and measurement errors (Cressie 2015). NIR spectroscopy is an indirect method, which adds a certain amount of noise to measurements of wood properties. This noise was somewhat attenuated by having several measurements per increment core. Despite its importance, short-scale variation in wood density and MOE was not explained by stand-level attributes. Sampling intensity was too weak at the local level, with only 2.4 increment cores per temporary plot

from the same species, on average, even when selecting only codominant and dominant trees. Furthermore, no strong linear relationships were measured with tree-level attributes among species. Groot and Cortini (2016) demonstrated in balsam fir and white spruce that several measurements within a tree are required to obtain strong correlations between wood density and tree-level variables such as slenderness, relative height, and ring width. They concluded that the weakness of relationships could reveal potential nonlinearities and interactions among tree-level attributes. The most predictive models successfully developed at the stand level have used a higher sampling intensity of increment cores per temporary plot (Lessard et al. 2014) and restrained the ecological conditions (Giroud et al. 2016).

Wood formation is also a complex natural phenomenon which can be influenced by various inherent factors (e.g., proximity of knot, slope of grain, tension wood) or external factors, such as very local and abrupt environmental changes related to competition dynamics, sudden wind exposure, water stress, or insect defoliation. The anatomical, chemical and physical properties of tension wood differ distinctly from those of normal wood (Giroud et al. 2015, Meder et al. 2010). However, Giroud et al. 2015 have demonstrated in black spruce that it was relatively easy to detect and remove the effects of compression wood on the radial profile of microfibril angle obtained by NIR spectroscopy. Detecting and removing the effects of reaction wood could possibly improve the stand-level modelling method. Wood formation is therefore difficult to model without an adequate sampling intensity and without setting and restraining the sources of variation. Finally, although the sampling intensity was insufficient to characterize the short-scale variations, it was sufficient to characterize the regional variation in wood density and MOE as originally intended.

Conclusion

A fast and reliable method of estimating wood density and MOE from increment cores was developed. The application of NIR spectroscopy on increment cores collected in thousands of inventory plots made it possible to obtain reliable regional estimates of wood density and MOE for Quebec's main boreal tree species. Spatial dependence was incorporated into predictive models, and intraspecific and interspecific regional differences were observed for the study area. This knowledge of the large-scale variation in wood properties could find numerous practical application, since many decisions in forestry are taken on scales larger than forest stands. Regional estimates of wood density and MOE could be averaged by management subdivisions for strategic or tactical decision-making in forest management or wood allocation. In addition, regions with a strong potential in MSR lumber could be prioritized in firefighting and insect outbreak control, which require major financial investments. The regional estimates could also be very useful in better assessing timber market value. These estimates could also reduce the uncertainty in forest carbon sequestration, especially since no strong relationship was observed between wood density and DBH. The short-scale variation in wood density and MOE may be due to low sampling intensity at the plot scale. Further studies are currently underway on this topic, as this knowledge would be very useful for operational decision-making.

Acknowledgements

This research was funded by the Fonds de recherche du Québec – Nature et technologies and the Ministère des Forêts, de la Faune et des Parcs du Québec. The reference samples were provided by the Canadian Wood Fibre Centre, Canadian Forest Service, and Natural Resources Canada. The automated near-infrared system was developed by Centre de recherche industrielle du Québec (CRIQ). Thanks to the staff of the Direction des inventaires forestiers du Québec, specifically to Max Taimela and Raynald Abel for their technical support and to Bastien Ferland-Raymond for statistical support and advice. We thank the two anonymous reviewers for their constructive comments, which helped us to improve the manuscript.

References

Alemdag, I.S. (1985). Wood density variation of 28 tree species from Ontario. Information Report PI-X-45F. Agriculture Canada, Canadian Forestry Service, Petawawa, Canada. 17 pp.

Antony, F., Jordan, L., Schimleck, L.R., Clark, A., Souter, R.A., and Daniels, R.F. (2011). Regional variation in wood modulus of elasticity (stiffness) and modulus of rupture (strength) of planted loblolly pine in the United States. Can. J. For. Res. 41(7), 1522-1533.

Briggs, D. (2010). Enhancing forest value productivity through fiber quality. J. For. 108(4), 174-182.

Cressie, N.A.C. (2015). Statistics for Spatial Data. John Wiley and Sons. 928 pp.

Chave, J., Muller-Landau, H.C., Baker, T.R., Easdale, T.A., Steege, H.T., and Webb, C.O. (2006). Regional and phylogenetic variation of wood density across 2456 neotropical tree species. Ecol. Appl. 16(6), 2356-2367.

Evans R. (1994). Rapid measurement of the transverse dimensions of tracheids in radial wood sections from Pinus radiate. Holzforschung 48(2), 168-172.

Evans, R., and Ilic, J. (2001). Rapid prediction of wood stiffness from microfibril angle and density. Forest Prod. J. 51(3), 53.

Giroud, G., Defo, M., Bégin, J., and Ung, C.H. (2015). Application of near-infrared spectroscopy to determine the juvenile-mature wood transition in black spruce. Forest Prod. J. 65(3), 129-138.

Giroud, G., Bégin, J., Defo, M., and Ung, C.H. (2016). Ecogeographic variation in black spruce wood properties across Quebec's boreal forest. Forest Ecol. Manag. 378, 131-143.

Groot, A., and Luther, J.E. (2015). Hierarchical analysis of black spruce and balsam fir wood density in Newfoundland. Can. J. Forest Res. 45(7), 805-816.

Groot, A., and Cortini, F. (2016). The effect of the interaction of tree slenderness and relative height with ring width on wood density in Abies balsamea and Picea glauca. Wood Sci. Technol. 51(1), 175-194.

Hung, T.D., Brawner, J.T., Lee, D.J., Meder, R., and Dieters, M.J. (2016). Genetic variation in growth and wood-quality traits of *Corymbia citriodora* subsp. *variegata* across three sites in south-east Queensland, Australia. South. Forests. 78(3), 225-239.

Jessome, A.P. (2000). Strength and related properties of woods grown in Canada. Special Publication SP-514E. Forintek Canada Corp., Quebec, Canada. 37 pp.

Jordan, L., Clark, A., Schimleck, L.R., Hall, D.B., and Daniels, R.F. (2008). Regional variation in wood specific gravity of planted loblolly pine in the United States. Can. J. For. Res. 38, 698–710.

Laflèche, V., Bernier, S., Saucier, J.-P. and Gagné, C. (2013). Indices de qualité de station des principales essences commerciales en fonction des types écologiques du Québec méridional. Ministère des Ressources naturelles (provincial Department of Natural Resources). Quebec, Canada. 115 pp.

Lenz, P., Deslauriers, M., Ung, C.-599 H., MacKay, J., and Beaulieu, J. (2014). What do ecological regions tell us about wood quality? A case study in eastern Canadian white spruce. Can. J. For. Res. 44, 1383–1393.

Lessard, E., Fournier, R.A., Luther, J.E., Mazerolle, M.J., and van Lier, O.R. (2014). Modeling wood fiber attributes using forest inventory and environmental data for Newfoundland's boreal forest. For. Ecol. Manag. 313, 307–318.

Littell, R.C., Stroup, W.W., Milliken, G.A., Wolfinger, R.D., and Schabenberger, O. (2006). SAS for mixed models. SAS institute. 828 pp.

Luther, J.E., Skinner, R., Fournier, R.A., Lier, O.R. van, Bowers, W.W., Coté, J.-F., Hopkinson, C., and Moulton, T. (2014). Predicting wood quantity and quality attributes of balsam fir and black spruce using airborne laser scanner data. Forestry 87, 313–326.

Meder, R., Marston, D., Ebdon, N., and Evans, R. (2011). Spatially-resolved radial scanning of tree increment cores for near infrared prediction of microfibril angle and chemical composition. J. Near Infrared Spec. 18(6), 499-505.

Mora, C.R., Schimleck, L.R., Isik, F., Mahon, J.M., Clark, A., and Daniels, R.F. (2009). Relationships between acoustic variables and different measures of stiffness in standing Pinus taeda trees. Can. J. For. Res. 39(8), 1421-1429.

Miller, J., Franklin, J., and Aspinall, R. (2007). Incorporating spatial dependence in predictive vegetation models. Ecol. Model. 202(3), 225-242.

Palmer, D.J., Kimberley, M.O., Cown, D.J., and McKinley, R.B. (2013). Assessing prediction accuracy in a regression kriging surface of Pinus radiata outerwood density across New Zealand. For. Ecol. Manag. 308, 9-16.

Paradis, N., Auty, D., Carter, P., and Achim, A. (2013). Using a standing-tree acoustic tool to identify forest stands for the production of mechanically-graded lumber. Sensor. 13(3), 3394-3408.

Pokharel, B., Dech, J.P., Groot, A., and Pitt, D. (2014). Ecosite-based predictive modeling of black spruce (*Picea mariana*) wood quality attributes in boreal Ontario. Can. J. For. Res. 44(5), 465-475.

Pokharel, B., Groot, A., Pitt, D.G., Woods, M., and Dech, J.P. (2016). Predictive Modeling of Black Spruce (*Picea mariana* (Mill.) BSP) Wood Density Using Stand Structure Variables Derived from Airborne LiDAR Data in Boreal Forests of Ontario. Forests 7(12), 311.

Raymond, C.A., Joe, B., Evans, R., and Dickson, R.L. (2007). Relationship between timber grade, static and dynamic modulus of elasticity, and SilviSvan properties for *Pinus radiata* in New South Wales. New Zeal. J. For. Sci. 37(2), 186.

Régnière, J., St-Amant, R., and Béchard, A. (2014). BioSIM 10 – User's manual. Natural Resources Canada, Canadian Forest Service, Laurentian Forestry Centre, Quebec, Canada. LAU-X-137E. 66 pp.

Rossi, S., Cairo, E., Krause, C., and Deslauriers, A. (2015). Growth and basic wood properties of black spruce along an alti-latitudinal gradient in Quebec, Canada. Ann. For. Sci. 72, 77–87.

Schimleck, L.R., Evans, R., and Ilic, J. (2001). Application of near infrared spectroscopy to a diverse range of species demonstrating wide density and stiffness variation. IAWA J. 22(4), 415-429.

Schimleck, L.R., Stürzenbecher, R., Mora, C., David Jones, P., and Daniels, R.F. (2005). Comparison of *Pinus taeda* L. wood property calibrations based on NIR spectra from the radial-longitudinal and radial-transverse faces of wooden strips. Holzforschung 59(2), 214-218.

Schimleck, L.R. (2008). Near-infrared spectroscopy: a rapid, non-destructive method for measuring wood properties and its application to tree breeding. New Zeal. J. For. Sci. 38(1), 14-35.

Schimleck, L.R., Hodge, G. R., and Woodbridge, W. (2010). Toward global calibrations for estimating the wood properties of tropical, sub-tropical and temperate pine species. J. Near Infrared Spec. 18(6), 355-365.

Singh, T. (1987). Wood density variations in thirteen Canadian tree species. Wood Fiber Sci. 19(4), 362-369.

Slik, J.W.F., Aiba, S.I., Brearley, F.Q., Cannon, C.H., Forshed, O., Kitayama, K., Nagamasu, H., Nilus, R., Payne, J., Paoli, G., Poulsen, A.D., Raes, N., Sheil, D., Sidiyasa, K., Suzuki, E., and van Valkenburg, J. (2010). Environmental correlates of tree biomass, basal area, wood specific gravity and stem density gradients in Borneo's tropical forests. Global Ecol. Biogeogr. 19(1), 50-60.

Swenson, N.G., and Enquist, B.J. (2007). Ecological and evolutionary determinants of a key plant functional trait: wood density and its community-wide variation across latitude and elevation. Am. J. Bot. 94(3), 451-459.

Tobler, W.R. (1970). A computer movie simulating urban growth in the Detroit region. Econ. Geogr. 46(sup1), 234-240.

Tsuchikawa, S. (2007). A review of recent near infrared research for wood and paper. Appl. Spectrosc. Rev. 42(1), 43-71.

Tsuchikawa, S., and Kobori, H. (2015). A review of recent application of near infrared spectroscopy to wood science and technology. J. Wood Sci. 61(3), 213-220.

Varmuza, K., and Filzmoser, P. (2016). Introduction to multivariate statistical analysis in chemometrics. CRC press. 336 pp.

Williams, P.C., and Sobering, D.C. (1993). Comparison of commercial near infrared transmittance and reflectance instruments for analysis of whole grains and seeds. J. Near Infrared Spec. 1(1), 25-32.

Xu, Q., Qin, M., Ni, Y., Defo, M., Dalpke, B., and Sherson, G. (2011). Predictions of wood density and module of elasticity of balsam fir (*Abies balsamea*) and black spruce (*Picea mariana*) from near infrared spectral analyses. Can. J. For. Res. 41, 352–358.

Zhang, S.B., Slik, J.W., Zhang, J.L., and Cao, K.F. (2011). Spatial patterns of wood traits in China are controlled by phylogeny and the environment. Global Ecol. Biogeogr. 20(2), 241-250.

Zobel, B.J., and Van Buijtenen, J.P. (2012). Wood variation: its causes and control. Springer Science and Business Media. 363 pp.

Conclusion générale

Tel que mentionné en introduction, les travaux de la présente thèse s'inscrivent dans une démarche visant dans un premier temps à établir des preuves de concept avec l'épinette noire (chapitres 1 et 2) et, dans un second temps, à proposer une méthode d'inventaire de la qualité de la fibre pour les principales essences boréales du Québec (chapitre 3).

Dans le chapitre 1, nous avons été en mesure de modéliser la variabilité naturelle des propriétés de la fibre de l'épinette noire en tenant compte de la station écologique et des conditions de croissance. Malgré son importance, clairement démontrée dans ce chapitre, l'influence de la station écologique n'est que très rarement prise en considération dans les études portant sur la variabilité naturelle des propriétés de la fibre. Pourtant, l'information écologique est disponible, de façon continue et détaillée, pour l'ensemble du territoire et à une échelle aussi fine que celle du peuplement forestier. À notre connaissance, cette publication est la première étude portant sur la variabilité naturelle des propriétés de la fibre à s'appuyer sur le système hiérarchique de classification écologique du territoire du MFFP.

De plus, dans le même chapitre, nous avons été en mesure de démontrer la faisabilité de modéliser les propriétés de la fibre à l'échelle du peuplement forestier. Les modèles au peuplement développés récemment dans le cadre du projet d'inventaire de la qualité de la fibre à Terre-Neuve sont les seuls comparables en forêt naturelle. Toutefois, contrairement à l'approche utilisée à Terre-Neuve, nous avons privilégié une modélisation au peuplement par saut d'échelle, en nous basant notamment sur les mesures de croissance d'arbres études provenant de 3350 placettes d'inventaire. Cette méthode a permis de mieux tenir compte de la variabilité des conditions de croissance à l'intérieur des deux végétations potentielles étudiées et, par la même occasion, d'améliorer la performance des modèles de prédiction. Une telle approche par saut d'échelle n'avait pas encore été évaluée pour estimer les propriétés de la fibre.

La réalisation d'un inventaire de la qualité de la fibre requiert des efforts et des coûts considérables, associés à l'échantillonnage de milliers d'arbres et aux analyses de laboratoire très exigeantes. C'est dans ce contexte que la spectroscopie proche infrarouge a été évaluée, comme technologie rapide et non destructive, pour mesurer la densité basale, la rigidité du bois et l'angle des microfibrilles de l'épinette noire, incluant l'âge de transition du bois juvénile au bois mature (chapitre 2). Le potentiel de la spectroscopie proche infrarouge avait déjà été évalué, avec succès, chez l'épinette noire et le sapin baumier, dans le cadre du projet d'inventaire de la qualité de la fibre à Terre-Neuve. Nos résultats ont simplement confirmé la faisabilité de développer des modèles spectroscopiques chez l'épinette noire dans un contexte forestier québécois. Toutefois, l'originalité de ce chapitre repose principalement sur la détermination de la transition du bois juvénile au bois mature par

spectroscopie proche infrarouge. Les perspectives d'utilisation semblent particulièrement intéressantes dans le contexte des prescriptions de reboisement. En effet, une telle application ouvre la porte à l'analyse, à moindres coûts, d'un grand nombre de carottes de bois provenant de plantations, afin de mieux évaluer l'influence de la densité de reboisement sur l'âge de transition du bois juvénile au bois mature. Il est toutefois important de rappeler que l'âge de transition a été déterminé en corrigeant aussi bien les fluctuations naturelles, associées à des stress de croissance, que les fluctuations artificielles, associées à la calibration proche infrarouge, connaissant la variabilité naturelle de l'angle des microfibrilles de la moelle vers l'écorce, en forme de « J » inversé. Les tendances naturelles, de la moelle vers l'écorce, de la densité, de la rigidité et de l'angle des microfibrilles ont été modélisées pour l'épinette noire, dans le premier chapitre de cette thèse, démontrant notamment l'influence déterminante de l'âge cambial, et dans une moindre mesure de la largeur de cerne sur celles-ci. Ces tendances sont également bien documentées et connues dans la littérature.

Dans le chapitre 3, nous avons proposé une méthode d'inventaire de la qualité de la fibre pour les principales essences boréales du Québec, basée sur l'analyse par spectroscopie proche infrarouge des carottes de bois, prélevées dans les placettes temporaires de la Direction des inventaires forestiers. Les résultats de ce chapitre sont uniques en plusieurs points. Il s'agit de la première utilisation à grande échelle de la spectroscopie proche infrarouge pour évaluer la variabilité régionale de la densité basale et de la rigidité du bois. Dans les limites de notre connaissance, il semble que la spectroscopie proche infrarouge n'avait jamais été calibrée pour mesurer ces propriétés chez l'épinette blanche, le pin gris, le bouleau à papier et le peuplier faux-tremble. Toutefois, l'originalité principale repose sur le développement d'une calibration proche infrarouge indépendante de l'essence, laissant entrevoir la possibilité d'étendre cet inventaire à d'autres essences, dans les limites de la variabilité mesurée. D'autre part, cette calibration a été développée à une résolution fine, soit à l'échelle du spot de lumière proche infrarouge, d'environ 3 mm^2 de surface. La méthode permet ainsi d'obtenir, à l'intérieur de chaque carotte, plusieurs mesures de densité basale et de rigidité du bois de la moelle vers l'écorce. L'approche permet ainsi d'évaluer la présence des tendances naturelles des propriétés de la fibre et, par la même occasion, le niveau de fluctuations autour de celles-ci.

Le chapitre 3 permet d'établir, pour la première fois au Québec, des valeurs régionales de densité basale et de rigidité du bois, pour les principales essences boréales. Ces valeurs régionales constituent de nouvelles références pour la qualité de la fibre au Québec. Elles permettent d'établir des comparaisons inter- et intraspécifiques de même que d'observer les gradients géographiques. Il est maintenant possible de déterminer les régions avec le plus fort potentiel de rigidité du bois. En ce qui concerne les retombées possibles, il semble que ces valeurs régionales de densité et de rigidité de bois pourraient être prises en considération, par le Bureau de mise en marché des bois, dans l'estimation de la valeur marchande des bois sur pied par zone de tarification

forestière. Actuellement, le Bureau de mise en marché des bois, de même que d'autres Directions du MFFP, utilise les valeurs canadiennes de Jessome (1977).

D'autre part, la variabilité naturelle de densité et de rigidité du bois est maintenant connue à l'intérieur de chaque essence étudiée, sur la base des milliers de carottes analysées. Il est désormais possible d'estimer les proportions de bois à plus fort potentiel MSR pour les essences résineuses considérées. Comme mentionné dans l'introduction, des facteurs d'ajustement, de l'ordre de -10% pour les résineux, et de -30% pour les feuillus, devraient être apportés aux valeurs de rigidité mesurées par proche infrarouge, afin de se rapprocher des valeurs de rigidité issues des tests mécaniques en flexion, comme ceux utilisés pour classer le bois MSR, par exemple. Dans les perspectives de développements futurs, il serait opportun de pouvoir estimer plus précisément le facteur d'ajustement associé à chaque essence.

En conclusion, la spectroscopie proche infrarouge s'est avérée une technologie particulièrement intéressante pour caractériser la densité basale et la rigidité du bois, à une échelle populationnelle. Toutefois, la méthode proposée s'est avérée insuffisamment précise pour caractériser la variabilité locale. À l'intérieur de chaque carotte, de la moelle à l'écorce, les tendances naturelles de densité et de rigidité sont observables, mais accompagnées d'importantes fluctuations, naturelles ou artificielles, ou combinées. Ces fluctuations occasionnent du bruit, expliquant probablement en partie les faibles relations obtenues à l'échelle de l'arbre ou du peuplement. D'autre part, l'utilisation d'une calibration purement spectrale fait en sorte d'ignorer une réalité physique pourtant déterminante, soit celle de l'influence de l'âge cambial, et dans une moindre mesure de la largeur de cerne. De plus, la régression des moindres carrés, qui est l'approche statistique la plus utilisée dans le domaine du proche infrarouge, ne permet pas, de tenir compte de la structure de covariance associée à des mesures répétées sur une même carotte. Le développement d'une approche de modélisation tenant à la fois compte de l'âge cambial, de la largeur de cerne et de la mesure spectrale, dans un contexte de mesures répétées, est en cours d'évaluation. L'objectif est d'estimer la densité basale et la rigidité du bois à l'échelle du peuplement forestier. La modélisation au peuplement est incontournable compte tenu de l'importance des retombées possibles, en termes d'évaluation de la valeur marchande des bois, d'analyse de rentabilité des traitements sylvicoles, ou encore de définition des aires potentielles pour l'intensification de la production de matière ligneuse. Une telle connaissance pourrait à terme influencer des prises de décision bien différentes, comme, par exemple, celles de prioriser, de façon spatio-temporelle, les secteurs de récolte en fonction des besoins des marchés en temps réel, ou encore de prioriser les peuplements à forte valeur et rigidité du bois dans la lutte contre les feux ou les épidémies. Finalement, il existe de nombreuses perspectives de développement, comme les possibilités d'inventorier d'autres propriétés d'intérêt, telles que la longueur des fibres, la masse linéique, et, dans un autre registre, la teneur en carbone.